

# Hierarchical Space-Time Point-Process Models (HIST-PPM): Software Documentation

Y. OGATA, K. KATSURA, M. TANEMURA, D. HARTE AND J. ZHUANG

Email: ogata@ism.ac.jp

Revised: 21 September 2020  
Beta Version: 28 March 2015

## Abstract

This documentation describes some FORTRAN and R programs used for fitting and displaying the Hierarchical Space-Time ETAS (HIST-ETAS) models, 2D spatial Poisson processes, 1D space vs time Poisson processes and location-dependent  $b$ -value estimates. The FORTRAN programs are used for the computationally intensive work of fitting the models, including a large dataset. The R programs provide graphical summaries of characteristics of the fitted models, which can be replaced by your preferred graphical software.

The document is split into five parts. In the first part, we outline the file naming convention that we use, how to compile the source code, and execution of jobs on standard Linux systems. In the second part, documentation is given for each of the FORTRAN programs. In the third part, various R programs are described for plotting spatial images that visualize the inversion outputs of the FORTRAN programs. In the fourth part, based on the estimated HIST-ETAS models, the FORTRAN programs for forecasting future seismicity rate are explained. R programs are then described to display snapshots of the spatial distribution of forecasts. In the fifth part, programs are given for simulating spatial nonhomogeneous Poisson model, spatial magnitude simulation using location-dependent  $b$ -values, and space-time simulation of HIST-ETAS models. The Appendix contains mathematical background of the models and optimization procedures.

**Keywords:** space-time ETAS model, space-time point process, location dependent parameters, penalized log-likelihood, maximum posterior estimates, non-homogeneous spatial Poisson process, location dependent  $b$ -value of the Gutenberg-Richter's formula, magnitude frequency, FORTRAN, R, Short-term seismicity forecast, simulations of HIST-PPM models

38

## 39 Contents

40 The sections and subsections in the content are linked to those in the text by using PDF heading  
41 (bookmark).

### 42 **Part I. File Organisation and Code Execution**

- 43 1 File Organization
- 44 1.1 Program Source Code
- 45 1.2 File Naming Convention
- 46 2 Compiling and Executing FORTRAN Programs
- 47 2.1 Compile FORTRAN Programs
- 48 2.2 Memory Issues
- 49 2.3 Execution of FORTRAN Jobs

### 50 **Part II. Parameter Estimation for Each Model**

- 51 3 Formatting of the ETAS data from hypocenter catalog (tseis2etas)
- 52 3.1 File Names
- 53 3.2 Program Execution
- 54 4 Identify Anisotropic Clusters of Events (etas2aniso)
- 55 4.1 File Names
- 56 4.2 Configuration File Format
- 57 4.3 Executing the Program
- 58 5 Spatial ETAS with All Parameters Constant (st-etas)
- 59 5.1 File Names
- 60 5.2 Configuration File Format
- 61 5.3 Executing the Program
- 62 5.4 Additional Advice
- 63 6 Delaunay Tessellation for Spatial Variation (delone1, delone2)
- 64 6.1 File Names to Perform Delaunay Tessellation
- 65 6.2 Configuration File Format
- 66 6.3 Executing Delaunay Tessellation Program
- 67 6.4 Generation of the Map Dada with Boundary Points
- 68 6.5 Plotting Delaunay Tessellations
- 69 6.6 Example Output
- 70 7 Spatially Varying  $b$ -Value of Magnitude Frequency
- 71 7.1 File Names
- 72 7.2 Configuration File Format
- 73 7.3 Program Execution
- 74 8 Spatial Occurrence Rate (delo2d-poisson)
- 75 8.1 File Names
- 76 8.2 Configuration File Format
- 77 8.3 Program Execution
- 78 9 ETAS: Spatially Varying  $\mu$  and  $K_0$  (hist-etas-mk)
- 79 9.1 File Names
- 80 9.2 Configuration File Format
- 81 9.3 Output of Calculation Process
- 82 9.4 Output of Calculation Process
- 83 9.5 Additional Advice
- 84 10 ETAS: Spatial Variation in 5 Parameters (hist-etas5pa)

85	10.1 File Names
86	10.2 Configuration File Format
87	10.3 Executing the Program
88	10.4 Output Produced by Program
89	<b>Part III. Plotting Spatial Parameter Estimates</b>
90	11 Plot Spatial Variation of Parameters
91	11.1 Delaunay Tessellation for Spatial Variation
92	11.2 Spatial Occurrence Rate
93	11.3 Spatially Varying $b$ -Value of Magnitude Frequency
94	11.4 ETAS: Spatially Varying $\mu$ and $K_0$
95	11.5 ETAS: Spatial Variation in 5 Parameters
96	12 Plot Interpolated Images by Delaunay Triangles
97	<b>Part IV. Short-Term Earthquake Forecasting</b>
98	13 Seismicity Forecasts by the HIST-ETAS Models
99	13.1 <code>hist-etas-mk</code> Forecast
100	13.2 <code>hist-etas-5pa</code> Forecast
101	13.3 Magnified Forecasting Image in a Localized Region
102	13.4 Plotting Snapshots of Short-Term Forecast Images
103	
104	<b>Part V. Simulations</b>
105	14 Nonhomogeneous Poisson simulation by spatial intensity rate function
106	14.1 File Names
107	14.2 Configuration File Format
108	14.3 Program Execution
109	15 Magnitude simulation given spatially varying $b$ -values of G-R law
110	15.1 File Names
111	15.2 Configuration File Format
112	15.3 Program Execution
113	16 HIST-ETAS simulation
114	16.1 File Names
115	16.2 Configuration File Format
116	16.3 Executing the Program
117	16.4 Output Produced by Program with configuration file of different first line
118	Case 1. <code>hist-etas-mk</code>
119	Case 2. <code>hist-etas-5pa</code>
120	
121	<b>APPENDICES</b>
122	A. Mathematical Outline of Models
123	A.1 Determination of Anisotropic Clusters
124	A.2 Delaunay Tessellation
125	A.3 Spatial Non-homogeneous Poisson Model
126	A.4 $b$ -value estimate and forecasting seismicity
127	A.5 Space-Time ETAS Models: General Model Formulation
128	A.5.1 Anisotropic Space-Time ETAS Model ( <code>etas2aniso</code> )
129	A.5.2 HIST-ETAS model; Location Dependent $\mu$ and $K_0$ -parameters
130	( <code>hist-etas7pa</code> )

131	A.5.3. HIST-ETAS model ( <code>hist-etas5pa</code> )
132	A.5.4. Forecasting by HIST-ETAS Models
133	A.6 Likelihoods and Penalised Likelihoods
134	A.6.1 Log-Likelihood Function and its Maximization
135	A.6.2 Penalised Log-Likelihood Function and its Optimization
136	B. Background to Computation Algorithms
137	B.1 Nonlinear Optimization for the Maximum Likelihood Estimates (MLE)
138	B.2 Computations of Bayesian Models through Gaussian Approximations
139	B.3 Notes on Location-Dependent $\mu$ and $K$ ETAS Fitting ( <code>hist-etas-mk</code> )
140	B.4 Notes on Location-Dependent $\mu$ , $K$ , $\alpha$ , $p$ and $q$ ETAS Fitting
141	( <code>hist-etas5pa</code> )
142	<b>References</b>
143	
144	

## 145 **Part I. File Organisation and Code Execution**

146 The programs are written in FORTRAN and R. FORTRAN is generally used for the  
147 computationally intensive work, and R is used for graphical displays. The  
148 documentation is written for UNIX like systems, and it is assumed that a satisfactory  
149 FORTRAN compiler is installed along with the R statistical software distributed by the  
150 R Project (R Development Core Team, 2009).

151 Alternatively, you can use your own graphical software such as Matlab. Data is  
152 exchanged between the FORTRAN and R software as standard text files, and hence  
153 could be read by other graphic software too.

154

### 155 **1 File Organization**

#### 156 **1.1 Program Source Code**

157 The original version of HIST-PPM is in the following program directory

158 <http://bemlar.ism.ac.jp/ogata/HIST-PPM/>

159 and its a revised version HIST-PPM-V2 can be taken from the following program  
160 directory

161 <http://bemlar.ism.ac.jp/ogata/HIST-PPM-V2/>

162 in which the following program subdirectory

163 <http://bemlar.ism.ac.jp/ogata/HIST-PPM-V2/estimation/>

164 is equivalent to the original HIST-PPM package, containing the same FORTRAN  
165 source codes, but some corrected R programs from those in the original package.

166 The additionally provided FORTRAN and R programs in HIST-PPM-V2 are for  
167 the implementation of Short-Term Earthquake Forecasting that are taken from the  
168 program subdirectory

169 <http://bemlar.ism.ac.jp/ogata/HIST-PPM-V2/forecasting/>

170 the use of which is explained in Part IV of this manual.

171 Finally, simulating spatial nonhomogeneous Poisson model, spatial magnitude  
172 simulation using location-dependent b-values, and space-time simulation of  
173 HIST-ETAS models are added to those in HIST-PPM-V3.

174 All the programs, inputs files and outputs files in this package HIST-PPM-V3 are  
175 selected and separately located in the directories that correspond to the subsections of  
176 Sections 3 ~ 16 in this manual, so that it will be useful that you can learn the  
177 implementation of the programs by reading the manual.

178

#### 179 **1.2 File Naming Convention**

180 Files are grouped with a common file name. This enables the user to determine the  
181 files that are associated with a particular program. It also ensures that later programs

182 do not overwrite the output of earlier programs. The files have been named as follows.  
183 The suffix determines the nature of the file:

184

185 `FILENAME.conf`: Configuration file (i.e. input parameters to `FILENAME.f`)

186 `FILENAME.f`: FORTRAN source code for single processor

187 `FILENAME`: Compiled object code for single processor

188 `FILENAME.prt`: `write(6,*)` output to keep by

189 `FILENAME |tee FILENAME.prt`

190 or

191 `FILENAME > FILENAME.prt &`

192 `FILENAME.out`: Various output files for single processor `out1, out2, ...`

193 number denotes I/O unit in Fortran code, where the transient output is

194 `out6`.

195 `FILENAME.upda`: Various output of the updated maximum a posteriori solution for

196 the weights that improved ABIC value in the searching by the simplex

197 method.

198 `FILENAME.omap` : Various output of the **optimal maximum a posteriori (OMAP)**

199 solution where “optimal” means MAP solution under the optimal weights

200 (i.e., minimum ABIC solution).

201 `FILENAME.R`: R program (usually to plot a graph)

202 `FILENAME.pdf`: Graphics output from R

203 `FILENAME.ts`: Hypocenter dataset (earthquake events) in the format, as given in

204 §3.2.

205 `FILENAME.etas`: Earthquake dataset in `etas`-format, as given in §3.2.

206

207

## 208 **2. Compiling and Executing FORTRAN Programs**

### 209 **2.1 Compile FORTRAN Programs**

210 The FORTRAN source code conforms to FORTRAN 77. Source code can be compiled in  
211 most Linux operating systems by using `gfortran`, as follows:

212

213 `gfortran FILENAME.f -o FILENAME`

214

215 You can use other FORTRAN packages such as Intel Fortran:

216

217 `ifort FILENAME.f -o FILENAME`

218

219 We have confirmed that both FORTRAN compilers above work well throughout

220 the presented programs. It has been observed that Intel FORTRAN (`ifort`) works

221 significantly faster than `gfortran` with some of the programs.

222

## 223 2.2 Memory Issues

224 The array dimensions in our FORTRAN programs are taken large enough for a  
225 moderately sized dataset. Usually, they are sufficiently large to accommodate a few  
226 tens of thousands of earthquakes. If the used memory is in excess of that defined,  
227 meaningless output can be produced. So, you have to be careful enough to check  
228 whether dimensions are set large enough. In Intel FORTRAN, for example, the  
229 following compilation command

```
230 ifort *.f -traceback -g -CB
```

231 allows a trace back when problems occur. However, there is no comparable command  
232 available in GNU FORTRAN, but you may find information by viewing the  
233 core-dump file in the Linux system.

234 Another potential problem is that the default FORTRAN settings may not allocate  
235 enough working memory in a standard Linux system compared to supercomputers. To  
236 increase such memory, the following command is available for Intel FORTRAN:

```
237  
238 ifort *.f -mcmmodel=large -shared-intel
```

239

240

## 241 2.3 Execution of FORTRAN Jobs

242 A job can be submitted interactively or in batch mode. Batch mode allows the user  
243 to log out of the system while the job continues to run in the background. The job  
244 could consist of a shell script (e.g. `job.sh`) or it may simply be a compiled FORTRAN  
245 binary file. The advantage of a shell script is that it can do other things before and  
246 after calling the compiled FORTRAN object.

247 An example script file (`job.sh`) is

```
248 ./FILENAME
```

```
249 R CMD BATCH FILENAME.R
```

```
250 mail -s "Job Complete" -r user@localhost
```

251 This would execute the compiled FORTRAN binary called `FILENAME`, run an R  
252 script which may do plots, then email the user on completion.

253

254 **Batch Mode – Submit Immediately:** Use Linux command `nohup`, e.g.

255

```
256 nohup batch.sh &
```

257

258 The ampersand at the end of the line frees the terminal after executing the  
259 command. In the above usage, any diagnostic output, including that which  
260 would normally be written to unit 6, will be written to `FILENAME.prt`.

261 To write the output to a file with a specific name, e.g. `program.prt`, run:

262

```
263 nohup batch.sh > program.prt &
```

264

265       **Batch Mode – Submit Later:** Use Linux command `at`, e.g. To execute a shell  
266       script called `batch.sh` at 21:06 on 08Nov, run the following in an XTERM  
267       within the program directory containing `batch.sh`:

268  
269       `at -f batch.sh -t 11082106`

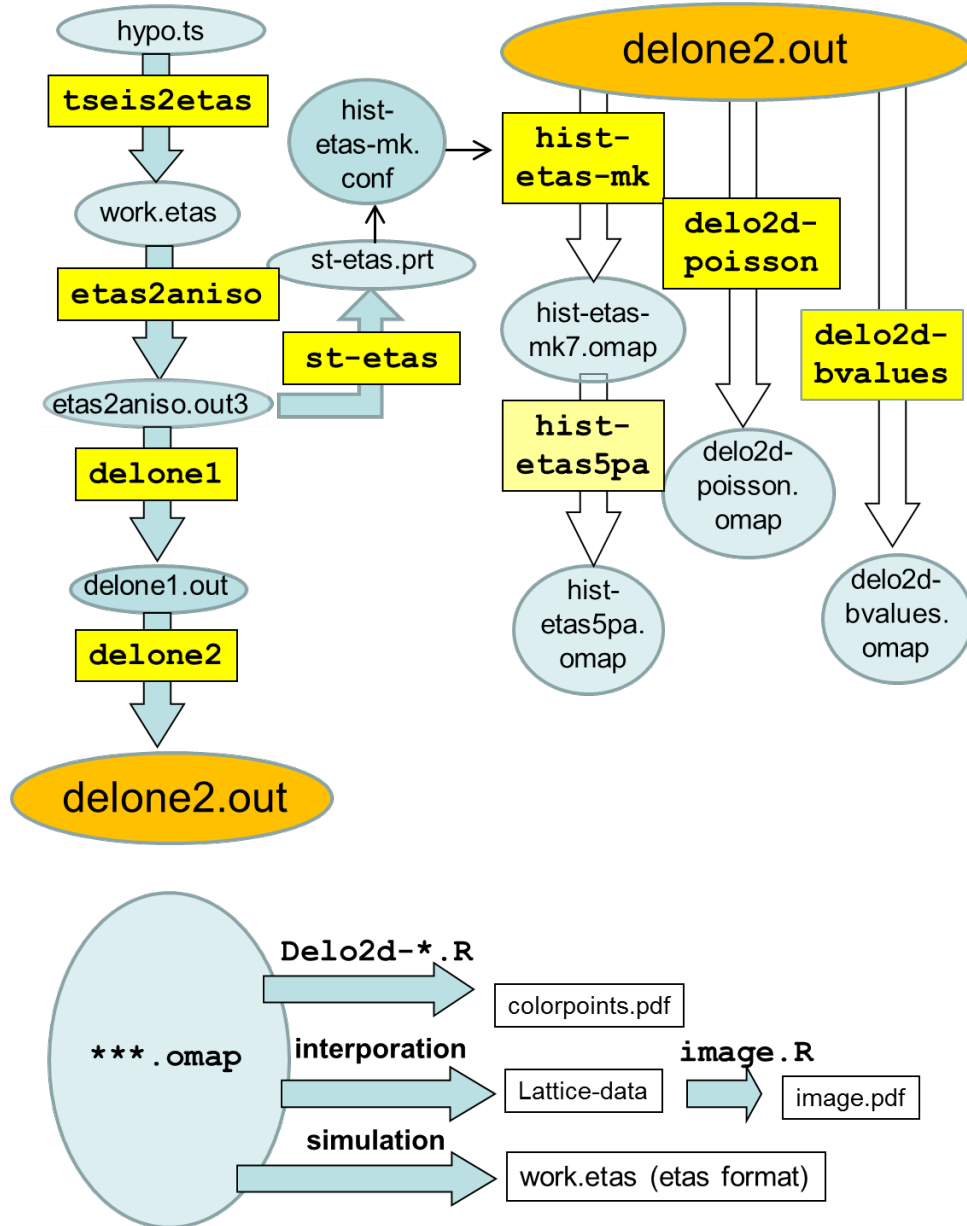
270  
271       The command `atq` lists jobs in the queue, and `atrm` removes jobs from the queue.  
272       More details about each can be found on the manual page (`man at`). Alternatively, jobs  
273       can be set up to run at regular time intervals by using `chron`.

274  
275

276  
277  
278  
279  
280  
281

## Part II. PARAMETER ESTIMATION FOR EACH MODEL

The programs documented in this part are not used independently of the each other. They will generally need to be executed in a certain order, as the outputs from some of the programs are required for the execution of other programs. A flowchart in **Figure 1** gives a summary of the output from each that is required in other programs.



282  
283  
284  
285  
286  
287

Fig. 1. The diagram shows the flow of output from each program to subsequent programs. Rectangular shapes represent programs, which are explained below. Elliptical shapes represent input/output files. The simulation components are given in Part V ( § 14 - § 16).

### 288 3 Formatting of the ETAS data from hypocenter catalog (tseis2etas)

289 Initially the earthquake catalog data are transformed into what we call an “etas”  
290 format. This format is more convenient for the use with the subsequent Fortran model  
291 fitting programs. Both input and output allow free format reading in our programs and  
292 several initial records at the beginning are shown. All the used files in this section are  
293 selected in the program directory of `Section3files/` in the package.  
294

#### 295 3.1 File Names

296  
297 Program: `tseis2etas.f`  
298 Object: `tseis2etas`  
299 input: `hypo.ts`  
300 output: `work.etas`  
301

#### 302 3.2 Program Execution

303 `./tseis2etas < hypo.ts`  
304

305 The file `hypo.ts` contains the earthquake catalog, and is assumed to have the  
306 following format.

```
307 1973 01 01 00 00 0.00 140.8700 33.4700 56.00 -9.5  
308 1973 01 05 05 31 5.80 140.8700 33.4700 56.00 4.5  
309 1973 01 05 11 48 37.50 140.9100 33.1600 33.00 3.9  
310 1973 01 06 10 21 16.30 140.8500 33.4900 33.00 4.2  
311 1973 01 06 11 21 54.70 140.9300 33.2700 46.00 4.5  
312 1973 01 06 14 55 52.80 140.7100 33.1500 61.00 4.7  
313 1973 01 09 02 21 14.80 141.6900 37.8100 59.00 3.5
```

314

<< omitted the middle.>>

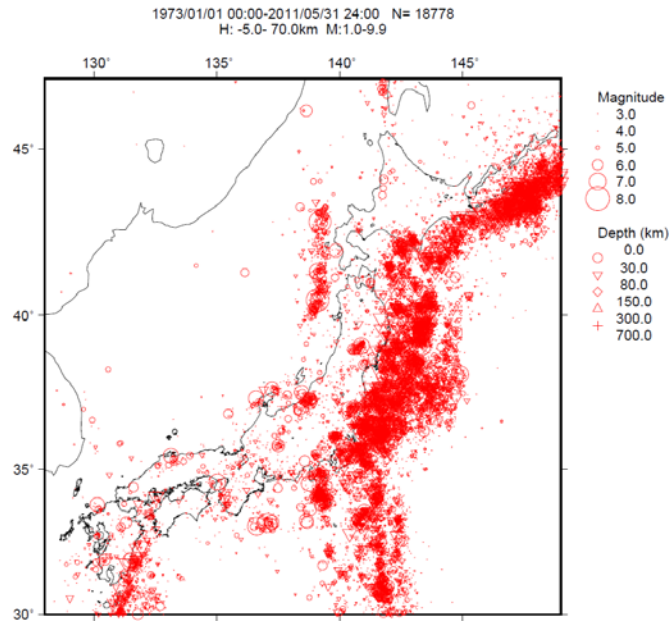
```
316 2011 05 30 00 05 39.30 142.6400 36.6200 32.00 4.9  
317 2011 05 30 01 04 36.02 142.7100 36.5400 6.00 4.8  
318 2011 05 30 19 36 42.25 140.8000 36.4200 49.00 4.9  
319 2011 05 30 23 53 44.79 143.2300 40.3400 32.00 4.9  
320 2011 05 31 07 50 16.83 140.8400 36.5100 42.00 4.6  
321 2011 05 31 11 26 50.06 141.2400 37.4900 20.00 4.7  
322 2011 05 31 12 28 36.09 141.9300 39.4000 40.00 5.6  
323 2011 05 31 16 26 12.41 143.2000 40.2500 38.00 4.9  
324 2011 05 31 17 14 0.38 146.5900 36.5900 14.00 4.8  
325 2011 05 31 23 53 59.18 142.1800 38.6000 59.00 4.7
```

326

327 Columns in the order from left to right are year, month, day, hour, minute, second,  
328 longitude (deg.), latitude (deg.), depth (km) and magnitude. The first record defines  
329 the beginning of the observation period, and the very small (negative) magnitude  
330 indicates that it is a non-event. The very small magnitude ensures that it has no effect  
331 in the analyses.

332 If you want make an aftershock analysis, the first row above starts with the main  
333 shock hypocenter.

334 The present data is shown in Figure 2.



336

337

338 Fig. 2. All detected earthquake by the JMA catalog, drawn by TSEIS visualization program  
339 package (Tsuruoka, 1996)

340

341 We recommend using all detected earthquakes to identify anisotropic clusters using  
342 `etas2aniso` program in the next section. Then, the corresponding `work.etas`  
343 comes as follows.

344

345 `formatted_for_etas`

346	1	140.87000	33.47000	-9.50	0.0000000	-56.00	1973	1	1
347	2	140.87000	33.47000	4.50	4.2299282	-56.00	1973	1	5
348	3	140.91000	33.16000	3.90	4.4921007	-33.00	1973	1	5
349	4	140.85000	33.49000	4.20	5.4314387	-33.00	1973	1	6
350	5	140.93000	33.27000	4.50	5.4735498	-46.00	1973	1	6
351	6	140.71000	33.15000	4.70	5.6221389	-61.00	1973	1	6
352	7	141.69000	37.81000	3.50	8.0980880	-59.00	1973	1	9
353	8	137.36000	36.84000	4.40	9.5782477	-33.00	1973	1	10
354	9	140.98000	33.11000	3.90	11.3227303	-20.00	1973	1	12
355	10	141.06000	33.28000	3.90	12.0151331	-40.00	1973	1	13

356

&lt;&lt; omitted the rest &gt;&gt;

357

358 Columns in order from left to right, are: event numbers, longitude (deg.), latitude  
359 (deg.), magnitude, time in days from the starting observation time, depth (negative  
360 km), and calendar date in year, month and day. Note that the first record is a  
361 comment.

362

#### 363 4 Identify Anisotropic Clusters of Events (`etas2aniso`)

364

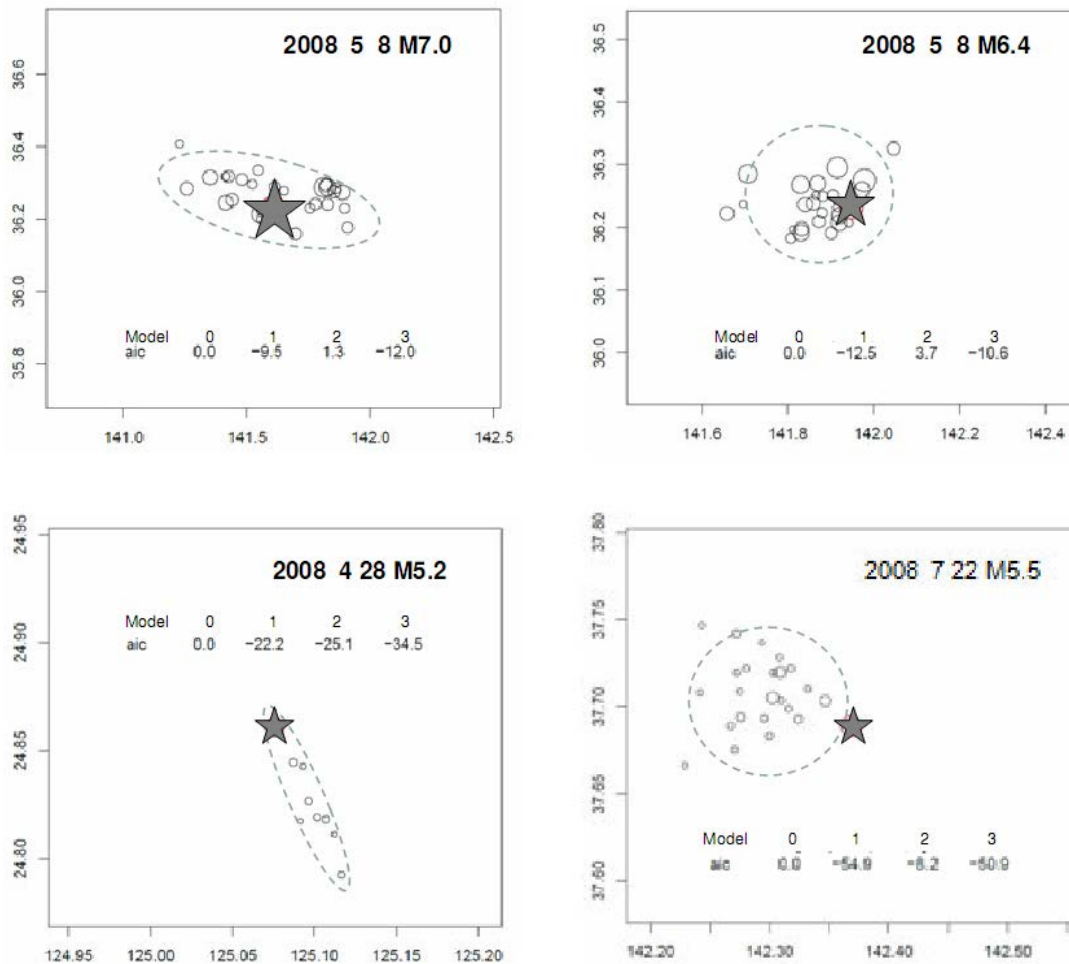
365 Before fitting the space-time models, we compile a dataset with a similar solution  
366 (but restricted on the 2-dimensional space) as the so-called centroid Moment tensor  
367 solution (Dziewonski *et al.*1981) using early aftershocks activity. This program first  
selects the large earthquakes and then selects their immediate aftershocks during a

368 certain time span. This is achieved using a fixed space window centered at each large  
369 earthquake.

370 For each such aftershock sequence, the normalized ellipsoidal coefficients (the  
371 variances and correlations of a fitted ellipse) are calculated as shown Figure 3. A new  
372 catalogue is printed containing the original earthquake origin values together with the  
373 two variances and rotation angle, written with each identified main shock. These  
374 additional data are used to fit the anisotropic space-time ETAS model (see §5). All the  
375 used files in this section are selected in the program directory of Section4files/ in  
376 the program package.

377 For more details, see §A.1.

378



379

380 Fig. 3. Examples of identified non-anisotropies.

381

382

### 383 4.1 File Names

384

385 Program: etas2aniso.f

386

Object: etas2aniso

387

Configuration: etas2aniso.conf (including work.etas as an input) writes:

388

389 `etas2aniso.out2:`  
 390 contains lists of immediate aftershocks that are triggered by large earthquakes,  
 391 specified magnitude threshold and a time span described in `etas2aniso.conf`,  
 392 together with results of best selected case of anisotropy analysis by the smallest AIC  
 393 value.  
 394 `etas2aniso.out3:`  
 395 contains the centroid locations and normalized ellipsoidal coefficients for all event  
 396 with magnitude not less than the cutoff magnitude.  
 397 `etas2aniso.out4:`  
 398 summarises changed data with either centroid coordinates or anisotropy matrix.  
 399 `etas2aniso.out8:`  
 400 summarises changed data of the identified earthquakes.  
 401 `etas2aniso.out9:`  
 402 contains the centroid locations of immediate aftershocks of large events with their  
 403 normalized ellipsoidal coefficients.  
 404

405 The input data are included in a file whose name is specified in the configuration  
 406 file (see below). Note that the first event in the input data file is a “no event”. Its time,  
 407 usually zero, indicates to the program the start of the analysis interval. A negative  
 408 magnitude will ensure that it has no effect.  
 409

## 410 4.2 Configuration File Format

411 The configuration (or initialisation) file is called `etas2aniso.conf` and has a  
 412 format as in the following example.

```
413
414 ./work.etas !input data
415 6.5 6.0 !clms cutm
416 1.0 !xxx(day)= time span for analyzing centroid and anisotropy
417
```

418 The first line is the name of the data file, here `work.etas`. Here it is recommended  
 419 to use all detected earthquakes without any magnitude cutoff. In the second line, the  
 420 number “6.5” is the smallest magnitude (`clsm` in the FORTRAN program) of  
 421 earthquake to analyse its cluster of triggering earthquakes that were followed within a  
 422 certain time span and certain range of neighborhood (may be called as aftershocks).  
 423 And “6.0” is used to set the cutoff magnitude (`cutm` in the FORTRAN program) of the  
 424 output (`etas2aniso.out3`) for a homogeneous data. It is read in using free  
 425 format.

426 The third line, “1.0” determines the time window in days for each cluster, here we  
 427 set one day or less time span in the case where we have a larger earthquake within the  
 428 considered space window. The time window can be longer in the low detected region  
 429 or during old period. On the other hand, from a real time forecasting perspective, one  
 430 may set  $1/24 = 0.04167$  day = one hour “to quickly determine the centroid location  
 431 and orientation characteristics of the impending aftershock sequence after a main  
 432 shock event. For the recent catalog, events within one-hour interval after the main  
 433 shock will be sufficient to give a reasonably good estimate of the centroid and  
 434 orientation characteristics of the evolving aftershock sequence.

435 If you want to use the original epicenters and isotropic clustering for all  
 436 earthquakes in the original catalog, you can take either a very large magnitude  
 437 `clsm=9.9` or a very small time span `xxx = 0.00001` in `etas2aniso.conf`.

### 438 4.3 Executing the Program

439 The current program directory must contain the configuration file  
 440 `etas2aniso.conf` and the data file, whose name is specified on the first line of  
 441 `etas2aniso.conf`. Other values in the configuration file must be specified by the  
 442 user.

443 The program code can then be run by executing the following shell script, after  
 444 editing the program directory location of the compiled object file called  
 445 `etas2aniso`.

```
446
447 ./etas2aniso | tee etas2aniso.prt
448
```

449 After execution, the current program directory will contain the following  
 450 additional files: `etas2aniso.out2`, `etas2aniso.out3`, `etas2aniso.out4`,  
 451 `etas2aniso.out8`, and `etas2aniso.out9`. Some of these are required by  
 452 programs documented in the following sections.  
 453

454 Example of output of `etas2aniso.prt` is omitted here.

455

456 Example of output of `etas2aniso.out3`

457

```
458 310 0.128E+03 0.149E+03 0.206E+02 0.300E+02 0.470E+02 0.170E+02
459 176 146.06919 42.94649 7.70 167.16323 1.00000 1.00000 0.00000
460 205 146.04000 42.71000 6.00 167.85969 1.00000 1.00000 0.00000
461 263 146.65053 43.15368 7.10 174.11349 1.00000 1.00000 0.00000
462 297 146.56000 43.17000 6.60 176.93889 1.00000 1.00000 0.00000
463 370 146.43000 43.45000 6.00 220.44753 1.00000 1.00000 0.00000
464
465 << omitted the middle >>
466 13914 141.71029 36.17382 6.90 12910.69813 0.18635 0.13324 -0.48998
467 14039 140.88000 39.03000 6.90 12947.98872 0.07126 0.11156 0.77508
468 14210 142.50500 37.48250 7.00 12983.11075 1.00000 1.00000 0.00000
469 14232 142.05000 37.19000 6.00 12985.47951 1.00000 1.00000 0.00000
470 14331 144.05375 41.75250 6.80 13037.01448 0.15116 0.07155 -0.68744
471 << omitted the rest >>
```

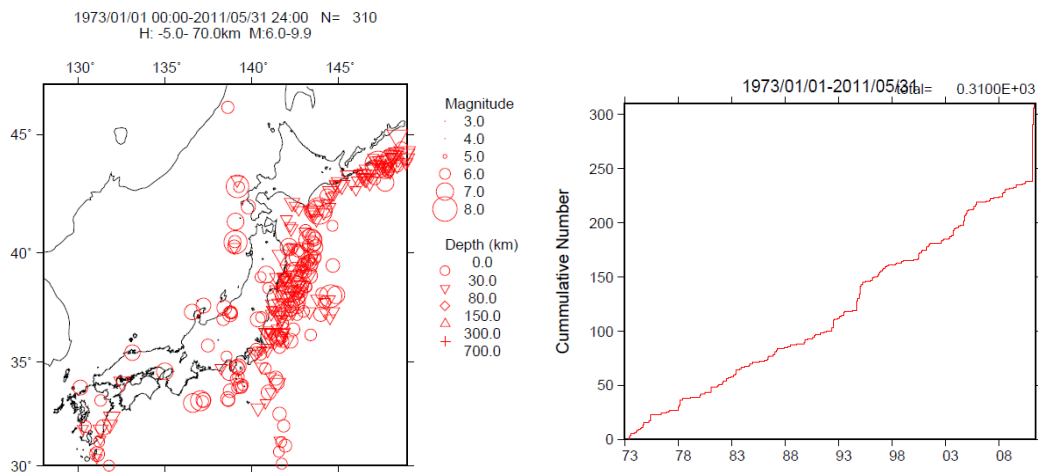
471

472 The first row record represents number of  $M \geq 6$  earthquakes, `minlong`, `maxlong`,  
 473 `maxlong-minlong`, `minlat`, `maxlat`, `maxlat-minlat`. The following records  
 474 represent earthquake number, longitudes, latitudes, magnitudes, occurrence times in days; the  
 475 last three columns represent the estimate of  $\sigma_1$ ,  $\sigma_2$  and  $\rho$  (correlation coefficients) for  
 476 modified epicenters of the centroid type. Relevantly, some of the epicenters are also modified  
 477 from the routine epicenters as shown in `etas2aniso.out4`.

478

479 The above output data are partially illustrated following in Figure 4.

480



481  
482  
483  
484

Fig. 4.  $M \geq 6.0$  earthquake by the JMA catalog

## 485 5 Spatial ETAS with All Parameters Constant (st-etlas)

486 This program fits various versions of the space-time ETAS model. It contains two  
487 main classes of model. The first class is where the function in (§A.5) that determines  
488 the spatial triggering component of the intensity function is assumed to be isotropic.  
489 The second class is where it is assumed to be anisotropic. The program does not  
490 estimate the anisotropy parameters, but uses those values calculated by the program  
491 described in §4. All the used files in this section are selected in the program directory  
492 of `Section5files/` in the program package.

493 Within each class, there are 4 possible models. In the program, the isotropic  
494 versions of these models are referred to as models 5–8, and their anisotropic  
495 counterpart as 15–18, respectively. The intensity functions of these models are  
496 defined by Ogata and Zhuang (2006), Equations 5–7, and 10, respectively. The matrix  
497  $S_j$  in those equations is a  $2 \times 2$  positive definite matrix. In the isotropic case, it will  
498 simply be the identity matrix. In the anisotropic case, its elements will contain those  
499 values estimated by the program in §4. Further mathematical details can be found in  
500 §A.5.1.

501

### 502 5.1 File Names

503 For the estimation phase, done in FORTRAN:

504

505 Program: `st-etlas.f`

506

Object: `st-etlas`

507

Configuration: `st-etlas.conf` (see §5.2)

508

Write outputs: `st-etlas.prt`

509

510

## 511 5.2 Configuration File Format

512 The configuration file is called `st-etas.conf` and has a format as in the  
513 following example. Note the symbol “→” below indicates that the record has been  
514 split in this document, and the symbol is not part of the configuration file.config.

```
515  
516 etas2aniso.out3          !hypodata  
517 7                        !nfunct  
518 21.0 17.0 14012.0 310    !tx,ty,tz,nn  
519 128.0 30.0 6.0 0.0 0.0 730.0 2.0 !xmin,ymin,xmg0,zmin,xmg1,tstar,bi2  
520 7                        !n=# of parameters  
521 0.95428E-06 0.40231E-02 0.12529E-02 0.11723E+01 0.94533E+00 →  
522 0.11215E-04 0.13821E+01      !μ0,K0,c,α,p,d,q  
523 7                          !ipr  
524
```

525 The numbers are read in as free format and have the following interpretation.

526 **Line 1:** Name of data file.

527 **Line 2:** Indicates the required space-time model. Valid values are: 5, 6, 7, 8, 15, 16,  
528 17, or 18. *Warning: The software has only been tested for cases 7 and 17, and*  
529 *others may be unstable.*

530 **Line 3:** Longitude region width (`tx` degrees), latitude region width (`ty` degrees),  
531 upper time boundary (`tz` days), and number (`nn`) of data points.

532 **Line 4:** Minimum longitude (`xmin` degrees), minimum latitude (`ymin` degrees),  
533 threshold magnitude (`xmg0`), minimum time (`zmin`), another magnitude (`xmg1`,  
534 currently not used), and starting time (`tstar` day). Parameter `bi2` is a  
535 multiplier used with the “*Utsu Spatial Distance (USD)*” defined explicitly in  
536 Appendix A5 (§A.5). The `bi2` is infinity (very large) in exact log-likelihood  
537 calculation, and this enables an approximation to shorten the computation time  
538 to have good initial ETAS parameter values. The *USD* is the width of a square,  
539 centred on the main shock, within which it is assumed that most of the  
540 aftershocks associated with the given main shock will occur. This assumption  
541 considerably lessens required calculations because the intensity at the location  
542 of subsequent events will only be affected by historical events if the given event  
543 is contained within the Utsu squares associated with the historical events.

544 **Line 5:** Number of initial model parameters listed on line 6.

545 **Line 6:** Initial parameter estimates.

546 **Line 7:** If `ipr = 7`, additional output is printed for the linear search procedure, and  
547 not printed if `ipr=0`

548

## 549 5.3 Executing the Program

550 The current program directory must contain `st-etas.conf` and the data file. The  
551 required data file is `etas2aniso.out3` which is one of the outputs from  
552 `etas2aniso`. See Appendix A.1 for some detail.

553 Appropriate initial parameter values must be edited into the configuration file by  
554 the user.

555 The job is executed by running the following execution command.

```

556
557 ./st-etas | tee st-etas.prt
558
559 Note that the number of events stated in st-etas.conf is the number of events in
560 etas2aniso.out3.
561
562 An example of the st-etas.prt is as follows:
563
564 ./etas2aniso.out3
565      17
566      21.      17.      14012.      310
567      128.0      30.0      6.0      0.0      0.0      730.0      2.0
568 data set      310 0.128E+03 0.149E+03 0.206E+02 0.300
569 input device      10
570 nn=      310
571 nfunct=      17
572 0tx,ty,tz,xmin,ymin,xmg0,xmg1,zmin,tsta
573 16.435 17.000 14012.000 128.000 30.000 6.000 0.000 0.000 →
574 0.000
575 nn = 310 nnc = 294
576 bi2 2.0000000000000000
577 jmax 67
578 tstar,nstar 730.00000000000000 16
579 0 input data
580 n= 7 itr=
581 0x= 0.95428E-06 0.40231E-02 0.12529E-02 0.11723E+01 0.94533E+00
582 0x= 0.11215E-04 0.13821E+01
583 linear ipr 7
584 - log likelihood = 0.153377032136182D+04 aic = 3081.5
585 lambda = 0.5000000000D+00 e2 = 0.1000000000000000D+31
586 lambda = 0.5000000000D-01 e4 = 0.1000000000000000D+31
587 lambda = 0.5000000000D-02 e4 = 0.1000000000000000D+31
588 lambda = 0.5000000000D-03 e4 = 0.1000000000000000D+31
589 lambda = 0.5000000000D-04 e4 = 0.10665559805887825D+06
590 lambda = 0.5000000000D-05 e4 = 0.28818211711226591D+04
591 lambda = 0.5000000000D-06 e4 = 0.11629651734330857D+04
592 lambda = 0.1900108183D-05 e5 = 0.17130527321761620D+04
593 lambda = 0.8710402217D-06 e6 = 0.13234771092168321D+04
594 lmbd = 0.5000000D-06 -ll = 0.132347710921683D+04 -0.24D+11 0.24D+11
595 lambda = 0.5000000000D-06 e2 = 0.11421402460408272D+04
596 lambda = 0.1000000000D-05 e3 = 0.11725055350543980D+04
597 lambda = 0.4534072998D-06 e5 = 0.11419671670520129D+04
598 lambda = 0.4581397976D-06 e6 = 0.11419644849252979D+04
599 lmbd = 0.4581398D-06 -ll = 0.114196448492530D+04 -0.97D+08 0.11D+09
600 << skipped >>
601 lambda = 0.2089781397D+01 e6 = 0.84830056255183285D+03
602 lmbd = 0.1393188D+01 -ll = 0.848300562551833D+03 -0.81D-15 0.15D-08
603 lambda = 0.1393187600D+01 e2 = 0.84830030469372718D+03
604 lambda = 0.2786375200D+01 e3 = 0.84830056255183172D+03
605 lambda = 0.1393187594D+01 e5 = 0.84830056255183490D+03
606 lambda = 0.2089781396D+01 e6 = 0.84830056255183433D+03
607 lmbd = 0.1393188D+01 -ll = 0.848300562551834D+03 -0.12D-15 0.23D-09
608 - log likelihood = 0.848300562551825D+03 aic = 1710.6
609 0----- x -----
610 -0.54093D-03 0.14630D+00 0.42172D-01 0.10343D+01 0.93246D+00 0.13550D+00 →
611 0.12333D+01
612 0*** gradient ***
613 -0.59377D-05 0.22362D-06 -0.32350D-06 0.26929D-07 -0.13557D-06 -0.18250D-06 →
614 0.10456D-06

```

```

615
616     mle = 0.29261E-06 0.21404E-01 0.17785E-02 0.10697E+01 0.86948E+00 →
617         0.18359E-01 0.15210E+01
618

```

619 The last 7 numbers are the MLEs of  $\mu$ ,  $K_0$ ,  $c$ ,  $\alpha$ ,  $p$ ,  $d$  and  $q$  of a space-time ETAS  
620 model, which will be used (copy & pasted) for the reference parameters in  
621 `hist-etas-mk.conf` in §9.2.  
622

## 623 5.4 Additional Advice

624 When the background rates in space are far from homogeneous, the MLE above  
625 may not converge well. In that case, firstly, set about a half of the average earthquake  
626 occurrence rate per unit time and unit area, say, for an initial estimate of the  $\mu$   
627 parameter as the case of the above; and set its gradient for the  $\mu$  parameter being  
628 always zero. Then, program `st-etas` implements the stable optimization for the  
629 other parameters than with the unfixed  $\mu$  parameter. This is implemented by  
630 additionally setting 1 in the 8th line in `st-etas.conf` as follows:

```

631
632 etas2aniso.out3           !hypodata
633 7                         !nfunc
634 21.0 17.0 14012.0 310     !tx,ty,tz,nn
635 128.0 30.0 6.0 0.0 0.0 730.0 2.0 !xmin,ymin,xmg0,zmin,xmg1,tstar,bi2
636 7                         !n=# of parameters
637 0.95428E-06 0.40231E-02 0.12529E-02 0.11723E+01 0.94533E+00 →
638 0.11215E-04 0.13821E+01     !  $\mu_0, K_0, c, \alpha, p, d, q$ 
639 7                         !ipr
640 1                         ! optimization by fixing  $\mu$ -parameter
641

```

642 and then run the program `st-etas`.

643 Having done that, use the above estimated  $\mu$ ,  $K_0$ ,  $c$ ,  $\alpha$ ,  $p$ ,  $d$  and  $q$  for initial  
644 estimates without the 8th line, again to run `st-etas` by the unfixed 7 parameters  
645 could lead an eventually stable MLE. This is implemented by setting the value other  
646 than 1 (say, 0 or nothing) in the 8th line in `st-etas.conf`.  
647  
648

## 649 6 Delaunay Tessellation for Spatial Variation (`delone1`, `delone2`)

650 This section describes a group of programs that are used to perform a Delaunay  
651 tessellation of the two-dimensional spatial coordinates. This tessellation is used by  
652 subsequent programs to provide spatial estimates of some or all of the ETAS  
653 parameters.

654 The first FORTRAN program (`delone1.f`) performs a Delaunay tessellation. It  
655 initially augments the spatial locations of the points closest to the boundary with the  
656 location of their mirror image in the boundary. The second (`delone2.f`) treats the  
657 locations where the triangle lines cross the observation region boundary as a new  
658 point, and excludes the mirror image added by `delone1.f`. Together with the  
659 original observed locations and these boundary points, it repeats the Delaunay  
660 tessellation, and then outputs the determined triangles in a satisfactory format so that

661 the R program `delone2.R` can be used to plot all of the triangles. This output is also  
662 used by programs for estimation where one or more parameters are assumed to vary in  
663 space. All the used files in this section are selected in the program directory of  
664 `Section6files/` in the program package.

665 Further mathematical detail can be found in §A.2.

666

667

## 668 6.1 File Names to Perform Delaunay Tessellation

669

670 Program: `delone1.f`

671 Object: `delone1`

672 Configuration: `delone1.conf`

673 Reads: `etas2aniso.out3`

674 Writes: `delone1.out`

675

## 676 6.2 Configuration File Format

677 An example of a configuration file follows.

```
678 1.00E-15      ! for EPS
679 1000 7000     ! for NEF0, NRG0
680 128.0 30.0   ! for xmin, ymin
681 21. 17.      ! for BXLX, BXLX
682 310          ! for NP (e.g., number of earthquakes)
```

683

684 Parameters are read as free format. The above parameters are fragile for successful  
685 computation; see §6.4 to check. The error bound is already very small and can be  
686 larger, which makes the computation faster in the case where the number of  
687 (earthquake) data points `NP` is very large. A rough rule of thumb is that `NEF0` should  
688 be approximately 0.8 times the number of data points `NP`, and `NRG0` should be larger,  
689 especially in the case where points are highly clustered. Note that “21.” for `BXLX` is  
690 the width of the analysis region (degrees longitude), “17.” for `BXLX` is the height of  
691 the analysis region (degrees latitude), “310” for `NP` is the number of points, “128” for  
692 `xmin` is the western boundary (longitude), and “30” for `ymin` is the southern  
693 boundary (latitude). In western hemisphere `xmin` should be positive taking between  
694 180 and 360 degrees, and in the southern hemisphere `ymin` is negative, taking values  
695 between -90 and 0 degrees.

696

## 697 6.3 Executing Delaunay Tessellation Program

698 The required data are contained in `etas2aniso.out3`. The source code  
699 `delone1.f` requires the configuration file (i.e. `delone1.conf`).

700

```
701 ./delone1 |tee delone1.prt
```

702

703 Running this job, we get the following output file (delone1.prt):

```
704
705 0      ***** input parameters *****
706      iperio=      0      np      =      0
707      dens =      1.00000      eps=      0.10000E-14
708      nef0 =      1000      nrg0 =      7000
709      nclx1 =      3      ncly1 =      3
710      ilist =      1      ifile =      0
711      incard=      1      idpat =      1
712
713      32  149.000000000000      44.0300000000000
714      302 131.780000000000      30.0000000000000
715      np      308
716      *** input coordinates ***
717      np= 308 idpat= 1 bxlx,bxly= 21.00000
718 17.00000 dens= 0.86835
719 0*** detailed outputs ***
720
721                                     << skipped >>.
722
723      ***** result of voronoi division *****
724      idpat np bxlx bxly brasq sum of pol.ar. box area
725      1 308 21.0000 17.0000 50.820 3.57000000E+02 3.57000000E+02
726      number of delaunay triangle = 618
727
728
729 Note here that the number of earthquakes in etas2aniso.conf (NP=310) is
730 reduced to 308 because the two earthquakes on the rectangular boundary are removed
731 in the computation.
732
733 In particular, in the second to last line on the right-hand side are values of “sum
734 of pol.ar.” and “box area”. The values for these should be the same if the
735 Delaunay tessellation is correct. If they are not, then the values of NEF0 and NRG0 in
736 the configuration file delone1.conf may need adjusting.
737
738
739 Another output file delone1.out to be used for the next subsection writes as
740 follows:
741
742
743      308 21.00000 17.00000 128.00000 30.00000
744      1 18.06954167 12.94617946 7.70000 167.16323 1.0000 1.0000 0.0000
745      2 18.03999678 12.70995838 6.00000 167.85969 1.0000 1.0000 0.0000
746      3 18.65051057 13.15371107 7.10000 174.11349 1.0000 1.0000 0.0000
747      4 18.56019533 13.17001224 6.60000 176.93889 1.0000 1.0000 0.0000
748      5 18.43048317 13.45037851 6.00000 220.44753 1.0000 1.0000 0.0000
749
750                                     << skipped >>
751
752      306 14.86989084 9.09956961 6.00000 13991.42554 1.0000 1.0000 0.0000
753      307 16.06046994 8.16971916 6.10000 14003.62383 1.0000 1.0000 0.0000
754      308 13.33026396 7.40966455 6.10000 14011.98325 1.0000 1.0000 0.0000
755      1 1 182 207 3
756      2 1 2 207 3
757      3 1 2 4 3
758      4 1 4 182 3
759      5 2 207 208 3
760      6 2 174 208 3
761
762                                     << skipped >>
763
764      614 274 280 306 3
```

```

755      615      275      280      306      3
756      616      275      282      306      3
757      617      275      276      282      3
758      618      275      276      280      3
759

```

760 The first line contains the number of earthquakes (NP), lengths of longitude (bxlx)  
761 and latitude (bxly) spans, the origin longitude and latitude of the rectangular region,  
762 in the order from the left. Then, the following first block provides the same data as in  
763 `etas2aniso.out3`. Here the order of earthquakes is given in the first column up to  
764 the number NP=308. Also note here that the number of earthquakes in  
765 `etas2aniso.conf` (NP=310) is reduced to 308 because the two earthquakes on the  
766 rectangular boundary are removed in the computation. The second block lists the  
767 Delaunay triangles, numbered from 1 to 618 in the first column, vertex points, and  
768 the id-number of each triangle.

#### 769 6.4 Generation of the Map Data with Boundary Points

770 The files associated with generating map data are as follows.

```

771
772 Program: delone2.f
773 Object: delone2
774 Reads: delone1.out
775 Writes: delone2.out
776

```

777 The above FORTRAN code can be executed by running the following shell script  
778 within the current program directory.

```

779
780 ./delone2 |tee delone2.prt
781

```

782 An example of the `delone2.prt` is as follows:

```

783
784 ss= 356.9999999999999          tx*ty= 357.0000000000000
785          10
786          12
787

```

788 We can confirm the accuracy of the tessellation program by equality of the two  
789 calculated areas in the first line; where `ss` represents the sum of the Delaunay triangle  
790 areas and `tx*ty` represents the whole rectangular area. The second line is the largest  
791 number of following connected earthquakes by the Delaunay tessellation. The last line  
792 indicates the largest number of preceding and following connected earthquakes by the  
793 Delaunay tessellation. The Incomplete Cholesky Conjugate Gradient (ICCG) method,  
794 used later, requires that the maximum number of connected edge points of the  
795 Delaunay triangulation `kkmax` is 12, which is given in the last line of `delone2.out`,  
796 and the last line of `delone2.prt` in the above.

797  
798 An example of the `delone2.out` is as follows:

```

799
800      308      342      648      21.00000      17.00000
801      1 18.06954167 12.94617946      7.70 167.1632300      1.0000      1.0000      0.0000
802      2 18.03999678 12.70995838      6.00 167.8596900      1.0000      1.0000      0.0000

```

803	3	18.65051057	13.15371107	7.10	174.1134900	1.0000	1.0000	0.0000
804	4	18.56019533	13.17001224	6.60	176.9388900	1.0000	1.0000	0.0000
805	5	18.43048317	13.45037851	6.00	220.4475300	1.0000	1.0000	0.0000

806

<< skipped >>

807

808

809	221	8.70176461	7.25834122	6.70	12501.0291400	0.1139	0.0798	0.6972
810	222	10.55744694	7.48449001	6.60	12614.0509500	0.1070	0.0790	0.6728
811	223	14.02977645	8.50037863	6.10	12776.5865100	1.0000	1.0000	0.0000
812	224	13.53967847	6.18031260	6.20	12910.6680900	1.0000	1.0000	0.0000
813	225	13.75989075	6.15983542	6.10	12910.6782000	1.0000	1.0000	0.0000
814	226	13.71057900	6.17401699	6.90	12910.6981300	0.1863	0.1332	-0.4900
815	227	12.88007256	9.02951694	6.90	12947.9887200	0.0713	0.1116	0.7751
816	228	14.50513802	7.48206907	7.00	12983.1107500	1.0000	1.0000	0.0000
817	229	14.05029992	7.18993243	6.00	12985.4795100	1.0000	1.0000	0.0000
818	230	16.05360444	11.75244392	6.80	13037.0144800	0.1512	0.0716	-0.6874

819

<< skipped >>

820

821

822	305	12.30031094	5.60951590	6.20	13989.5673500	1.0000	1.0000	0.0000
823	306	14.86989084	9.09956961	6.00	13991.4255400	1.0000	1.0000	0.0000
824	307	16.06046994	8.16971916	6.10	14003.6238300	1.0000	1.0000	0.0000
825	308	13.33026396	7.40966455	6.10	14011.9832500	1.0000	1.0000	0.0000
826	309	0.00000000	0.00000000	0.00	0.00000000	0.0000	0.0000	0.0000
827	310	21.00000000	0.00000000	0.00	0.00000000	0.0000	0.0000	0.0000
828	311	21.00000000	17.00000000	0.00	0.00000000	0.0000	0.0000	0.0000

829

<< skipped >>

830

831

832	340	21.00000000	0.99002710	0.00	0.00000000	0.0000	0.0000	0.0000
833	341	21.00000000	7.05039114	0.00	0.00000000	0.0000	0.0000	0.0000
834	342	21.00000000	7.35957019	0.00	0.00000000	0.0000	0.0000	0.0000
835	1	1	182	207	0.796487629875D-01			
836	2	1	2	207	0.113149385584D+00			
837	3	1	2	4	0.546448113038D-01			
838	4	1	4	182	0.346708339754D-01			

839

<< skipped >>

840

841

842	645	275	280	306	0.132964341353D-01				
843	646	275	282	306	0.158110057792D-01				
844	647	275	276	282	0.302560585723D-01				
845	648	275	276	280	0.252603344595D-01				
846	1	4	2	4	182	207			
847	2	9	3	4	97	100	165	174	190
848	3	4	4	13	40	165			
849	4	4	13	75	159	182			
850	5	7	48	75	138	140	159	182	207
851	6	5	77	184	295	298	299		
852	7	8	52	99	188	189	191	206	220
853								232	

853

<< skipped >>

854

855

856	335	1	339	
857	336	0		
858	337	1	338	
859	338	0		
860	339	0		
861	340	1	341	
862	341	1	342	
863	342	0		
864	12			

865

866 The first record gives the number of earthquakes (NP), number of points Delaunay  
867 tessellation including those on boundaries, number of Delaunay triangles, and lengths  
868 of longitude (BXUP) and latitude (BYUP) spans, in the order from the left. Then, the  
869 first block provides the same data as st-etaz.out. Here the order of earthquakes  
870 are given in the first column up to the number NP=308. The second block of the index

871 numbers from NP=309 to 342 includes the Delaunay vertex points on the boundary of  
872 the rectangular region. The third block lists the Delaunay triangles numbered from 1  
873 to 648 in the first column, vertex points id-number of each triangle, and area of the  
874 triangle in the last column. The forth block indicates neighboring points connected by  
875 the sides of the triangle; the first record specifies the id-numbers of points, the second  
876 indicates the number of the connected points by the side of the triangles, and the rest  
877 of the columns show the id-numbers of the nearest points. The bottom raw number  
878 shows the largest numbers of the nearest points.

879 These provide necessary information to the Bayesian smoothing procedure,  
880 especially for the Hessian matrix and incomplete Cholesky conjugate gradient (ICCG)  
881 method: see Appendix B.2.

## 882 6.5 Plotting Delaunay Tessellations

883 The files associated with plotting the Delaunay tessellations using the R statistical  
884 language are as follows.

885  
886 Program: delone-plot.R  
887 Reads: delone2.out  
888 Writes: delone-plot.pdf  
889

890 The above R program can be executed by running R within the current program  
891 directory (Section6files), and executing the R function source to run the  
892 contents of the file interactively as:

893  
894 R  
895 > source('delone-plot.R')  
896

897 The plot will be written into the file delone-plot.pdf.

## 898 6.6 Example Output

899 An example of the Delaunay tessellation plot example data is shown in the  
900 following figure (Fig.5).

901

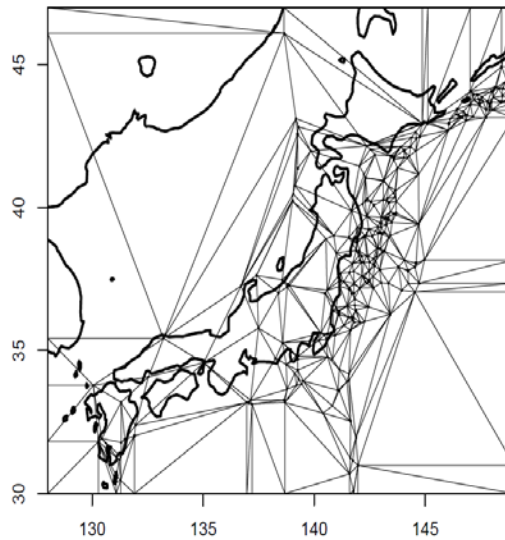


Fig. 5: Delaunay tessellation plot, delone-plot .pdf

## 7 Spatially Varying $b$ -Value of Magnitude Frequency ( $b$ -values)

These programs calculate and plot estimates of the  $b$ -value over a spatial region. The program calculates  $b$ -values at the nodes of the Delaunay tessellations (§6). Estimates at other spatial points can be made using the interpolation program. All the used files in this section are selected in the program directory of `Section7files/` in the program package. Further mathematical detail can be found in §A.4.

### 7.1 File Names

For the estimation phase, done in FORTRAN:

```

Program:      delo2d-bvalues.f
Object:      delo2d-bvalues
Configuration: delo2d-bvalues.conf
Reads:      delone2.out
Writes:      delo2d-bvalues.omap

```

For the spatial plot, done in R:

```

Program: delo2d-bvalues.R
Reads:  delone2.out, delo2d-bvalues.omap
Writes: delo2d-bvalues.pdf.

```

### 7.2 Configuration File Format

The configuration file `delo2d-bvalues.conf` includes the following three lines:

```

930
931 128.30.5.95 !xmin, ymin, threshmag = magnitude threshold
932 6.0d0      !w1 = initial weight of the penalty to be optimized.
933 7          ! ipr

```

934 containing the following records; the first line includes the origin of the considered  
935 region in longitude and latitude, and then magnitude threshold. The second line is an  
936 initial weight value for the penalty function. In the third line, if ipr = 7, more detailed  
937 output about the linear search procedure is given, and is not given if ipr = 1.  
938 Parameters are read as free format.

939  
940 **Magnitude rounding issue:** if magnitude data are rounded to 0.1 units, the  
941 threshold magnitude here should be modified to 5.95 (=  $Mc - 0.05$ ) to avoid the  
942 *b*-value MLE bias. This is because a rounded value of 6.0 may have been as small as  
943 5.95 or large as 6.05. This applies to the traditional catalogs such as the JMA,  
944 NEIC-PDE, and ISC catalog. Otherwise, namely, less than 0.01 magnitude unit, we  
945 can keep threshmag = 6.0.

### 946 7.3 Program Execution

947  
948 FORTRAN execution command:

```

949
950 ./delo2d-bvalues |tee delo2d-bvalues.prt
951

```

952 The contents of delo2d-bvalues.prt includes the calculation processes as  
953 follows:

```

954
955 xmin,ymin,threshmag= 128.00000000000000      30.00000000000000
956 5.9500000000000000
957 weight= 6.0000000000000000
958 linear ipr      7
959      308      342      648      21.00000000000000
960      17.0000000000000000
961 an = 1.0000000000000000
962 npex      342
963 w1,w2,w3 6.0000000000000000      0.0000000000000000E+000
964 0.0000000000000000E+000
965 ptdet = 0.1286030538956D+04
966 #1: w1 = 0.60000000D+01
967 penalized-log-likelihood = 0.463684636109451D+02
968 lambda2 = 0.5000000000D+00      e2 = 0.30828181796202939D+04
969 lambda4 = 0.5000000000D-01      e4 = 0.62135776017985577D+02
970 lambda4 = 0.5000000000D-02      e4 = 0.45023517036283550D+02
971 lambda5 = 0.1285750683D-01      e5 = 0.44224067911271810D+02
972 lambda6 = 0.1284875160D-01      e6 = 0.44224065397758963D+02
973 1      1 lambda = 0.1284875D-01      pell = 0.442240653977590D+02      0.33D+03
974 lambda2 = 0.1284875160D-01      e2 = 0.50878298842753544D+02
975 lambda4 = 0.1284875160D-02      e4 = 0.43818395118639856D+02
976 lambda5 = 0.2832311965D-02      e5 = 0.43645759409649770D+02
977 lambda6 = 0.2832374825D-02      e6 = 0.43645759408993605D+02
978 1      2 lambda = 0.2832375D-02      pell = 0.436457594089936D+02      0.41D+03
979 lambda2 = 0.2832374825D-02      e2 = 0.43616306798161546D+02
980 lambda3 = 0.5664749651D-02      e3 = 0.43586937733633853D+02
981 lambda3 = 0.1132949930D-01      e3 = 0.43528450272154494D+02
982 lambda3 = 0.2265899860D-01      e3 = 0.43412478220408836D+02
983 lambda3 = 0.4531799721D-01      e3 = 0.43184547213016458D+02

```

```

984   lambda3 = 0.9063599442D-01   e3 = 0.42744750536460081D+02
985   lambda3 = 0.1812719888D+00   e3 = 0.41929523194600279D+02
986   lambda3 = 0.3625439777D+00   e3 = 0.40557386459155495D+02
987   lambda3 = 0.7250879553D+00   e3 = 0.38853488561817301D+02
988   lambda3 = 0.1450175911D+01   e3 = 0.39668601393578882D+02
989   lambda5 = 0.9826636726D+00   e5 = 0.38493436628796665D+02
990   lambda6 = 0.9834376482D+00   e6 = 0.38493427204469839D+02
991   1      3 lambda = 0.9834376D+00   pell = 0.384934272044698D+02  0.49D+01
992   lambda2 = 0.9834376482D+00   e2 = 0.38489324810747796D+02
993   lambda3 = 0.1966875296D+01   e3 = 0.38493117194215735D+02
994   lambda5 = 0.1002746347D+01   e5 = 0.38489323394303419D+02
995   lambda6 = 0.1002091162D+01   e6 = 0.38489323392487314D+02
996   1      4 lambda = 0.1002091D+01   pell = 0.384893233924873D+02  0.67D-02
997   lambda2 = 0.1002091162D+01   e2 = 0.38489323390150034D+02
998   lambda3 = 0.2004182325D+01   e3 = 0.38489323392506961D+02
999   lambda5 = 0.9999924475D+00   e5 = 0.38489323390150027D+02
1000  lambda6 = 0.9992774566D+00   e6 = 0.38489323390150084D+02
1001  1      5 lambda = 0.9999924D+00   pell = 0.384893233901500D+02  0.18D-08
1002  penalized log likelihood = 0.384893233901500D+02
1003  #e: w1 = 0.60000000D+01
1004  abic = 0.8410057591D+02   -l == -0.2930057833D+03   pn = 0.1298666099D+04
1005  ----- xd -----   1.000000000000000   6.000000000000000   84.1005759128927

1006  << skipped >>

1007  w1,w2,w3  2.00974825755177   0.000000000000000E+000 →
1008  0.000000000000000E+000
1009  ptdet = 0.9130617889564D+03
1010  #1: w1 = 0.20097483D+01
1011  penalized-log-likelihood = 0.287800079161731D+02
1012  lambda2 = 0.5000000000D+00   e2 = 0.29546166935190861D+02
1013  lambda4 = 0.5000000000D-01   e4 = 0.28777011048782104D+02
1014  lambda5 = 0.3346968607D-01   e5 = 0.28776042319021148D+02
1015  lambda6 = 0.3346159299D-01   e6 = 0.28776042318756339D+02
1016  1      1 lambda = 0.3346159D-01   pell = 0.287760423187563D+02  0.24D+00
1017  lambda2 = 0.3346159299D-01   e2 = 0.28782452945428989D+02
1018  lambda4 = 0.3346159299D-02   e4 = 0.28775473430799885D+02
1019  lambda5 = 0.8752834473D-02   e5 = 0.28775122438782077D+02
1020  lambda6 = 0.8752857664D-02   e6 = 0.28775122438782141D+02
1021  1      2 lambda = 0.8752834D-02   pell = 0.287751224387821D+02  0.21D+00
1022  lambda2 = 0.8752834473D-02   e2 = 0.28775048199836448D+02
1023  lambda3 = 0.1750566895D-01   e3 = 0.28774974613552200D+02
1024  lambda3 = 0.3501133789D-01   e3 = 0.28774829398984622D+02
1025  lambda3 = 0.7002267579D-01   e3 = 0.28774546801964874D+02
1026  lambda3 = 0.1400453516D+00   e3 = 0.28774012937290273D+02
1027  lambda3 = 0.2800907031D+00   e3 = 0.28773070532623031D+02
1028  lambda3 = 0.5601814063D+00   e3 = 0.28771687079862836D+02
1029  lambda3 = 0.1120362813D+01   e3 = 0.28770926064465890D+02
1030  lambda3 = 0.2240725625D+01   e3 = 0.28777431321669166D+02
1031  lambda5 = 0.9995936669D+00   e5 = 0.28770863947998595D+02
1032  lambda6 = 0.9996405857D+00   e6 = 0.28770863947986673D+02
1033  1      3 lambda = 0.9996406D+00   pell = 0.287708639479867D+02  0.39D-02
1034  lambda2 = 0.9996405857D+00   e2 = 0.28770863945859837D+02
1035  lambda3 = 0.1999281171D+01   e3 = 0.28770863947983585D+02
1036  lambda5 = 0.100003763D+01   e5 = 0.28770863945859844D+02
1037  lambda6 = 0.9954337900D+00   e6 = 0.28770863945859880D+02
1038  1      4 lambda = 0.9996406D+00   pell = 0.287708639458598D+02  0.38D-08
1039  penalized log likelihood = 0.287708639458598D+02
1040  #e: w1 = 0.20097483D+01
1041  abic = 0.8153752949D+02   -l == -0.1162398678D+03   pn = 0.9425712218D+03
1042
1043  ----- xd -----   6.000000000000000   2.00974825755177 →
1044  81.5375294926255
1045  ##### iteration, f, epsilon = 6 0.81537529D+02 0.35904191D-03
1046  x = 0.13960189D+01
1047  0.20097E+01 0.81538E+02 342

```

1048

1049 The records including `lambd#` ('#' for a number) show linear search for the  
1050 minimum of the negative penalized log likelihood (`pell`), and the rows including  
1051 `pell` show the minimized value and the sum of squares of the gradient vector  
1052 components of the `pell` function with respect to the minimizing parameters.  
1053 Furthermore, the `abic` value is minimized with respect to a weight `w1`, assuming  
1054 isotropic smoothing constraint. The rows with “----- `xd` -----“ shows every step  
1055 where the minimum was updated by the simplex algorithm. The third to last rows  
1056 from the bottom starting at ##### show that the iterated simplex algorithm updated the  
1057 ABIC for 6 times with the minimum `abic` = 0.8153752949D+02 and the difference with the  
1058 previous smallest ABIC is 0.82721787D-04. This is attained by `w1` = 0.20097483D+01  
1059 (5th row from the bottom), and the bottom row shows its logarithm. See Appendix A  
1060 for the definitions and Appendix B for the numerical procedures.

1061

1062 The file `delo2d-bvalues.prt` includes a large volume of output. It may be  
1063 useful to use UNIX command `egrep` (`grep`) to restrict output to records of interest.  
1064 For example,

```
1065 egrep xd delo2d-bvalues.prt
```

1066 and

```
1067 egrep xd |abic delo2d-bvalues.prt
```

1068 shows you a series of only the updated smallest ABIC values and of all searched  
1069 ABIC values in the simplex minimization procedure, respectively.

1070

```
1071 ./delo2d-bvalues > delo2d-bvalues.omap
```

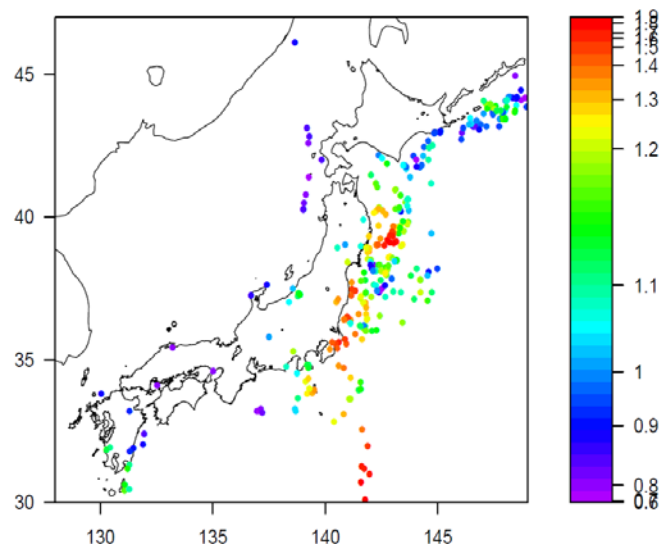
1072

```
1073 R
```

```
1074 > source('delo2d-bvalues.R')
```

1075

1076 The output shows Fig. 6.



1077

1078 Fig. 6. `bvalues.pdf`; colors are ordered in frequency-linearized scale.

1079

1080

## 1081 **8 Spatial Occurrence Rate (delo2d-poisson)**

1082 This program fits a nonhomogeneous spatial Poisson model with no time component  
1083 to the location of earthquakes. This is done by estimating the Poisson rates at the  
1084 nodes of the Delaunay tessellations (§6). All the used files in this section are selected  
1085 in the program directory of `Section8files/` in the program package. Further  
1086 mathematical detail can be found in §A.5.2.

1087

### 1088 **8.1 File Names**

1089 For the estimation phase, done in FORTRAN:

1090

1091 Program: `delo2d-poisson.f`

1092 Object: `delo2d-poisson`

1093 Configuration: `delo2d-poisson.conf`

1094 Reads: `delone2.out`

1095 Writes: `delo2d-poisson.omap`

1096

1097 For the spatial plot, done in R:

1098

1099 Program: `delo2d-poisson.R`

1100 Reads: `delone2.out`, `delo2d-poisson.omap`

1101 Writes: `delo2d-poisson.pdf`

1102

1103

### 1104 **8.2 Configuration File Format**

1105

1106 The configuration file `delo2d-poisson.conf` includes the following three lines:

1107

1108 `128. 30. 5.95 !xmin, ymin, threshmag = magnitude threshold`

1109 `6.0d0 !w1= initial weight of the penalty to be optimized.`

1110 `7 ! ipr`

1111

1112 containing the following records; the first line includes the origin of the considered  
1113 region in longitude and latitude, and then magnitude threshold. The second line is an  
1114 initial weight value for the penalty function. In the third line, if `ipr = 7`, more detailed  
1115 output about the linear search procedure is given, and is not given if `ipr = 0`.

1116 Parameters are read as free format.

1117

### 1118 **8.3 Program Execution**

1119

1120 FORTRAN execution command:

1121

```

1122  ./delo2d-poisson |tee delo2d-poisson.prt
1123
1124  The example of delo2d-poisson.prt includes the calculation processes as
1125  follows:
1126
1127      308      342      648      16.434778690338135      17.000000000000000 →
1128  0.95798319327731085
1129  an = 1.0000000000000000
1130  tx,ty 16.435 17.000 nn,np,npex,nd = 308 308 342 648
1131  ptdet = 0.1218006057961D+04
1132  #1: w1,w2,w3,w4 = 0.60000000D+01 0.60000000D+01 0.00000000D+00 0.10000000D+01
1133  wx,wy= 0.60000D+01wxx,wyy= 0.00000D+00 pell = 0.293388497473962D+03
1134  lambda = 0.5000000000D+00 e2 = 0.27484230578836838D+03
1135  lambda = 0.1000000000D+01 e3 = 0.26290412013045670D+03
1136  lambda = 0.2000000000D+01 e3 = 0.25722684413266461D+03
1137  lambda = 0.4000000000D+01 e3 = 0.31070799318271708D+03
1138  lambda = 0.1762692124D+01 e5 = 0.25648282432909440D+03
1139  lambda = 0.1745673777D+01 e6 = 0.25647816623906681D+03
1140  lambda = 0.1745674D+01 pell = 0.256478166239067D+03 -0.44D+02 0.27D+04
1141  cgres_0 31 2.51817502773355539E-009 5.18160438220919444E-013
1142  #iteration= 1
1143  cgres_0 35 8.16996669971836904E-010 4.73376310296145925E-013
1144  lambda = 0.1745673777D+01 e2 = 0.12575332143434689D+04
1145  lambda = 0.1745673777D+00 e4 = 0.18238027528344378D+03
1146  lambda = 0.4214208914D+00 e5 = 0.10619977032668238D+03
1147  lambda = 0.5037843862D+00 e6 = 0.89583483392868573D+02
1148  lambda = 0.5037844D+00 pell = 0.895834833928686D+02 -0.47D+03 0.17D+04
1149  cgres_0 31 1.96048463382195580E-010 4.13813896662551007E-013
1150  #iteration= 2
1151  cgres_0 31 3.02592639283617553E-010 7.26217704144932776E-013
1152  lambda = 0.5037843862D+00 e2 = 0.69744102731447668D+02
1153  lambda = 0.1007568772D+01 e3 = 0.63752199016021812D+02
1154  lambda = 0.2015137545D+01 e3 = 0.96660591021549394D+02
1155  lambda = 0.9574016612D+00 e5 = 0.63709613227398854D+02
1156  lambda = 0.9673758963D+00 e6 = 0.63706622422671018D+02
1157  lambda = 0.9673759D+00 pell = 0.637066224226710D+02 -0.53D+02 0.42D+03
1158  cgres_0 29 9.76411103241434597E-011 2.51836405349217590E-013
1159  #iteration= 3
1160  cgres_0 33 8.39914763820138480E-013 3.42533485175028649E-013
1161  lambda = 0.9673758963D+00 e2 = 0.63386328627224401D+02
1162  lambda = 0.1934751793D+01 e3 = 0.63625716518613871D+02
1163  lambda = 0.1037296374D+01 e5 = 0.63385217407971851D+02
1164  lambda = 0.1029415522D+01 e6 = 0.63385196860218286D+02
1165  lambda = 0.1029416D+01 pell = 0.633851968602183D+02 -0.63D+00 0.25D+01
1166  cgres_0 33 1.23078004902940045E-012 5.04589483633406912E-013
1167  #iteration= 4
1168  cgres_0 36 1.23479568721858537E-015 6.82639669277830308E-013
1169  lambda = 0.1029415522D+01 e2 = 0.63385147363602783D+02
1170  lambda = 0.2058831044D+01 e3 = 0.63385202811382449D+02
1171  lambda = 0.1000227585D+01 e5 = 0.63385147321246720D+02
1172  lambda = 0.1000170025D+01 e6 = 0.63385147321246102D+02
1173  lambda = 0.1000170D+01 pell = 0.633851473212461D+02 -0.99D-04 0.18D-02
1174  cgres_0 36 1.38678649094504771E-015 7.66666188308590379E-013
1175  #iteration= 5
1176  cgres_0 41 3.70006474981530149E-023 7.93982954620509432E-013
1177  penalized log likelihood = 0.633851473212461D+02 rss1 = 0.00000D+00
1178  #2: w1,w2,w3,w4 = 0.60000000D+01 0.60000000D+01 0.00000000D+00 0.10000000D+01
1179  abic = 0.1423320648D+03 -l = -0.2322598418D+03 pn = 0.1233567828D+04
1180
1181  ----- xd ----- 1.0000000000000000 142.33206476053772
1182  << skipped >>
1183  cgres_0 11 1.54020947332860286E-015 2.29884192443332537E-013
1184  lambda = 0.1043609807D+01 e2 = -0.22403882242063287D+03
1185  lambda = 0.2087219613D+01 e3 = -0.22403690586438574D+03
1186  lambda = 0.9992959948D+00 e5 = -0.22403882557855775D+03

```

```

1187 lambda = 0.9994767724D+00          e6 = -0.22403882557861556D+03
1188 lambda = 0.9994768D+00      pell = -0.224038825578616D+03  -0.32D-02  0.67D-02
1189 cgres_0      11  1.30812015597880167E-015  1.95274516420379816E-013
1190 #iteration=      2
1191 cgres_0      15  3.46131678207414862E-021  5.61917090100347095E-013
1192 penalized log likelihood = -0.224038825578616D+03      rss1 = 0.00000D+00
1193 #2: w1,w2,w3,w4 = 0.24251537D+00 0.24251537D+00 0.00000000D+00 0.10000000D+01
1194 abic = -0.2578557275D+03  -l = 0.2735685405D+02  pn = 0.3141466440D+03
1195
1196 ----- xd -----      7.000000000000000      -257.85572753556761
1197 ##### iteration, f, epsilon =      10 -0.25785573D+03  0.40149378D-02
1198
1199                                     <<  skipped  >>
1200 ptdet = 0.1266242306393D+03
1201 #1: w1,w2,w3,w4 = 0.24444285D+00 0.24444285D+00 0.00000000D+00 0.10000000D+01
1202 wx,wy= 0.24444D+00wxx,wy= 0.00000D+00      pell = -0.223521871356295D+03
1203 lambda = 0.5000000000D+00          e2 = -0.22352266609096029D+03
1204 lambda = 0.1000000000D+01          e3 = -0.22352295814051013D+03
1205 lambda = 0.2000000000D+01          e3 = -0.22352203375141028D+03
1206 lambda = 0.1040406199D+01          e5 = -0.22352295978543751D+03
1207 lambda = 0.1040441881D+01          e6 = -0.22352295978543987D+03
1208 lambda = 0.1040442D+01      pell = -0.223522959785440D+03  -0.21D-02  0.79D-02
1209 cgres_0      11  1.61880861331118845E-015  1.50704974760771075E-013
1210 #iteration=      1
1211 cgres_0      11  3.85521606748695143E-016  2.26906058674522855E-013
1212 lambda = 0.1040441881D+01          e2 = -0.22352336816547259D+03
1213 lambda = 0.2080883761D+01          e3 = -0.22352289158507637D+03
1214 lambda = 0.1000350532D+01          e5 = -0.22352336882549560D+03
1215 lambda = 0.1000261750D+01          e6 = -0.22352336882549969D+03
1216 lambda = 0.1000262D+01      pell = -0.223523368825500D+03  -0.82D-03  0.17D-02
1217 cgres_0      11  3.70289506047125967E-016  2.17923635050981849E-013
1218 #iteration=      2
1219 cgres_0      16  3.06587908896622114E-023  7.84642264502102871E-014
1220 penalized log likelihood = -0.223523368825500D+03      rss1 = 0.00000D+00
1221 #2: w1,w2,w3,w4 = 0.24444285D+00 0.24444285D+00 0.00000000D+00 0.10000000D+01
1222 abic = -0.2578532621D+03  -l = 0.2652255568D+02  pn = 0.3158177062D+03
1223
1224 ##### iteration, f, epsilon =      11 -0.25785573D+03  0.87167224D-03
1225 x = 0.49245849D+00

```

1226 The rows including “lambda =” show values of the negative penalized log  
1227 likelihood (`pell`) in the linear searching procedure. The rows including `lambda`  
1228 without a number attached show the minimized value and sum of squares of the  
1229 gradient vector components of the `pell` function with respect to the minimizing  
1230 parameters. Furthermore, the `abic` value is minimized with respect to a weight `w1`.  
1231 The rows with “----- xd -----“ shows every step where the minimum is updated  
1232 by the simplex algorithm. The second to last rows show that the iterated simplex  
1233 algorithm updated the ABIC for 11 times with the minimum `abic` =  
1234 `-0.2578532621D+03`. This is attained by `w1 = w2 = 0.24444285D+00` (4th row from  
1235 the bottom in the last second block, and the bottom row shows its logarithm). See  
1236 Appendix A for the definitions and Appendix B for the numerical procedures.

1237  
1238 The file `delo2d-poisson.prt` also includes a large volume of outputs. It may be  
1239 useful to use UNIX command `egrep` (`grep`) to select specific items of interests. For  
1240 example,

```

1241 egrep xd delo2dpoisson.prt
1242
1243 egrep `xd|abic` delo2d-poisson.prt

```

1244

1245 shows you just updated and all history of ABIC values, respectively .

1246

1247 For the spatial plot, done in R:

1248

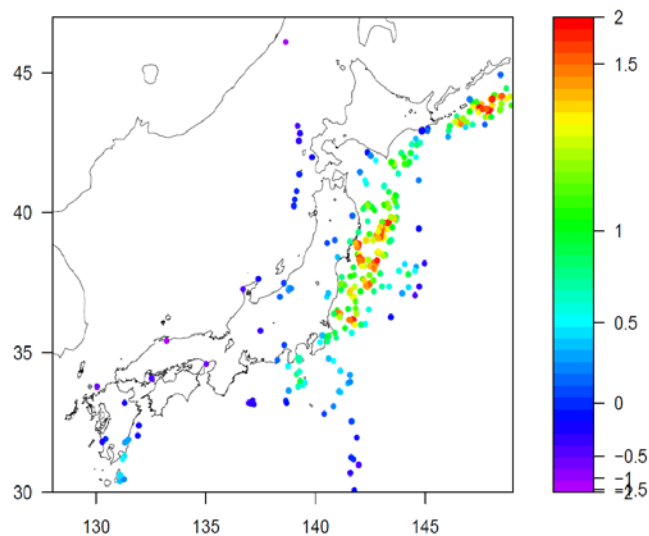
1249 Program: delo2d-poisson.R

1250 Reads: delone2.out, delo2d-poisson.omap

1251 Writes: delo2d-poisson.pdf

1252

1253 which gives the following plot.



1254

1255

1256

1257 Fig. 7. Rainbow colors are in frequency-linearised associated with logarithmic scale values

1258

## 1259 9 ETAS: Spatially Varying $\mu$ and $K_0$ parameters (hist-etask)

1260 This model in §A5.2 is almost the same as the space-time ETAS model as  
1261 described in §5 except that the background rate  $\mu$  and aftershock productivity  $K$  are  
1262 location dependent. The parameters  $\mu$  and  $K$  use a piecewise linear function defined  
1263 on the Delaunay tessellations (§6). On the other hand, the location-independent  
1264 parameters  $\alpha$ ,  $c$ ,  $p$ ,  $d$  and  $q$  are compensated from those obtained as the MLEs  
1265 calculated by the above space-time ETAS program `st-etask`, depending on the  
1266 estimation of location-dependent  $\mu$  and  $K$ . All the used files in this section are  
1267 selected in the program directory of `Section9files/` in the program package.

1268 The program can take a considerable amount of time to converge, as the data size get  
1269 large. An approximation of the model for a faster likelihood calculation is adjusted by  
1270 `bi2`; that restrict the range of spatial distance of interaction between earthquakes; see  
1271 “Line 4” of the configuration file in §5.2.

1272

### 1273 9.1 File Names

1274 For the estimation phase, done in FORTRAN:

```

1275
1276 Program: hist-etas-mk.f
1277 Object: hist-etas-mk
1278 Configuration: hist-etas-mk.conf
1279 Reads: delone2.out
1280 Writes: hist-etas-mk.prt
1281         simplex.root
1282         hist-etas-mk.upda
1283         hist-etas-mk.omap
1284

```

## 1285 9.2 Configuration File Format

1286 An example of the configuration file is as follows. Parameters are read as free  
1287 format. Note that “→” indicates that the record continues onto the following line, i.e.  
1288 it is not split in the configuration file. It is *not* part of the input data configuration.

```

1289
1290 ./delone2.out                !maindata
1291 21.0 17.0 14012.0 308        !tx,ty,tz,nn=#erthquakes
1292 128.0 30.0 6.0 0.0 730.0 2.0 !xmin,ymin,xmg0,zmin,tstart,bi2
1293 0                             !init
1294 0                             !inits
1295 1                             !initf
1296 ./hist-etas-mk.upda         !to be used in case init=1 to succeed calculations
1297 0.0 1.d0 1.d0              !w01,w1,w2
1298 7                             !n=#of parameters
1299 0.29261E-06 0.21404E-01 0.17785E-02 0.10697E+01 0.86948E+00 0.18359E-01 →
1300 0.15210E+01                !μo,Ko,c,α,p,d,q
1301 0                             !if ipr = 7, printing the linear search
1302 0 1.d0 1.d-0              !nhesapp, dist,eps (in subroutine simplex)
1303

```

1304 The data are interpreted as follows.

1305 **Line 1:** Name of the data file, preceded by ./.

1306 **Line 2:** Width of region ( $t_x$  degrees longitude), height of region ( $t_y$  degrees  
1307 latitude), end of observation period ( $t_z$  days), number of events ( $nn$ ) in dataset.

1308 **Line 3:** Minimum longitude ( $x_{min}$  degrees), minimum latitude ( $y_{min}$  degrees),  
1309 reference magnitude ( $x_{mg0}$ ) that can be usually a threshold magnitude of  
1310 completely detected ( $cut_m$  in §4.2), starting time of all data including  
1311 precursory period for the history ( $z_{min} = 0$  day), starting time of target period  
1312 of estimation ( $t_{start} = 730$  days, in the current case), and an adjustment  
1313 parameter called  $bi2$  ( $=2.0$ , in the current case), which restrict the range of  
1314 spatial distance of interaction between earthquakes. For an explanation of  $bi2$ ,  
1315 see “Line 4” in §5.2.

1316 **Line 4:** Value of  $init$ . If  $init$  is 0, then estimation starts at the beginning using  
1317 the data file specified in Line 1 and initial parameter estimates given in Line 10.  
1318 If  $init$  is 1, estimation continues from where a previous run was terminated.

1319           The results of the previous run are placed in the file specified in Line 8  
1320           (hist-etas-mk.upda).

1321       **Line5:** Value of `inits`. If 1, the file containing the simplex optimization history  
1322           from the previous run is used, 0 if it is not to be read. This information is  
1323           contained in the file with `simplex.root`. There is a possibility that this will  
1324           not work, in which case `inits` should be set to 0.

1325       **Line 6:** Value of `initf`. This is related to the grid search of the weights `w3`, `w5`,  
1326           and `w7` the “hist-etas5pa” model (see §5 and §11.5 and §A5).

1327       **Line 7:** File name containing estimation information from a previously incomplete  
1328           run. It is the file `hist-etas-mk.upda`. This information can be used as a  
1329           good starting point for the new run. This file includes the updated estimates of  
1330           baseline parameters and the numbers in lines 10~11 are ignored in the case  
1331           where `init=1`.

1332       **Line 8:** Weights for the flatness constraints (`w1`, `w2`) of Delaunay piecewise linear  
1333           function. The first weight `w01` represents the dumping penalty that is imposed  
1334           only on the vertices on the boundary of the region. See A.6.2 for definition and  
1335           details.

1336       **Line 9:** Number of initial model parameters listed on lines 10~11.

1337       **Line 10~11:** Initial estimates of baseline parameters. We recommend using the  
1338           estimates is computed by the program `st-etas` given in `st-etas.prt` (see  
1339           §5). These inputs estimates are ignored in the case where `init=1`

1340       **Line 12:** Index `ipr` for printing the linear search results in `hist-etas-mk.prt`.  
1341           If `ipr = 0`, no printing, otherwise printing the linear search result.

1342       **Line 13:** Adoption of the approximated Hessian matrix (`nhesapp=1`); initial  
1343           distance for simplex search; and error bounds for the criteria of the simplex  
1344           convergence (penalized log-likelihood ) used in subroutine `simplex`. The  
1345           other parameters that may require adjusting within the FORTRAN code are `dist`  
1346           and `eps`. The first adjusts the search criterion (size of the simplex), and the  
1347           second sets the convergence criterion.

1348

### 1349   9.3 Executing the Program

1350       When `init=0`, parameter estimation does not start from where a previous run of  
1351       `hist-etas-mk` terminated. Hence the file specified in Line 6 of the configuration  
1352       file is not used. The model fitting starts from the initial parameter values specified in  
1353       the configuration file. Execute as

```
1354       ./hist-etas-mk |tee hist-etas-mk.prt
```

1355       When `init=1` information from a previous run is used, namely that contained in  
1356       the file `hist-etas-mk.upda`. For more accurate estimation, we set a larger value of  
1357       `bi2` such as 4 or 8, and we can use the previously obtained estimates. Since the new  
1358       job will also write a file with the same name, we recommend copying and keeping the  
1359       original `hist-etas-mk.upda`. Hence this name is specified on Line 9 of the  
1360       configuration file.

1361

1362 9.4 Output of Calculation Process

1363 An example of the program output (hist-etas-mk.prt) is as follows.

```

1364
1365 delone2.out
1366     21.0      17.0   14012.0      308
1367     730.0
1368     128.00   30.00    6.00    0.00   730.00    2.00
1369 input device      10
1370 nfunct=          17
1371 nn,ntstar,nnc    308      16      292
1372 tx,ty,tz,xmin,ymin,xmg0,zmin,tsta
1373     16.435   17.000 14012.000   128.000   30.000   6.000   0.000   730.000
1374 nn = 308 nnc = 292
1375 jmax           61
1376 n=             7
1377 para-init=     0.29261E-06   0.21404E-01   0.17785E-02   0.10697E+01   0.86948E+00 →
1378 0.18359E-01   0.15210E+01
1379 linear ipr      0
1380 nhesapp,simplex(dist,eps)      0  1.0000000000000000      1.0000000000000000
1381 n=             7
1382 non-pos diag.      339  -8.7469312074247600      586.78388345246196
1383 non-pos diag.      339  -8.7469312074247600      586.78388345246196
1384     588.42278020120909      588.42278020120909
1385 ptdet = 0.1176845560402D+04
1386 #s: w1,w2 = 0.100D+01  0.100D+01
1387 Initial Penalized log likelihood = 10089.469022236997
1388 lambda = 0.4228466D+00 pell = 0.478286492088103D+04 -0.51D+05  0.49D+06
1389 lambda = 0.3465761D+00 pell = 0.303540668222858D+04 -0.36D+05  0.75D+05
1390 lambda = 0.1063103D+01 pell = 0.194855632224969D+04 -0.18D+04  0.20D+05
1391 lambda = 0.1064288D+01 pell = 0.185052756355960D+04 -0.16D+03  0.61D+03
1392 lambda = 0.7674186D+00 pell = 0.183141972939415D+04 -0.52D+02  0.18D+03
1393 lambda = 0.8041680D+00 pell = 0.182171531754999D+04 -0.23D+02  0.49D+02
1394 lambda = 0.7680201D+00 pell = 0.181722348272042D+04 -0.12D+02  0.31D+02
1395 lambda = 0.7644997D+00 pell = 0.181447949500491D+04 -0.69D+01  0.98D+01
1396 lambda = 0.7265978D+00 pell = 0.181309094850632D+04 -0.39D+01  0.68D+01
1397 lambda = 0.7025772D+00 pell = 0.181225563224721D+04 -0.23D+01  0.26D+01
1398 lambda = 0.6575894D+00 pell = 0.181181504512178D+04 -0.14D+01  0.18D+01
1399 lambda = 0.6419689D+00 pell = 0.181154264428305D+04 -0.82D+00  0.81D+00
1400 lambda = 0.6188474D+00 pell = 0.181139001000143D+04 -0.50D+00  0.62D+00
1401 lambda = 0.6180905D+00 pell = 0.181129162444832D+04 -0.31D+00  0.29D+00
1402 lambda = 0.6092636D+00 pell = 0.181123423083046D+04 -0.19D+00  0.23D+00
1403 lambda = 0.6101669D+00 pell = 0.181119729576200D+04 -0.12D+00  0.11D+00
1404 lambda = 0.6068614D+00 pell = 0.181117528517862D+04 -0.73D-01  0.87D-01
1405 lambda = 0.6069101D+00 pell = 0.181116129443409D+04 -0.46D-01  0.40D-01
1406 lambda = 0.6059907D+00 pell = 0.181115284215355D+04 -0.28D-01  0.33D-01
1407 lambda = 0.6053561D+00 pell = 0.181114752142969D+04 -0.17D-01  0.15D-01
1408 lambda = 0.6055761D+00 pell = 0.181114427741159D+04 -0.11D-01  0.13D-01
1409 lambda = 0.6045714D+00 pell = 0.181114224762131D+04 -0.67D-02  0.59D-02
1410 lambda = 0.6053656D+00 pell = 0.181114100240355D+04 -0.41D-02  0.48D-02
1411 lambda = 0.6041784D+00 pell = 0.181114022595194D+04 -0.26D-02  0.22D-02
1412 lambda = 0.6052692D+00 pell = 0.181113974761236D+04 -0.16D-02  0.18D-02
1413 lambda = 0.6039944D+00 pell = 0.181113944988561D+04 -0.98D-03  0.85D-03
1414 lambda = 0.6052458D+00 pell = 0.181113926593057D+04 -0.61D-03  0.70D-03
1415 lambda = 0.6039214D+00 pell = 0.181113915152839D+04 -0.38D-03  0.33D-03
1416 lambda = 0.6052650D+00 pell = 0.181113908069490D+04 -0.23D-03  0.27D-03
1417 lambda = 0.6039132D+00 pell = 0.181113903665419D+04 -0.15D-03  0.12D-03
1418 lambda = 0.6053139D+00 pell = 0.181113900934350D+04 -0.90D-04  0.10D-03
1419 lambda = 0.6039305D+00 pell = 0.181113899236161D+04 -0.56D-04  0.48D-04
1420 lambda = 0.6054994D+00 pell = 0.181113898181821D+04 -0.35D-04  0.40D-04
1421 lambda = 0.6035771D+00 pell = 0.181113897526049D+04 -0.22D-04  0.18D-04
1422 lambda = 0.6059521D+00 pell = 0.181113897118520D+04 -0.13D-04  0.15D-04
1423 lambda = 0.6035625D+00 pell = 0.181113896864956D+04 -0.84D-05  0.70D-05
1424 lambda = 0.6059704D+00 pell = 0.181113896707257D+04 -0.52D-05  0.59D-05
1425 lambda = 0.6035741D+00 pell = 0.181113896609097D+04 -0.33D-05  0.27D-05
1426 lambda = 0.6060786D+00 pell = 0.181113896548008D+04 -0.20D-05  0.23D-05
1427 lambda = 0.6035508D+00 pell = 0.181113896509967D+04 -0.13D-05  0.10D-05

```

```

1428 lambda = 0.6062551D+00 pell = 0.181113896486279D+04 -0.78D-06 0.87D-06
1429 lambda = 0.6048568D+00 pell = 0.181113896471523D+04 -0.49D-06 0.40D-06
1430 lambda = 0.6036937D+00 pell = 0.181113896462330D+04 -0.30D-06 0.34D-06
1431 lambda = 0.6061852D+00 pell = 0.181113896456600D+04 -0.19D-06 0.16D-06
1432 lambda = 0.6038110D+00 pell = 0.181113896453029D+04 -0.12D-06 0.13D-06
1433 lambda = 0.6061742D+00 pell = 0.181113896450802D+04 -0.73D-07 0.60D-07
1434 lambda = 0.6061742D+00 pell = 0.181113896449415D+04 -0.46D-07 0.50D-07
1435 lambda = 0.6016804D+00 pell = 0.181113896448548D+04 -0.29D-07 0.23D-07
1436 lambda = 0.6085610D+00 pell = 0.181113896448009D+04 -0.18D-07 0.20D-07
1437 lambda = 0.5957944D+00 pell = 0.181113896447671D+04 -0.11D-07 0.90D-08
1438 lambda = 0.6163351D+00 pell = 0.181113896447461D+04 -0.68D-08 0.75D-08
1439 lambda = 0.5983139D+00 pell = 0.181113896447330D+04 -0.44D-08 0.35D-08
1440 lambda = 0.6122871D+00 pell = 0.181113896447248D+04 -0.27D-08 0.29D-08
1441 lambda = 0.6122871D+00 pell = 0.181113896447197D+04 -0.17D-08 0.13D-08
1442 lambda = 0.5848831D+00 pell = 0.181113896447165D+04 -0.11D-08 0.11D-08
1443 lambda = 0.5848831D+00 pell = 0.181113896447145D+04 -0.64D-09 0.52D-09
1444 lambda = 0.6719067D+00 pell = 0.181113896447133D+04 -0.37D-09 0.43D-09
1445 lambda = 0.5502216D+00 pell = 0.181113896447125D+04 -0.28D-09 0.20D-09
1446 lambda = 0.5983607D+00 pell = 0.181113896447120D+04 -0.14D-09 0.17D-09
1447 penalized log likelihood = 0.181113896447120D+04
1448 #e: w1,w2 = 0.100D+01 0.100D+01
1449 abic = 0.3655784386D+04 -l = 0.1850351202D+04 pn = 0.1210352017D+04
1450 repeated davidn = 1
1451 Surface Sliding: Old a1, a2= 2.92610000000000024E-007 2.14039999999999994E-002
1452 Surface Sliding: sss1, sss2= 1678.3115727728357 -1349.0295398812370
1453 Surface Sliding: New a1, a2= 3.95841650338503000E-005 4.14387812724830850E-004
1454 ----- xd ----- 1 0.365578438575E+04 0.000
1455 a1-7 0.396E-04 0.414E-03 0.178E-02 0.107E+01 0.869E+00 0.184E-01 0.152E+01
1456 w1-2 0.100E+01 0.100E+01

1457 << skipped >>

1458 lambda = 0.1591954D+00 pell = 0.167273796149464D+04 -0.64D-09 0.11D-09
1459 lambda = 0.3881579D+00 pell = 0.167273796149461D+04 -0.16D-09 0.98D-10
1460 lambda = 0.1665214D+00 pell = 0.167273796149459D+04 -0.27D-09 0.76D-10
1461 lambda = 0.4590164D+00 pell = 0.167273796149457D+04 -0.95D-10 0.61D-10
1462 lambda = 0.1529797D+00 pell = 0.167273796149455D+04 -0.22D-09 0.45D-10
1463 penalized log likelihood = 0.167273796149455D+04
1464 #e: w1,w2 = 0.823D-01 0.809D+00
1465 abic = 0.3526282973D+04 -l = 0.2172458180D+04 pn = 0.4366366499D+03
1466 repeated davidn = 1
1467 Surface Sliding: Old a1, a2= 1.13588618541079640E-004 6.72600220400718243E-005
1468 Surface Sliding: sss1, sss2= 2.5486238908657164 -238.50222149897596
1469 Surface Sliding: New a1, a2= 1.14438256042319838E-004 3.34881323324280578E-005
1470 ----- xd ----- 9 0.352628297294E+04 -5.110
1471 a1-7 0.114E-03 0.335E-04 0.647E-02 0.146E+01 0.104E+01 0.210E-01 0.233E+01
1472 w1-2 0.823E-01 0.809E+00

1473 << skipped >>

1474 lambda = 0.2309417D+00 pell = 0.167026661988171D+04 -0.11D-09 0.47D-10
1475 lambda = 0.3459302D+00 pell = 0.167026661988169D+04 -0.84D-10 0.42D-10
1476 lambda = 0.1827652D+00 pell = 0.167026661988168D+04 -0.13D-09 0.38D-10
1477 lambda = 0.4000000D+00 pell = 0.167026661988167D+04 -0.58D-10 0.33D-10
1478 lambda = 0.1842672D+00 pell = 0.167026661988166D+04 -0.11D-09 0.30D-10
1479 penalized log likelihood = 0.167026661988166D+04
1480 #e: w1,w2 = 0.916D-01 0.443D+00
1481 abic = 0.3533595745D+04 -l = 0.2254182084D+04 pn = 0.2805016139D+03
1482 repeated davidn = 1
1483 #### iteration, f, epsilon = 43 0.35262830D+04 0.96234391D+00
1484 x = -0.24971914D+01 -0.21167911D+00 -0.50405642D+01 0.37993810D+00 →
1485 x = 0.37616517D-01 -0.38631250D+01 0.84729410D+00
1486

```

1487 The above lists ABIC values, the final parameter estimates, and the penalised  
1488 log-likelihoods. The numbers in last column are the sum of squares of all the gradient  
1489 vector components of the coefficients. The progression to smaller values as one goes

1490 down the output indicates that the computations are converging. The third to last rows  
 1491 show that the iterated (7-dimensional) simplex algorithm updated the ABIC value, 9  
 1492 times updates, out of 43 ABIC calculation trials to get the smallest value of ABIC =  
 1493 0.352628297294E+04 (indicated by ` - xd - `; the 16th row from the output bottom)  
 1494 which is attained by  $w_1 = 0.823E-01$  and  $w_2 = 0.809E+00$  ('w1-2'; the 15th row from the  
 1495 bottom), and the third last row (indicated by #####) from the output bottom  
 1496 summarizes iterated numbers, the smallest ABIC value, and the difference from the  
 1497 second smallest ABIC is 0.96234391D+00. The 16th row from the output bottom  
 1498 ('a1-7') shows the baseline parameters of  $\mu$ ,  $K_0$ ,  $c$ ,  $\alpha$ ,  $p$ ,  $d$  and  $q$ , and the bottom two  
 1499 rows show their logarithmic values. See Appendix A for the definitions and Appendix  
 1500 B for the numerical procedures.

1501 The file `hist-etas-mk.prt` includes a large amount of output. It may be useful  
 1502 to use the UNIX command `egrep(grep)` to extract items of interest, as done earlier,

```
1503 egrep xd hist-etas-mk.prt
1504 egrep xd|abic hist-etas-mk.prt
```

1505 These will show you just the updated and all history of ABIC values, respectively.  
 1506

1507 An example of the program output (`hist-etas-mk.omap`) is as follows.

```
1508
1509 -0.2497E+01  -0.2117E+00  3533.60  684
1510 0.114438261954E-03  0.334881320043E-04  0.647009682182E-02  0.146219408001E+01 →
1511 0.103833297334E+01  0.210022642758E-01  0.233332455954E+01
1512 -0.768090420081E+01 -0.980188281878E+01 -0.830621370392E+01 -0.797115464193E+01
1513 -0.893480205512E+01 -0.695269893920E+01 -0.889522839754E+01 -0.867387791505E+01
1514 -0.935157675729E+01 -0.898946493741E+01 -0.679076775508E+01 -0.912639592929E+01
1515 -0.793894681451E+01 -0.944728426317E+01 -0.942753542139E+01 -0.848239207321E+01
```

1516 << skipped till the end >>

1517 Here the first line writes  $\ln(w_1)$ ,  $\ln(w_2)$ , abic and twice of the number of coefficients  
 1518 in the Delaunay functions representing  $\mu$  and  $K$ . The second and third lines give the  
 1519 optimized baseline parameters  $\mu_0$ ,  $K_0$ ,  $c$ ,  $\alpha$ ,  $p$ ,  $d$  and  $q$ . The fourth and following  
 1520 lines down to the bottom give logarithm of deviations from the baseline parameters  $\mu_0$   
 1521 and  $K_0$ .

1522 See R display procedure and example figures of the optimal maximum a posterior  
 1523 (OMAP) estimate in §11.5.

1524 For a good initial estimation with the program `hist-etas5pa` in the next section,  
 1525 and the forecasting in §13.1, the following is the updated output file

```
1526 hist-etas-mk.upda:
1527
1528 0.82316E-01  0.80922E+00  3526.28  684
1529 0.114438256042E-03  0.334881323324E-04  0.647009682182E-02  0.146219408001E+01 →
1530 0.103833297334E+01  0.210022642758E-01  0.233332455954E+01
1531 0.139457092658E+01 -0.726407678229E+00  0.769261411269E+00  0.110432047804E+01
1532 0.140673083157E+00  0.212277617056E+01  0.180246755834E+00  0.401597166657E+00
1533 -0.276101629785E+00  0.860101851354E-01  0.228470737143E+01 -0.509208017719E-01
1534 0.113652828785E+01 -0.371809145881E+00 -0.352060305758E+00  0.593083039677E+00
1535 -0.683893507324E+00 -0.816700951127E+00  0.902848610295E-01  0.557331993929E+00
1536 -0.138820519275E+01  0.108533576988E+01 -0.180759606983E+00 -0.107075073680E+00
```

1537 << skipped >>

```

1538  0. 241695424598E+00  0. 511075481092E+00 -0. 283118737557E+00  0. 953208296924E+00
1539  0. 114626199422E+00  0. 231870568842E+00 -0. 398161180796E+00 -0. 180628788391E+00
1540 -0. 114291272430E+01 -0. 378213066618E+00 -0. 859583923866E-01 -0. 129659654388E+00
1541 -0. 117930858809E+00 -0. 528690530145E+00 -0. 605507186335E+00 -0. 173845062437E+00
1542 -0. 152130753387E+00 -0. 108836609546E+01 -0. 907255257880E+00 -0. 737753342053E+00
1543 -0. 460987874419E+00 -0. 232974758562E+00 -0. 557155856504E+00 -0. 591710718465E+00
1544 -0. 471950174999E+00 -0. 289090736345E+00 -0. 239500503238E+00 -0. 261449294363E+00
1545 -0. 377911671516E+00 -0. 547351463463E+00 -0. 225341192861E+00 -0. 606005843722E+00
1546 -0. 246721505150E+00 -0. 638621609165E+00 -0. 383947873387E+00 -0. 540608762369E+00
1547 -0. 244800152526E+00 -0. 179074966412E+00 -0. 137299967512E+00 -0. 135008778881E+00
1548

```

1549 Here the first line has  $w_1$ ,  $w_2$ ,  $abc$  and twice of number of coefficients in the  
1550 Delaunay functions representing  $\mu$  and  $K$ . The second and third lines give the  
1551 optimized baseline parameters  $\mu_0, K_0, c, \alpha, p, d$  and  $q$ . The fourth line down to  
1552 the bottom give logarithm of the OMAP estimates taking account of the baseline  
1553 parameters  $\mu_0$  and  $K_0$ .

1554  
1555

## 1556 9.5 Additional Advice

1557 The current program `hist-etaz-mk` is the most time consuming because of the 7  
1558 dimensional simplex optimization procedure for the reference parameters of  $\mu, K_0, c,$   
1559  $\alpha, p, d$  and  $q$  besides the high-dimensional quasi-Newton and Newton optimizations.  
1560 Nevertheless, assuming that we can use initial reference parameters with the MLEs of  
1561 (`st-etaz`) in §5 that converged well (see §5.4), it can take a shorter time in  
1562 converging the `hist-etaz-mk` program than the default case; specifically, try a short  
1563 distance in the step-size of the simplex procedure. This implementation corresponds  
1564 to replacing `dist=1.0` (the default) by `dist=0.05`, for example, in the last line of  
1565 `hist-etaz-mk.conf` and then run it.

1566  
1567

## 1568 10 ETAS: Spatial Variation in 5 Parameters (`hist-etaz5pa`)

1569 This model is referred to as the five-parameter model because it allows five of the  
1570 parameters to vary in space, i.e.  $\mu, K_0, \alpha, p$  and  $q$ . The parameters  $c$  and  $d$  are  
1571 assumed to be constant in space, and fixed throughout the computation procedure. For  
1572 further mathematical detail, see §A.5.3. This program should be undertaken after  
1573 having obtained the optimal estimates by `hist-etaz-mk` as described in the previous  
1574 section. All the used files in this section are selected in the program directory of  
1575 `Section10files/` in the program package.

1576

### 1577 10.1 File Names

1578 For the estimation phase, done in FORTRAN:

1579

1580 Program: `hist-etaz5pa.f`

1581 Object: `hist-etaz5pa`

```

1582 Configuration: hist-etas5pa.conf
1583 Reads:         delone2.out, hist-etas-mk.upda
1584 Writes:        hist-etas5pa.upda,
1585                hist-etas5pa.omap
1586

```

## 1587 10.2 Configuration File Format

1588 The program can take a considerable amount of time to converge, depending on the  
1589 number of earthquakes. It is possible that a job may exceed queue time and be  
1590 terminated by the system before it has converged. An approximation of the model,  
1591 giving a faster likelihood calculation, is provided by `bi2`; see “Line 5” in §5.2. To  
1592 restart the job at roughly the same place, specifically where it last wrote solution  
1593 information to the disk, the configuration file needs modification. The files that track  
1594 the convergence process are `hist-etas5pa.prt` and `simplex.rootu` (simplex  
1595 root information).

1596 An example of the configuration file `hist-etas5pa.conf` is as follows.  
1597 Parameters are read as free format. Note that “→” indicates that the record continues  
1598 onto the following line, i.e. it is not split in the configuration file. It is *not* part of the  
1599 input data. The configuration file would generally have the following format when  
1600 one first runs this program (see detailed explanation of each line below). Notice that,  
1601 unlike the previous programs, `init` on line 6 is generally set to one. In the present  
1602 example, this has the effect of using the output in file `hist-etas-mk.omap`.

```

1603
1604 ./delone2.out                !main data
1605 21.0 17.0 14012.0 308        !tx,ty,tz,nn=#earthquakes
1606 128.0 30.0 6.0 0.0 730.0 2.0 !xmin,ymin,xmg0,zmin,tstart,bi2
1607 0                            !init
1608 0                            !inits
1609 1                            !initf
1610 ./hist-etas-mk.upda         !approximate solution for initial estimate
1611 0. 1000.                    !w00, w01,
1612 10. 100. 1000.              !w3, w4, w5
1613 0                            !if ipr = 7, printing the linear search results
1614 0.1d-3 0.1d-3                !tau1,tau2(davidn)
1615 0.1d-3 0.1d-3                !eps1,eps2(davidn)
1616 0 1.d0 0.5d-0                !nhesapp, dist,eps (in subroutine simplex)
1617

```

1618 The data are interpreted as follows:

- 1619 **Line 1:** Name of the data file, preceded by `./`.
- 1620 **Line 2:** Width of region (`tx` degrees longitude), height of region (`ty` degrees  
1621 latitude), end of observation period (`tz` days), number of events (`nn`) in dataset.
- 1622 **Line 3:** Minimum longitude (`xmin` degrees), minimum latitude (`ymin` degrees),  
1623 threshold magnitude (`xmg0`), minimum time (`zmin`), starting time (`tstart` 730  
1624 days), and an adjustment parameter called `bi2`. For and explanation of `bi2`, see  
1625 “Line 5” in §5.2.
- 1626 **Line 4:** Value of `init`. If `init` is 0, then estimation starts at the beginning using  
1627 the data file `delone2.out` as specified in Line 1 and `hist-etas-mk.upda` as

1628 given in Line 7. If `init` is 1, estimation starts by replacing  
1629 `hist-et-as-mk.upda` in Line 7 by `hist-et-as5pa.upda`.

1630 **Line 5:** Value of `inits`. If 1, the file containing the simplex optimization history  
1631 from a previous run is used, 0 if it is not to be read. This information is  
1632 contained in the file with `simplex.root`. There is a possibility that this will  
1633 not work, in which case `inits` should be set to 0.

1634 **Line 6:** Value of `initf`. If `initf` = 1 then the program will only utilise the  
1635 weights  $w_3, w_4$ , and  $w_5$  as given in line 8. If `initf` = 0 then the simplex program  
1636 searches for optimal weights  $(w_1, w_2, w_3, w_4, w_5)$  by minimizing ABIC, which  
1637 takes a substantial CPU time. For the grid search of  $(w_3, w_4, w_5)$  with the fixed  
1638  $(w_1, w_2)$  that are optimized by `hist-et-as-mk.f` the former should be used.

1639 The coefficient parameters may not always be converged in case of `initf` =  
1640 1 because the Hessian matrix does not become positive-definite, when, for  
1641 example, the weights of  $(w_3, w_4, w_5)$  is too small. Usually, weights for  $\alpha, p$  and  
1642  $q$  of the HIST-ETAS model are not necessary to seek the values in accurate, and  
1643 it is not bad idea to make a grid search. To execute grid searches, set `initf` = 0.  
1644 Regarding grid exploration, the ninth line provides the default weights, but if  
1645 the data size is a large, they can be (1000., 1000., 1000.), for example, to  
1646 converge it in one loop, so remember its ABIC value for the comparisons as  
1647 follows: namely, in addition for example, (1000., 10000., 10000.), (100., 100.,  
1648 10000.), (100., 1000., 10000.) (10., 10., 1000.), and so on, to find the smaller  
1649 ABIC value. Ignore combinations of smaller weights that still do not converge.  
1650 In our experience, if the weight of  $(w_3, w_4, w_5)$  is too small, the Hessian matrix  
1651 will not be positive-definite and the coefficient parameters will not converge.  
1652 Especially, the weight  $w_5$  may be large because the variable parameter  $q$  does  
1653 not likely change so much.

1654 **Line 7:** File name containing estimation information from a previously incomplete  
1655 run. It is the file with the suffix `.upda`. This information can be used as a  
1656 starting point for the new run. In the case where `init` is 0,  
1657 `hist-et-as-mk.upda` as given in Line 7 provides an optimal initial estimates  
1658 of the baseline parameters  $\mu_0, K_0, c, \alpha, p, d$  and  $q$ , and the coefficients of  
1659 Delaunay functions representing  $\mu$  and  $K$ . The coefficients of the Delaunay  
1660 functions representing  $\alpha, p$  and  $q$  are all set to 0 in the program. In the case  
1661 where `init` is 1, the baseline parameters are the same, but the coefficients of  
1662 Delaunay functions representing  $\mu, K, \alpha, p$  and  $q$  are all going to be updated,  
1663 starting from those in `hist-et-as5pa.upda`.

1664 **Line 8:** Weights for the flatness constraints of Delaunay piecewise linear function.  
1665 The first weight  $w_{00}$  represents the dumping penalty for all parameters at all  
1666 vertices of Delaunay triangles, and  $w_{01}$  represents the same dumping penalty  
1667 imposed only on the vertices on the boundary of the region. See A.6.2 for  
1668 definition and details.

1669 **Line 9:** Initial weights for the flatness constraints  $(w_3, w_4, w_5)$  of the Delaunay  
1670 piecewise linear functions. See A.6.2 for definition and details. In the case of  
1671 grid search of weights  $w_3, w_4$  and  $w_5$  for the penalty of  $\alpha, p$  and  $q$ , these are  
1672 different by exponential orders as given in Line 8, according to our experience  
1673 in finding optimal weights by minimizing ABIC value.

1674 **Line 10:** Index `ipr` for printing the linear search results in `hist-etas5pa.prt`.  
 1675 If `ipr = 0`, no printing, otherwise printing the linear search result.  
 1676 **Lines 11 and 12:** convergence criteria in subroutine `davidn`.  
 1677 **Line 13** Adoption of the approximated Hessian matrix (`nhesapp=1`); initial  
 1678 distance for simplex search; and error bounds for the criteria of the simplex  
 1679 convergence (penalized log-likelihood) used in subroutine `simplex`. The  
 1680 other parameters that may require adjusting within the FORTRAN code are `dist`  
 1681 and `eps`. The first adjusts the search criterion (size of the simplex), and the  
 1682 second sets the convergence criterion.  
 1683

### 1684 10.3 Executing the Program

1685 The following command executes the compiled FORTRAN code.  
 1686 `./hist-etas5pa |tee hist-etas5pa.prt`  
 1687

### 1688 10.4 Output Produced by Program

1689 An example of the program output (`hist-etas5pa.prt`) is as follows.

```

1690 delone2.out
1691      21.0      17.0  14012.0      308
1692      128.      30.      6.      0.      730.      2.
1693 input device      10
1694 Otx,ty,tz,xmin,ymin,xmg0,zmin,tsta
1695      16.435      17.000 14012.000      128.000      30.000      6.000      0.000      730.000
1696 nn = 308 nnc = 292
1697 jmax,bi2      61  2.0000000000000000
1698      308
1699 w0-w7 0.0000000000000000E+000 1000.000000000000      8.2320000000000000E-002
1700      0.8092000000000000      10.000000000000000      100.00000000000000 →
1701      1000.000000000000
1702 linear ipr      0
1703 davidn tau 1.0000000000000000E-004 1.0000000000000000E-004
1704 davidn eps 1.0000000000000000E-004 1.0000000000000000E-004
1705 nhesapp,simplex(dist,eps)      0 1.0000000000000000 0.5000000000000000
1706 n=      7
1707 w1-w7 8.2320000000000000E-002 0.8092000000000000      10.000000000000000 →
1708      100.00000000000000      1000.000000000000
1709 a1-a7 1.144382542340000E-004 3.348813210360000E-005 6.470096821820000E-003 →
1710      1.46219408001000 1.03833297334000 2.100226427580000E-002 2.33332455954000
1711 w00,w01 = 0.0000000000000000E+000 1000.000000000000
1712 non-pos diag.      339 -106.26040147013342 -257.26626201915627
1713 non-pos diag.      339 -10.809089255604786 515.23453657230607
1714 ptdet = 0.7637790019860D+04
1715 repeated davidn =      1
1716 #s: w1,w2,w4,w5,w7 = 0.823D-01 0.809D+00 0.100D+02 0.100D+03 0.100D+04
1717 Initial Penalized log likelihood = 1672.7379602189433
1718 lambda = 0.8744497D+00 pell = 0.167044234940854D+04 -0.52D+01 0.60D+04
1719 lambda = 0.9592622D+00 pell = 0.166605016259747D+04 -0.93D+01 0.27D+04
1720 lambda = 0.3613464D+00 pell = 0.166533962998344D+04 -0.38D+01 0.22D+04
1721 lambda = 0.1055977D+01 pell = 0.166495986340342D+04 -0.73D+00 0.47D+02
1722 lambda = 0.3649882D+00 pell = 0.166475860787496D+04 -0.11D+01 0.79D+03
1723 lambda = 0.6678868D+00 pell = 0.166467378583788D+04 -0.25D+00 0.19D+02
1724
1725 <<skipped>>
1726 lambda = 0.9000000D+00 pell = 0.166426648388209D+04 -0.55D-10 0.32D-07
1727 lambda = 0.1377750D+00 pell = 0.166426648388207D+04 -0.31D-09 0.25D-07

```

```

1728 lambda = 0.1152778D+01 pell = 0.166426648388205D+04 -0.41D-10 0.24D-07
1729 lambda = 0.1151316D+00 pell = 0.166426648388203D+04 -0.32D-09 0.18D-07
1730 lambda = 0.2285714D+01 pell = 0.166426648388200D+04 -0.28D-10 0.17D-07
1731 penalized log likelihood = 0.166426648388199D+04
1732 #e: w1,...,w5 = 0.823D-01 0.809D+00 0.100D+02 0.100D+03 0.100D+04
1733 abic= 0.3569086244E+04 -l= -0.5841625728E+03 pn= 0.7878343296E+04
1734 ----- xd ----- 1 3569.0862435900335
1735 a1-7 0.114E-03 0.335E-04 0.647E-02 0.146E+01 0.104E+01 0.210E-01 0.233E+01
1736 w1-7 0.000E+00 0.100E+04 0.823E-01 0.809E+00 0.100E+02 0.100E+03 0.100E+04

```

1737 << skipped >>

```

1738 lambda = 0.7812500D+00 pell = 0.167574329557346D+04 -0.60D-10 0.34D-07
1739 lambda = 0.1547237D+00 pell = 0.167574329557345D+04 -0.23D-09 0.27D-07
1740 lambda = 0.1063830D+01 pell = 0.167574329557342D+04 -0.44D-10 0.26D-07
1741 lambda = 0.1424074D+00 pell = 0.167574329557340D+04 -0.27D-09 0.18D-07
1742 lambda = 0.1904255D+01 pell = 0.167574329557337D+04 -0.28D-10 0.18D-07
1743 penalized log likelihood = 0.167574329557337D+04
1744 #e: w1,...,w5 = 0.125D+00 0.599D+00 0.152D+02 0.415D+02 0.152D+04
1745 abic= 0.3562608863E+04 -l= -0.5869629136E+03 pn= 0.7877466597E+04
1746 ----- xd ----- 4 3562.6088628260377
1747 a1-7 0.114E-03 0.335E-04 0.647E-02 0.146E+01 0.104E+01 0.210E-01 0.233E+01
1748 w1-7 0.000E+00 0.100E+04 0.125E+00 0.599E+00 0.152E+02 0.415E+02 0.152E+04
1749

```

```

1750 ##### iteration, f, epsilon = 2 0.35626089D+04 0.10703394D+01
1751 x = -0.41543796D+01 -0.10233689D+01 0.54451702D+01 0.74503404D+01 →
1752 x = 0.14655511D+02

```

1753 << skipped >>

```

1754 lambda = 0.1500000D+00 pell = 0.168438504518700D+04 -0.78D-09 0.25D-07
1755 lambda = 0.1542857D+01 pell = 0.168438504518697D+04 -0.39D-10 0.24D-07
1756 lambda = 0.1542857D+00 pell = 0.168438504518694D+04 -0.30D-09 0.15D-07
1757 lambda = 0.1266667D+01 pell = 0.168438504518693D+04 -0.24D-10 0.15D-07
1758 lambda = 0.1449091D+00 pell = 0.168438504518692D+04 -0.16D-09 0.10D-07
1759 penalized log likelihood = 0.168438504518692D+04
1760 #e: w1,...,w5 = 0.159D+00 0.506D+00 0.130D+02 0.670D+02 0.135D+04
1761 abic= 0.3563238642E+04 -l= -0.6202776694E+03 pn= 0.7944725887E+04
1762 ##### iteration, f, epsilon = 5 0.35626089D+04 0.30092985D+00
1763 x = -0.41543796D+01 -0.10233689D+01 0.54451702D+01 0.74503404D+01 →
1764 x = 0.14655511D+02
1765

```

1766 The numbers in last column are the sum of squares of all the gradient vector  
1767 components of the coefficients. The progression to smaller values as one goes down  
1768 the output indicates that the computations are converging. The second to last row  
1769 shows that the iterated simplex algorithm updated the ABIC for 16 times with the  
1770 smallest abic= 0.3562608863E+04. This is attained by w1,...,w5 = 0.125D+00 0.599D+00  
1771 0.152D+02 0.415D+02 0.152D+04 (in the two lines before “----- xd ----- 4  
1772 3562.6088628260377”), and the bottom row shows their logarithms. See Appendix A for  
1773 the definitions and Appendix B for the numerical procedures.

1774 The file hist-etasp5pa.prt includes a large amount of output. It may be useful  
1775 to use the UNIX command egrep (grep) to extract lines of interest, for example,

```

1776 egrep xd hist-etasp5pa.prt
1777 egrep `xd | abic` hist-etasp5pa.prt

```

1778 show you just updated and all history of ABIC values, respectively.

1779 An example of the program output (hist-etasp5pa.omap) is as follows.

```

1780
1781 0.125287875259E+00 0.599470104176E+00 0.152196155562E+02 0.414782911682E+02 →
1782 0.152196155562E+04 0.356323892700E+04 1710 0.100000000000E+04

```

1783 0.114438254234E-03 0.334881321036E-04 0.647009682182E-02 0.146219408001E+01 →  
 1784 0.103833297334E+01 0.210022642758E-01 0.233332455954E+01  
 1785 0.374513210667E-03 0.675979122716E-04 0.265190771687E-03 0.354908735402E-03  
 1786 0.146433535062E-03 0.916947720816E-03 0.146338679517E-03 0.177204790397E-03  
 1787 0.922917100686E-04 0.114314194061E-03 0.106254935918E-02 0.112398922637E-03  
 1788 0.359109874846E-03 0.917853243391E-04 0.926876136674E-04 0.210983087983E-03  
 1789 0.513378081538E-04 0.610030246154E-04 0.151535542538E-03 0.237911207613E-03

1790 << skipped >>

1791 Here the first and second lines contain  $w_1, w_2, w_4, w_5, w_7, abic$ , and number of all  
 1792 coefficients  $1710 = 5 * (308+34)$  where 308 represents the number of earthquake and  
 1793 34 represents Delaunay apex on the boundary of the region; the last column represents  
 1794 the fixed dumping weight  $w_{0l}$  in the 8<sup>th</sup> row of the configuration file  
 1795 `hist-etass5pa.conf`.

1796 The third and fourth lines give the optimized baseline parameters  $\mu_0, K_0, c, \alpha, p, d$   
 1797 and  $q$ . The remaining values from fifth line to the bottom give logarithm of the  
 1798 location-dependent deviations from the baseline parameter values  $\mu_0, K_0, \alpha, p$  and  $q$ .

1799 See R display procedure and example figures of the optimal maximum a posterior  
 1800 (OMAP) estimate in §11.5.

1801  
 1802

### 1803 **Part III. PLOTTING SPATIAL PARAMETER ESTIMATES**

#### 1804 **11 Plot Spatial Variation of Parameters**

1805 This R program plots the Delaunay tessellation of various datasets; spatial intensity  
 1806 rate, location-dependent b-values of Gutenberg-Richter magnitude distribution, the  
 1807 spatial estimates of the ETAS parameters  $\mu$  and  $K_0$ , and location-dependent 5  
 1808 parameters  $\mu, K_0, \alpha, p$  and  $q$ . All of these are defined based on the Delaunay  
 1809 tessellations, over the observed spatial region. Incidentally, the users can use any  
 1810 available graphical packages for the display such as Matlab, Mathematica, GMT, etc.,  
 1811 by making their own program scripts using the present Fortran programs. The  
 1812 provided R and below figures are to show the examples. All the used files in this  
 1813 section are selected in the program directory of `Section11files/` in the program  
 1814 package.

1815

#### 1816 **11.1 Delaunay Tessellation for Spatial Variation**

1817

1818 Program: `delone-plot.R`

1819 Reads: `delone2.out`

1820 Requires: `drawmap.R, f2.R`

1821 Writes: `delone-plot.pdf`; see §6.5 for an example figure.

1822

#### 1823 **11.2 Spatial Occurrence Rate**

1824

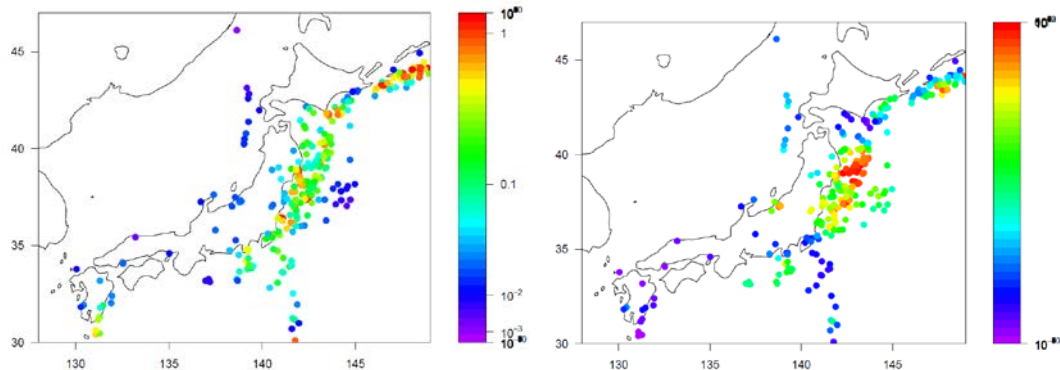
1825 Program: delo2d-poisson.R  
 1826 Reads: delone2.out, delo2d-poisson.omap  
 1827 Requires: drawmap.R, f2.R  
 1828 Writes: delo2d-poisson.pdf; see §8.3 for an example figure.  
 1829

### 1830 11.3 Spatially Varying $b$ -Value of Magnitude Frequency

1831  
 1832 Program: delo2d-bvalues.R  
 1833 Reads: delone2.out, delo2d-bvalues.omap  
 1834 Requires: drawmap.R, f2.R  
 1835 Writes: delo2d-bvalues.pdf; see §7.3 for an example figure.  
 1836

### 1837 11.4 ETAS: Spatially Varying $\mu$ and $K_0$

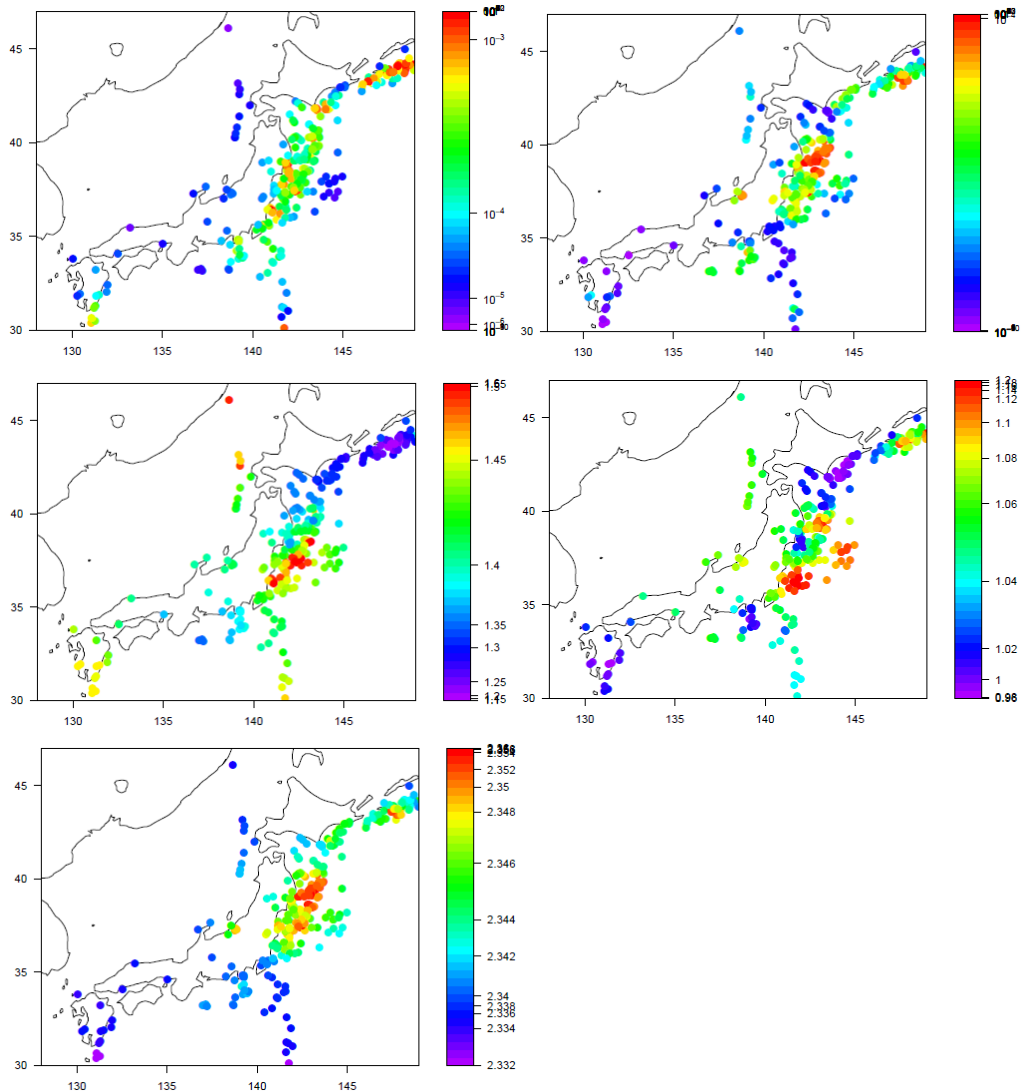
1838  
 1839 Program: hist-etask-mk.R  
 1840 Reads: delone2.out, hist-etask-mk.omap  
 1841 Requires: drawmap.R, f2.R  
 1842 Writes: hist-etask-mk.pdf; see the following for an example figure (Fig. 8).  
 1843



1844  
 1845 Fig. 8. hist-etask-mk.pdf:  $\mu$  and  $K_0$  in the order from the left to the right. The color  
 1846 table of  $K_0$ -values indicate that range of  $K_0$ -values change are very narrow.  
 1847

### 1848 11.5 ETAS: Spatial Variation in 5 Parameters

1849  
 1850 Program: hist-etask5pa.R  
 1851 Reads: delone2.out, hist-etask5pa.omap  
 1852 Requires: drawmap.R, f2.R  
 1853 Writes: hist-etask5pa.pdf; see the following for an example figure (Fig. 9).  
 1854



1855

1856

1857

1858 Fig. 9. `hist-etax5pa.pdf`: The estimated parameters ( $\mu$ ,  $K$ ,  $\alpha$ ,  $p$  and  $q$ ) in the order  
 1859 from the left to the right. The color table of  $K_0$ -values and  $q$ -values indicate that range of  
 1860  $K_0$ -values and  $q$ -values change are very narrow.

1861

1862

## 12 Plot interpolated images by Delaunay triangles

1863

1864

1865

1866

1867

The plotted color points in the last section shows the optimal maximum a posteriori (MAP) estimates on earthquake event locations which are also vertices of the Delaunay triangles (see the figure in §6.6). The MAP estimates are subject to the interpolation on any lattice points by the Delaunay triangles which include the lattice point.

1868

1869

1870

1871

1872

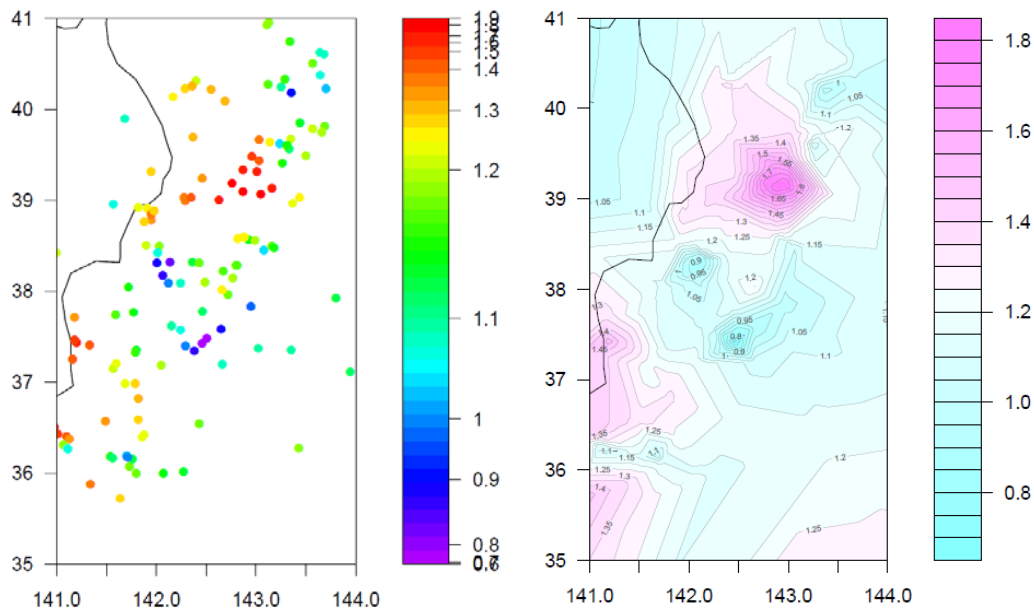
1873

1874

Note: The R-plotting procedures have been partly modified because the sub-module “filled1.contour” that was used in the previous version is no more available in the current R programme. Please use the followings from the program directory “estimations” in HIST-PPM-V2. In this version, we use `f2.r` instead, and to understand the new module, please consult “`help(filled contour)`” in R command. All the used files in this section are selected in the program directory of `Section12files/` in the program package.

1875  
1876  
1877 Program: interpolated.f ! Interpolation of the optimal MAP solution to lattice  
1878 image  
1879 Reads: interpolated.conf, delone2.out, and  
1880 either delo2d-bvalues.omap or delo2d-poisson.omap  
1881 Writes: interplated.pixel ! Output pixel images on lattice points  
1882  
1883 The FORTRAN program interpolated.f works for both *b*-value images and  
1884 Poisson intensity-rate image, whose configuration file interpolated.conf  
1885 includes the following three lines:  
1886  
1887 delone2.out  
1888 delo2d-bvalues.omap  
1889 128.0 30.0 141. 144. 35. 41. 100 100 !lon0, lat0, minlon maxlon, minlat, maxlat, nx, ny  
1890  
1891 For *b*-value images, this contains the following records; the first line includes the  
1892 Delone structural data, and the second line includes the optimal MAP solution of  
1893 *b*-values. The first two items (128.0, 30.0) in the third line indicate the origin of the  
1894 considered region in longitude and latitude, and the following four items are  
1895 longitudes and latitudes for the restricted region, and the last two numbers indicate  
1896 division of the restricted rectangular region into pixels.  
1897  
1898 Then the following are output example of interpolated.f, with filename  
1899 Interplated.pixel.  
1900  
1901 141.01 35.03 0.299E+00  
1902 141.01 35.09 0.306E+00  
1903 141.01 35.15 0.312E+00  
1904 141.01 35.21 0.319E+00  
1905 141.01 35.27 0.325E+00  
1906 141.01 35.33 0.331E+00  
1907 << skipped >>  
1908 143.99 40.73 0.727E-01  
1909 143.99 40.79 0.773E-01  
1910 143.99 40.85 0.727E-01  
1911 143.99 40.91 0.682E-01  
1912 143.99 40.97 0.636E-01  
1913  
1914  
1915 Then we can use:  
1916  
1917 Program: interpolated-bvalues.R  
1918 Reads: interplated-bvalue.pixel, interpolated-bvalues-conf  
1919 Requires: drawmap.R, delone2.out  
1920 Writes: interpolated-bvalues.pdf; see the right side for an example  
1921 figure (Fig. 10).  
1922

1923 Also, we can use:  
 1924  
 1925 Program: enlarge.R  
 1926 Reads: delone2.out, interpolated.conf  
 1927 Requires: drawmap.R, f2.R  
 1928 Writes: enlarged.pdf (= enlarged-bvalues.pdf); see the left-hand-side  
 1929 figure (Fig. 10).  
 1930  
 1931



1932  
 1933 Fig. 10: enlarged-bvalues.pdf, image.pdf (=interpolated-bvalues.pdf)  
 1934  
 1935

1936 For Poisson intensity rate image, the configuration file  
 1937 interpolated-poisson.conf includes the following three lines:  
 1938

```
1939 delone2.out
1940 delo2d-poisson.omap
1941 128.0 30.0 141. 144. 35. 41. 100 100 !lon0, lat0, minlon maxlon, minlat, maxlat, nx, ny
```

1942  
 1943 containing the following records; the first line includes the Delone data, and the  
 1944 second line includes the OMAP solution of Poisson intensity rates. The first two items  
 1945 (128.0, 30.0) in the third line indicate the origin (longitude, latitude) of the full  
 1946 region, and the following four items are longitude and latitude for the enlarged region,  
 1947 and the last two numbers indicate division of the enlarged rectangular region into  
 1948 pixels.

1949  
 1950 Then the following interpolated.poisson.pixel are output example of  
 1951 interpolated.f.

1952  
 1953

1954 141.01 35.03 0.129E+01  
 1955 141.01 35.09 0.134E+01  
 1956 141.01 35.15 0.140E+01  
 1957 141.01 35.21 0.145E+01  
 1958 141.01 35.27 0.150E+01

1959 << skipped >>

1960 143.99 40.73 0.162E+01  
 1961 143.99 40.79 0.166E+01  
 1962 143.99 40.85 0.163E+01  
 1963 143.99 40.91 0.160E+01  
 1964 143.99 40.97 0.157E+01

1965

1966 Then we can use:

1967

1968 Program: `interplated-poisson.R`

1969 Reads: `interplated-poisson.pixel, interplated-poisson.conf`

1970 Requires: `drawmap.R, f2.R`

1971 Writes: `image.pdf (= interpolated-poisson.pdf)`; see the right-side figure  
 1972 (Fig. 11).

1973

1974 Also, we can use:

1975

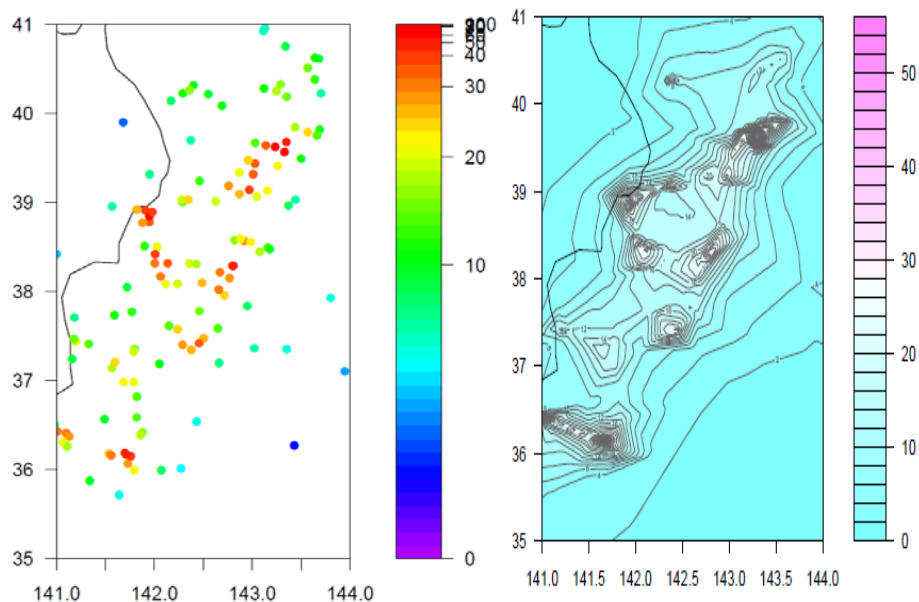
1976 Program: `enlarge.R`

1977 Reads: `delone2.out, interpolated.conf`

1978 Requires: `drawmap.R, f2.R`

1979 Writes: `enlarged.pdf (=enlarged-poisson.pdf)`; see left-side figure below  
 1980 (Fig. 11).

1981



1982

1983

1984 Fig. 11: `enlarged-poisson.pdf, image.pdf (=interpolated-poisson.pdf)`

1985

1986

1987  
 1988  
 1989  
 1990  
 1991  
 1992  
 1993  
 1994  
 1995  
 1996  
 1997  
 1998  
 1999  
 2000  
 2001  
 2002  
 2003  
 2004  
 2005

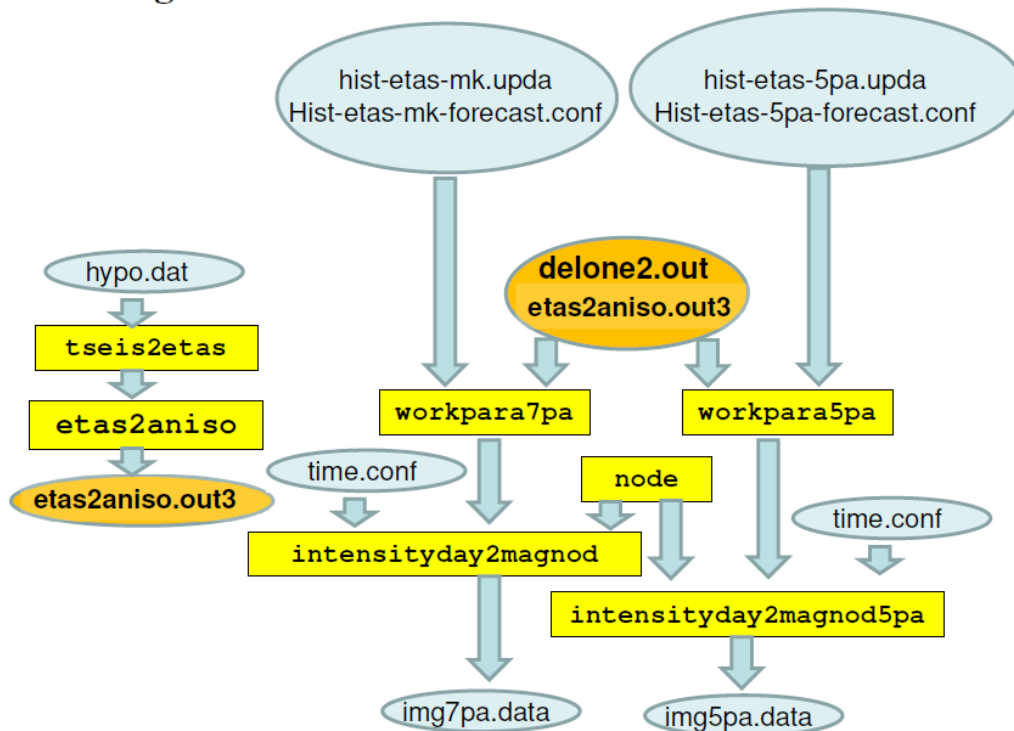
## Part IV. Short-Term Earthquake Forecasting

The estimated HIST-ETAS models of the previous period until a certain time instant is used to implement space-time forecasting of history-dependent seismicity rate after the previous period as moving images. Here, we assume that the model parameters do not change during the updated data until the present, and that the predictions are made on the basis of consecutively observed earthquakes.

The diagram (Fig. 12) below shows the flow chart of programs for estimations of the HIST-ETAS models and their forecasting. The hypocenter data `hypo.ts` and `hypo.dat` is connecting in time, that the first row of hypocenter data is last date of the `hypo.dat` in the same region. The flow chart details in the top block is the estimating procedure that were already explained in the above sections.

A job can be submitted interactively or in batch mode. Batch mode allows the user to log out of the system while the job continues to run in the background. The job could consist of a shell script (e.g. `job.sh`) or it may simply be a compiled FORTRAN binary file. The advantage of a shell script is that it can do other things before and after calling the compiled FORTRAN object.

### Forecasting flow chart



2006  
 2007  
 2008  
 2009  
 2010

Fig. 12: The diagram shows the flow of output from each program to subsequent programs. Rectangular shapes represent programs, which are explained below. Elliptical shapes represent input/output files.

2011 **13 Seismicity forecasts by the HIST-ETAS models**

2012 All the used files in this section are selected in the program directory of  
2013 Section13files/ in the program package.  
2014

2015 **13.1 hist-etas-mk forecast**

2016 Specifically, assume the estimated hist-etas-mk model  
2017 (hist-etas-mk.upda) calculated in §9 based on the data configuration in §9.2 for  
2018 the whole Japan  $M \geq 6$  earthquake data as illustrated in §4.3. Remember that the last  
2019 date of the data was the end of May 2011. After that, consider the following  
2020 hypocenter data of earthquakes of  $M \geq 4$  in the same Japan region as §11.4. The  
2021 following explains the consecutive implementation of unix (linux) shell script of  
2022 [japan.sh]:

```
2023  
2024 ifort tseis2etas.f -o tseis2etas  
2025 ./tseis2etas < hypo.dat (output-file, work.etas)  
2026  
2027 ifort etas2aniso.f -o etas2aniso  
2028 ./etas2aniso (input-files, work.etas, etas2aniso.conf; output-file,  
2029 etas2aniso.out2, etas2aniso.out3, etas2aniso.out4,  
2030 etas2aniso.out8, etas2aniso.out9)  
2031  
2032 ifort workpara7pa.f -o workpara7pa  
2033 ./workpara7pa (input-files,, hist-etas-mk-forecast.conf,  
2034 hist-etas-mk.upda, delone2.out, node.dat, etas2aniso.out3; output-file,  
2035 work.para)  
2036  
2037 ifort node.f -o node  
2038 ./node (input-files, node.conf, work.etas; output-file, node.dat)  
2039  
2040 ifort intensityday2magnod.f -o intensityday2magnod  
2041 ./intensityday2magnod (input-files, time.conf, hist-etas-mk.conf,  
2042 hist-etas-mk.upda, node.dat, work.para; output-file, img1.data)
```

2043

2044 Instead of Intel-Fortran, gfortran can be also used here.

2045

2046 Firstly, by using the HIST-ETAS model estimations based on [hypo.ts] in §3.2,  
2047 we will forecast sequentially using the following updating earthquake data  
2048 [hypo.ts]:

2049

2050 2011 06 01 01 26 7.97 143.3522 40.2497 11.65 5.1

```

2051 2011 06 01 01 30 57.07 143.2218 35.2540 76.00 4.4
2052 2011 06 01 01 41 19.63 141.7620 37.6593 43.71 4.2
2053 2011 06 01 02 15 17.19 141.9967 38.8785 49.52 4.1
2054 2011 06 01 06 27 33.93 143.4100 39.8478 27.23 4.5
2055 2011 06 01 07 07 45.40 143.4283 39.8302 20.98 4.1
2056 2011 06 01 07 28 40.90 143.8588 37.6817 36.00 4.1
2057 2011 06 01 08 53 59.04 141.9093 38.6377 48.79 4.2
2058 2011 06 01 12 14 11.03 143.7070 39.7765 33.00 5.1
2059 2011 06 01 13 00 1.01 142.2350 36.7177 16.24 4.5
2060
2061
2062 2018 09 25 14 19 23.31 148.1022 43.9925 0.00 4.4
2063 2018 09 25 22 03 13.75 148.4427 44.0177 0.00 4.0
2064 2018 09 26 01 22 13.29 148.2313 44.0835 0.00 4.0
2065 2018 09 27 10 25 21.45 141.9518 34.1040 34.65 4.3
2066 2018 09 28 04 32 25.27 141.1032 37.1130 52.21 4.0
2067 2018 09 28 10 01 2.37 148.3172 44.0750 0.00 4.2
2068 2018 09 29 18 25 54.33 142.0007 42.7707 35.36 4.2
2069 2018 09 29 20 56 34.07 140.9535 35.8075 29.75 4.0
2070 2018 09 30 17 54 4.49 141.9897 42.5498 36.86 4.9
2071 2018 10 01 11 22 3.35 142.0100 42.7940 34.81 4.7
2072

```

2073 Here, to save file memory size, we restrict `hypo.dat` to including only  $M \geq 4$   
2074 earthquakes, but practically for accuracy of the analysis of the anisotropy, it is  
2075 certainly preferred to take all detected earthquakes with hypocenter data.

2076 Then, the program `tseis2etas` transforms this data to `[work.etas]` as given in  
2077 the same format as given in §3.2. We use same program `etas2aniso` with the same  
2078 configuration file, `etas2aniso.conf`:

```

2079
2080 ./work.etas !input data
2081 6.0 6.0 !clms cutm
2082 0.04666667 !xxx(day)= time span for analyzing centroid and anisotropy

```

2083  
2084 Here, from a real-time forecasting perspective, we usually set `xxx=1/24 =`  
2085 `0.041666667 day = one hour` “to quickly determine the centroid location and  
2086 orientation characteristics of the impending aftershock sequence after a main shock  
2087 event. For the recent catalog, events within an hour interval after the main shock to  
2088 give a reasonably good estimate of the centroid and orientation characteristics of the  
2089 evolving aftershock sequence.

2090 Then, by implementing the program `etas2aniso` that is actually the same  
2091 program in §3 and §4, we get the output `etas2aniso.out3`:

```

2092
2093      82 0.128E+03 0.149E+03 0.209E+02 0.300E+02 0.469E+02 0.169E+02
2094      31 143.83320 37.30250 6.10 2.37850 1.00000 1.00000 0.00000
2095     125 143.58270 37.81170 6.00 13.92144 1.00000 1.00000 0.00000
2096     155 141.82130 37.61770 6.00 17.85491 1.00000 1.00000 0.00000
2097     187 142.59080 39.94780 6.90 22.28531 1.00000 1.00000 0.00000
2098     289 143.29852 38.06312 7.30 39.41467 1.00000 1.00000 0.00000
2099     405 142.09120 38.87370 6.40 52.56555 1.00000 1.00000 0.00000
2100     414 141.62670 37.70870 6.30 54.16071 1.00000 1.00000 0.00000
2101     457 141.22130 36.90320 6.50 60.16239 1.00000 1.00000 0.00000

```

```

2102      473 138.54880 34.70700 6.20 61.99874 1.00000 1.00000 0.00000
2103      . . .
2104      5379 144.48870 38.03600 6.30 2304.06758 1.00000 1.00000 0.00000
2105      5387 142.45530 40.26670 6.10 2310.22374 1.00000 1.00000 0.00000
2106      5396 143.94830 37.43530 6.30 2319.70802 1.00000 1.00000 0.00000
2107      5468 144.80580 38.00620 6.00 2357.30843 1.00000 1.00000 0.00000
2108      5473 140.74530 32.35200 6.00 2360.78026 1.00000 1.00000 0.00000
2109      5568 142.44800 41.00970 6.30 2429.82731 1.00000 1.00000 0.00000
2110      5646 132.58320 35.17803 6.10 2504.06425 0.00546 0.00724 -0.73698
2111      5733 135.62170 34.84430 6.10 2574.33234 1.00000 1.00000 0.00000
2112      5760 140.59200 35.16530 6.00 2593.84987 1.00000 1.00000 0.00000
2113      5840 142.00670 42.69080 6.70 2654.13055 0.02837 0.06975 0.52842

```

2114

2115 contains the centroid locations and normalized ellipsoidal coefficients for all event  
2116 with magnitude not less than the cutoff magnitude, except for the first row that is the  
2117 number of the additional  $M \geq 6$  data, ranges of longitudes and latitudes (see  
2118 `hist-etas-mk-forecast.conf`). The other outputs, `etas2aniso.out2`,  
2119 `etas2aniso.out4`, `etas2aniso.out8`, and `etas2aniso.out9` are also explained in  
2120 §4.1.

2121

2122 We then use the input configuration file `hist-etas-mk-forecast.conf`:

2123

```

2124 21.0 17.0 14012.0 308 !longitude span, latitude span, time span, starting time (days)
2125 of forecasting (= end time of the estimated period) for the hist-etas-mk model, and
2126 number of  $M \geq 6$  earthquakes to forecast.

```

2127

```

2128 128.0 30.0 6.0 0.0 730.0 2.0 !origin of the target rectangular region, cutoff
2129 magnitude, origin of time and end time of the short-term forecasting period. for the ranges of
2130 spatial rectangular region, time span, magnitude cutoff, etc.

```

2130

2131 We also use the Delaunay tessellation of the precursory period [`delone2.out`] in  
2132 §6.4 to obtain [`work.para`] above by interpolating the `hist-etas-mk` coefficients  
2133 [`hist-etas-mk.upda`] for each node; these coefficients are unchanged for the data.

2134

2134 Then we apply the program `workpara7pa` to make the summarized file

2135

2135 [`work.para`]:

2136

```

2137 -0.195903E+01 -0.770966E-01 143.8332 37.3025 6.1 14014.37850 1.0000 1.0000 0.0000
2138 -0.114274E+01 0.493784E-01 143.5827 37.8117 6.0 14025.92144 1.0000 1.0000 0.0000
2139 0.143420E+01 0.690773E-01 141.8213 37.6177 6.0 14029.85491 1.0000 1.0000 0.0000
2140 0.252823E+00 0.274905E+00 142.5908 39.9478 6.9 14034.28531 1.0000 1.0000 0.0000
2141 -0.156295E+00 0.200900E+00 143.2985 38.0631 7.3 14051.41467 1.0000 1.0000 0.0000
2142 0.180846E+01 0.622751E+00 142.0912 38.8737 6.4 14064.56555 1.0000 1.0000 0.0000
2143 0.167737E+01 -0.147276E-01 141.6267 37.7087 6.3 14066.16071 1.0000 1.0000 0.0000
2144 -0.204882E-01 0.155726E+00 141.2213 36.9032 6.5 14072.16239 1.0000 1.0000 0.0000
2145 -0.497493E+00 -0.208164E+00 138.5488 34.7070 6.2 14073.99874 1.0000 1.0000 0.0000
2146 -0.391050E-01 0.153219E+00 141.1610 36.9688 6.1 14084.14033 1.0000 1.0000 0.0000

```

2147

```

2148 -0.205721E+01 0.309927E-01 144.4887 38.0360 6.3 16316.06758 1.0000 1.0000 0.0000
2149 0.325441E+00 0.119500E+00 142.4553 40.2667 6.1 16322.22374 1.0000 1.0000 0.0000
2150 -0.203715E+01 -0.457134E-01 143.9483 37.4353 6.3 16331.70802 1.0000 1.0000 0.0000

```

```

2151  -0.215702E+01  -0.979918E-01  144.8058 38.0062 6.0 16369.30843  1.0000  1.0000  0.0000
2152  -0.392149E+00  -0.275451E+00  140.7453 32.3520 6.0 16372.78026  1.0000  1.0000  0.0000
2153   0.453226E+00  -0.209358E+00  142.4480 41.0097 6.3 16441.82731  1.0000  1.0000  0.0000
2154  -0.312373E+01  -0.554472E+00  132.5832 35.1780 6.1 16516.06425  0.0055  0.0072 -0.7370
2155  -0.179847E+01  -0.457204E+00  135.6217 34.8443 6.1 16586.33234  1.0000  1.0000  0.0000
2156   0.471500E+00  -0.303005E+00  140.5920 35.1653 6.0 16605.84987  1.0000  1.0000  0.0000
2157  -0.148886E+01  -0.325565E+00  142.0067 42.6908 6.7 16666.13055  0.0284  0.0698  0.5284

```

2158

2159 for the additional earthquake in each raw, and the first two columns represent location  
2160 dependent deviations from the baseline parameters  $\log(\mu_0)$  and  $\log(K_0)$  of the  
2161 `hist-etas-mk` model, respectively; 3 - 6 column stands for longitudes, latitudes,  
2162 magnitudes and occurrence times in days unit, respectively. The last three columns  
2163 indicate the anisotropic information of triggered descendants (same as those of  
2164 `etas2aniso.out3` in the above); and `hist-etas-mk.upda` is the estimated  
2165 coefficients of  $\mu$  and  $K$  by the program `hist-etas-mk` in §9 for each  $M \geq 6$   
2166 earthquakes and some added points including those of boundaries from precursory  
2167 period for the estimation.

2168 Finally, given the time of the snapshot image `time.conf`:

2169

```

2170 1780.05 ! one-hour after M6.5; time of intensity in days = see work.etas for the
2171 time in days

```

2172

2173 in addition to the program `node` set coordinates of pixel node on which predicted  
2174 intensity rate are given where the input configuration file is `node.conf`:

2175

```

2176 128. 149. 30. 47. ! longitude and latitude ranges for all Japan Area
2177 210 170 ! number of pixels for image,

```

2178

2179 which means that the resolution degree of the intensity image is unit pixel of  $0.1^2 \text{ deg}^2$   
2180 and unit time of 1 day, so that the each probability of  $M \geq 6$  earthquake in the  
2181 space-time unit is  $100^{-1}$  times of the intensity value; note that the estimated intensity  
2182 values are per  $1.0 \text{ deg}^2$  and per day.

2183 The output file is given in such a way that `node.dat`:

2184

```

2185 128.0500 30.0500
2186 128.0500 30.1500
2187 128.0500 30.2500
2188 128.0500 30.3500
2189 128.0500 30.4500
2190 128.0500 30.5500
2191 128.0500 30.6500
2192 128.0500 30.7500
2193 128.0500 30.8500
2194 128.0500 30.9500

```

2195 . . .

```

2196 148.9500 46.0500
2197 148.9500 46.1500
2198 148.9500 46.2500
2199 148.9500 46.3500
2200 148.9500 46.4500
2201 148.9500 46.5500

```

```

2202      148.9500    46.6500
2203      148.9500    46.7500
2204      148.9500    46.8500
2205      148.9500    46.9500
2206

```

2207 for the locations at which the intensity is calculated.

2208 For the snapshot at the time instances in `time.conf`, the program  
2209 `intensityday2magnod` provides the location-dependent seismicity rates on the  
2210 given node locations as the output [`img1.data`]:

```

2211
2212      1780.05000  128.0500  30.0500  -4.48152
2213      1780.05000  128.0500  30.1500  -4.35851
2214      1780.05000  128.0500  30.2500  -4.22291
2215      1780.05000  128.0500  30.3500  -4.07589
2216      1780.05000  128.0500  30.4500  -3.92018
2217      1780.05000  128.0500  30.5500  -3.76075
2218      1780.05000  128.0500  30.6500  -3.60562
2219      1780.05000  128.0500  30.7500  -3.46630
2220      1780.05000  128.0500  30.8500  -3.35696
2221      1780.05000  128.0500  30.9500  -3.29134

```

```

2222      . . .

```

```

2223      1780.05000  148.9500  46.0500  -5.00901
2224      1780.05000  148.9500  46.1500  -5.04269
2225      1780.05000  148.9500  46.2500  -5.14049
2226      1780.05000  148.9500  46.3500  -5.17804
2227      1780.05000  148.9500  46.4500  -5.21446
2228      1780.05000  148.9500  46.5500  -5.24642
2229      1780.05000  148.9500  46.6500  -5.27794
2230      1780.05000  148.9500  46.7500  -5.31176
2231      1780.05000  148.9500  46.8500  -5.34829
2232      1780.05000  148.9500  46.9500  -5.38806

```

```

2233

```

2234 for the forecasting based on `hist-etas-mk` model, where the last column represents  
2235 the ordinary logarithm of the intensity values.

```

2236

```

```

2237

```

## 2238 13.2 hist-etas-5pa forecast

2239 The shell script `japan.sh` provides the same procedure as the above `japan.sh`  
2240 except for using `workpara5pa` instead of `workpara7pa`, and  
2241 `intensityday2magnod5pa` instead of `intensityday2magnod`. The program  
2242 `workpara7pa` make the summarized file [`work para`]:

```

2243

```

```

2244      -0.173143E+01  -0.235180E+00  -0.177008E-01  0.525061E-01  0.450011E-02  143.8332  37.3025  6.1 14014.37850  1.0000  1.0000  0.0000
2245      -0.968881E+00  -0.969090E-01  -0.150673E-01  0.472810E-01  0.520681E-02  143.5827  37.8117  6.0 14025.92144  1.0000  1.0000  0.0000
2246      0.141514E+01  -0.370253E-01  -0.112767E-01  0.830377E-02  0.581182E-02  141.8213  37.6177  6.0 14029.85491  1.0000  1.0000  0.0000
2247      0.308055E+00  0.249292E+00  -0.574826E-01  0.147485E-01  0.628059E-02  142.5908  39.9478  6.9 14034.28531  1.0000  1.0000  0.0000
2248      -0.105439E+00  0.816887E-01  -0.764281E-02  0.320480E-01  0.580723E-02  143.2985  38.0631  7.3 14051.41467  1.0000  1.0000  0.0000
2249      0.178974E+01  0.628283E+00  -0.426934E-01  0.234688E-01  0.707487E-02  142.0912  38.8737  6.4 14064.56555  1.0000  1.0000  0.0000
2250      0.156352E+01  -0.108644E+00  -0.226194E-01  0.775780E-02  0.544244E-02  141.6267  37.7087  6.3 14066.16071  1.0000  1.0000  0.0000
2251      0.174968E+00  0.100107E+00  -0.824457E-02  0.477913E-01  0.566260E-02  141.2213  36.9032  6.5 14072.16239  1.0000  1.0000  0.0000
2252      -0.457258E+00  -0.190316E+00  -0.559044E-01  -0.398870E-02  0.304299E-02  138.5488  34.7070  6.2 14073.99874  1.0000  1.0000  0.0000
2253      0.149485E+00  0.993812E-01  -0.990510E-02  0.416871E-01  0.569163E-02  141.1610  36.9688  6.1 14084.14033  1.0000  1.0000  0.0000

```

2254

. . .

2255	-0.187238E+01	-0.790851E-01	-0.247511E-01	0.697094E-01	0.493365E-02	144.4887	38.0360	6.3	16316.06758	1.0000	1.0000	0.0000
2256	0.330056E+00	0.121612E+00	-0.695166E-01	0.102073E-01	0.592056E-02	142.4553	40.2667	6.1	16322.22374	1.0000	1.0000	0.0000
2257	-0.180773E+01	-0.188937E+00	-0.187992E-01	0.553893E-01	0.458487E-02	143.9483	37.4353	6.3	16331.70802	1.0000	1.0000	0.0000
2258	-0.202072E+01	-0.218767E+00	-0.327643E-01	0.612950E-01	0.439912E-02	144.8058	38.0062	6.0	16369.30843	1.0000	1.0000	0.0000
2259	-0.463733E+00	-0.276171E+00	-0.344978E-01	0.223125E-02	0.136756E-02	140.7453	32.3520	6.0	16372.78026	1.0000	1.0000	0.0000
2260	0.375490E+00	-0.212455E+00	-0.715324E-01	-0.159353E-01	0.450233E-02	142.4480	41.0097	6.3	16441.82731	1.0000	1.0000	0.0000
2261	-0.300655E+01	-0.604138E+00	-0.335803E-01	0.646442E-02	0.977202E-03	132.5832	35.1780	6.1	16516.06425	0.0055	0.0072	-0.7370
2262	-0.180156E+01	-0.483693E+00	-0.572613E-01	0.122522E-01	0.188226E-02	135.6217	34.8443	6.1	16586.33234	1.0000	1.0000	0.0000
2263	0.486403E+00	-0.386306E+00	-0.298320E-01	0.209163E-01	0.284362E-02	140.5920	35.1653	6.0	16605.84987	1.0000	1.0000	0.0000
2264	-0.140339E+01	-0.302433E+00	-0.730526E-01	-0.172558E-01	0.320788E-02	142.0067	42.6908	6.7	16666.13055	0.0284	0.0698	0.5284

2265

2266 for the additional earthquakes in each raw, where the first 5 columns represent  
 2267 location dependent deviations from the logarithm of reference values  $\mu_0, K_0, \alpha_0, p_0$   
 2268 and  $q_0$  (the top five numbers in `hist-etas5pa.upda`), respectively, at each  
 2269 hypocenter location of longitudes, latitudes, magnitudes and occurrence times in days  
 2270 unit, respectively, given in 6 - 9 columns. The last three columns indicate the  
 2271 anisotropic information of triggered descendants (same as `etas2aniso.out3`). The  
 2272 input files are:

2273 [`hist-etas5pa-forecast.conf`]

2274

2275	21.0	17.0	14012.	308								
2276	128.0	30.0	6.0	0.0	730.0	2.0						

2277

2278 for the ranges of spatial rectangular region, time span, magnitude cutoff, etc., as  
 2279 explained for `hist-etas7pa-forecast.conf` in the above.

2280

2281 The program `intensityday2magnod` provides the location-dependent  
 2282 seismicity rates on the given node locations as the output [`img1.data`]:

2283

2284	1780.05000	128.0500	30.0500	-4.47764
2285	1780.05000	128.0500	30.1500	-4.35814
2286	1780.05000	128.0500	30.2500	-4.22522
2287	1780.05000	128.0500	30.3500	-4.08007
2288	1780.05000	128.0500	30.4500	-3.92552
2289	1780.05000	128.0500	30.5500	-3.76672
2290	1780.05000	128.0500	30.6500	-3.61197
2291	1780.05000	128.0500	30.7500	-3.47310
2292	1780.05000	128.0500	30.8500	-3.36457
2293	1780.05000	128.0500	30.9500	-3.30022

2294

. . .

2295	1780.05000	148.9500	46.0500	-4.90040
2296	1780.05000	148.9500	46.1500	-4.93188
2297	1780.05000	148.9500	46.2500	-5.01747
2298	1780.05000	148.9500	46.3500	-5.05222
2299	1780.05000	148.9500	46.4500	-5.08627
2300	1780.05000	148.9500	46.5500	-5.11626
2301	1780.05000	148.9500	46.6500	-5.14587
2302	1780.05000	148.9500	46.7500	-5.17757
2303	1780.05000	148.9500	46.8500	-5.21170
2304	1780.05000	148.9500	46.9500	-5.24869

2305  
2306 for the forecasting based on `hist-etas-5pa` model.  
2307  
2308

### 2309 13.3 Magnified forecasting image in a localized region

2310 The shell script `kumamoto.sh` provides the same procedure as the above `japan.sh`  
2311 except for the restriction of regions as given by `node.conf`:

```
2312  
2313 130. 132. 32. 34.    !longitude and latitude ranges for Kumamoto Area  
2314 200 200              ! number of pixels for image
```

2315  
2316 where the number of pixels adjust the resolution of image.  
2317  
2318

### 2319 13.4 Plotting Snapshots of Short-Term Forecast Images

2320 The example output images with relevant maps are given by R language:

```
2321 Program:  japan.r  
2322 Reads:    img1.data, work.para, node.conf  
2323 Requires: drawmap.r, f2.r > filled2contour.r > see  
2324           help(filled.contour) in R command.  
2325 Writes:   Rplots.pdf; see the left-hand-side figure below (Fig. 13).  
2326
```

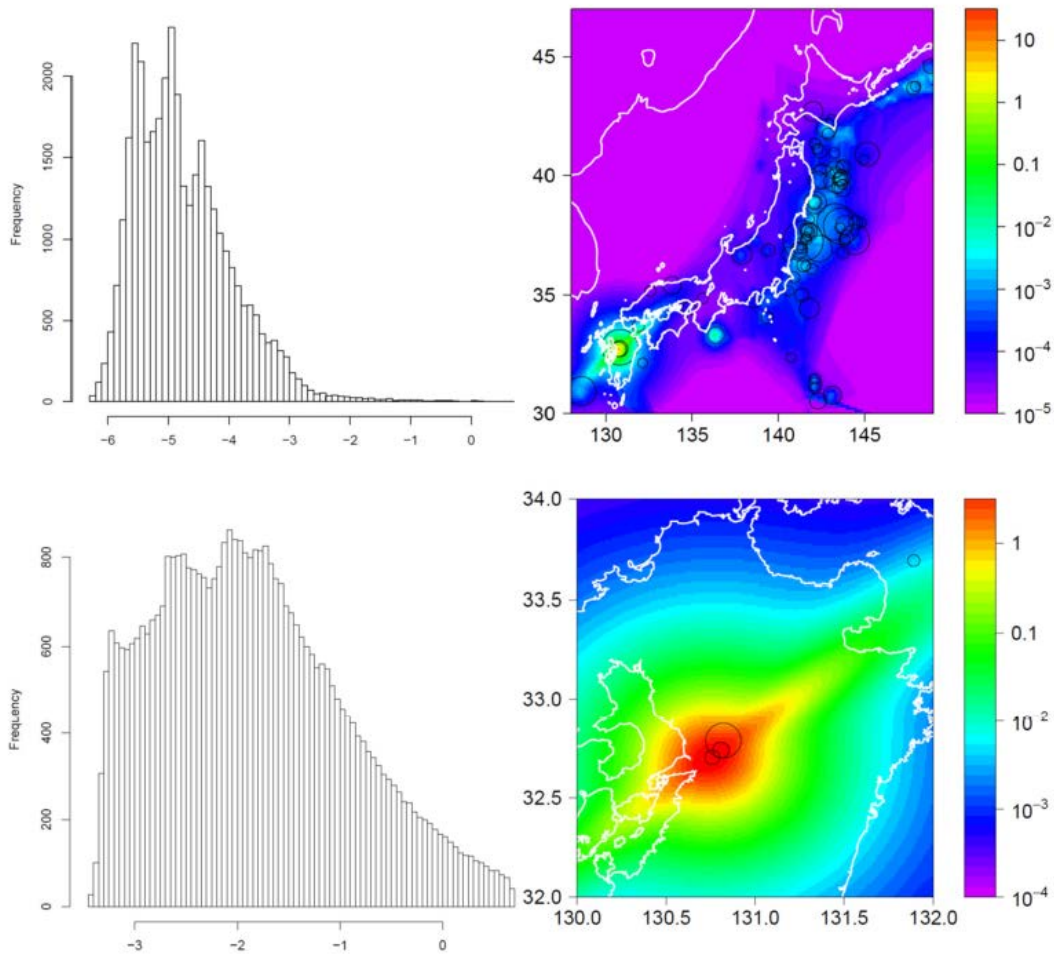
2327 The example output images for the magnified region can be seen in:

```
2328  
2329 Program:   kumamoto.r  
2330 Reads:     img1.data, work.para, nodekuma.conf  
2331 Requires:  drawmap.r, f2.r  
2332 Writes:    Rplors.pdf; see the right-hand-side of the below figure (Fig.13).  
2333
```

2334 We get the following panels of `Rplot.pdf` that delineates snapshots of the  
2335 short-term probability forecast at the time of one-hour after the M6.5 Kumamoto  
2336 Earthquake (see `time.conf` above). These are conditional intensity function  
2337  $\lambda(t, x, y | H_t)$  as mathematically defined in §A.5

2338  
2339

2340  
2341



2342  
2343  
2344  
2345  
2346  
2347  
2348  
2349  
2350  
2351

Fig. 13: Snapshots of probability forecasts of  $M \geq 6$  earthquakes at one-hour after the largest  $M6.4$  foreshock before the 2016  $M7.3$  Kumamoto earthquake; image in the main Japan area and enlarged image in Kyushu area. The circles indicate actual  $M \geq 6$  earthquakes occurring during the forecast periods. The histograms show the frequency of intensity values at each pixel against the ordinary logarithm of the intensity. Color scale of the image shows expected number of  $M \geq 6$  earthquakes per one square degree ( $\sim 100\text{km}^2$ ) per day.

2352  
2353  
2354  
2355  
2356  
2357  
2358  
2359  
2360

## Part V. Simulations

This chapter provides the simulation of hypocenters using the nonhomogeneous Poisson model, spatial magnitudes using by space-dependent b-values, HIST-ETAS-mk model and HIST-ETAS-5pa model. Examples here use the intensity b-values and conditional intensities estimated in §7 ~ §10.

### 14. Nonhomogeneous Poisson simulation by spatial intensity rate function

2361  
2362

This program fits a nonhomogeneous spatial Poisson model with stationary Poisson time component to the location of earthquakes. The simulation is done using the 2D

2363 spatial Poisson intensity given by coefficients at the nodes of the Delaunay  
2364 tessellations (§6) and their interpolations can be found §12. All the used files in this  
2365 section are in the program directory of `Section14files/` in the program package.

2366     Mathematical explanation of Poissonian spatial intensity is described in §A.3.

2367

#### 2368 14.1 File Names

2369 For the example we use the intensity estimated in §8:

2370 Program: `simNHPoisson.f`

2371 Object: `simNHPoisson`

2372 Configuration: `poisson.conf`

2373 Reads: `delone2.out`, `delo2d-poisson.omap`

2374 Writes: `fort.2` (= `simNHPoi.hypo`)

2375

2376 For the spatial plot, done in R:

2377 Program: `fort2.R`

2378 Reads: `fort.2`, `drawmap.r`, `../MapsData/jp.br.dat` & `jp.pp.dat`

2379 Writes: `Rplots.pdf` (= `1993.1119.1046.pdf`)

2380

#### 2381 14.2 Configuration File Format

2382 The configuration file `poisson.conf` includes the following three lines:

2383 `128.0 21.0 30.0 17.0 ! xmin, ymin, tx, ty`

2384 `1993 1119 1046 !4 digit seeds of for a series of uniform random numbers, where different`

2385     seeds are expected to provide mutually independent random number series.

2386

#### 2387 14.3 Program Execution

2388 For the simulations, done in FORTRAN:

2389 `./simNHPoisson |tee simNHPoisson.prt !which is given in Section14files/.`

2390

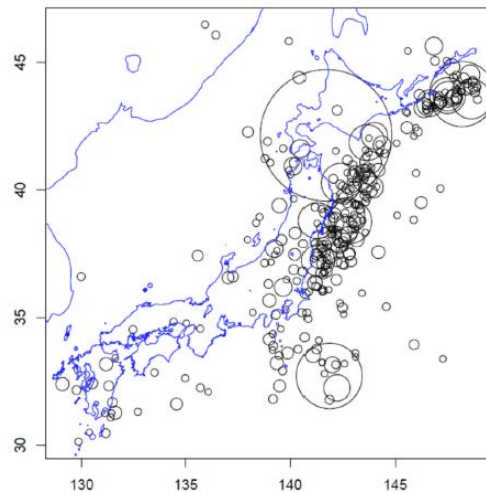
2391 For the spatial plot, done in R:

2392 `> source('r.fort2')`

2393 Writes: `Rplots.pdf` (= `1993.1119.1046.pdf`); which shows the following plot (Fig.

2394 14):

2395



delo2d-poisson.pdf:

Fig. 14. Simulated epicenter coordinates by the nonhomogeneous Poisson intensity §8.3 in and around mainland Japan. Sizes of circle radii are proportional to exponential of the same magnitude series ( $M \geq 6$ ) of the original JMA data.

After simulation we can make reestimation of nonhomogeneous Poisson intensity, starting from constructing the new Delone tessellation of the simulated data.

## 15. Magnitude simulation given spatially varying $b$ -values of G-R law

These programs simulate magnitudes given the  $b$ -value over a spatial region. Magnitude are simulated by GR-law at any location based on  $b$ -values interpolated on the Delaunay tessellations (§6). All used files in this section are selected in the program directory of Section15files/ in the program package.

### 15.1 File Names

For the simulations, done in FORTRAN:

Program: bvalue2magsim.f

Object: bvalue2magsim

Configuration: delo2d-bvalues.conf !same as poisson.conf in §14.2

Reads: delone2.out

Writes: fort.2 (= fort.2Mc595, fort.2.Poiconfig)

For the spatial plot, done in R:

Program: fort2.R

Reads: fort.2, drawmap.r, ../MapsData/jp.br.dat & jp.pp.dat

Writes: Rplots.pdf (= original2magsim.pdf, binterpo2magsim.pdf)

## 2425 15.2 Configuration File Format

2426 The configuration file `delo2d-bvalues.conf` includes the following three lines:

```
2427 128 . 30 . 5.95 !xmin, ymin, threshmag = magnitude threshold
```

```
2428 6.0d0 !w1, which used in §8, but not used here.
```

```
2429 7 !ipr, which used in §8, but not used here.
```

2430

2431 Magnitude rounding issue: if magnitude data are rounded to 0.1 units, the threshold  
2432 magnitude here should be modified to 5.95 ( $= M_c - 0.05$ ) to avoid the  $b$ -value MLE  
2433 bias. This is because a rounded value of 6.0 may have been as small as 5.95 or large  
2434 as 6.05. This applies to the traditional catalogs such as the JMA, NEIC-PDE, and ISC  
2435 catalogs. Otherwise, namely, less than 0.01 magnitude unit, we can keep `threshmag =`  
2436 `6.0`.

2437

## 2438 15.3 Program Execution

2439 FORTRAN execution command:

```
2440 ./delo2d-bvalues |tee delo2d-bvalues.prt !which is given in
```

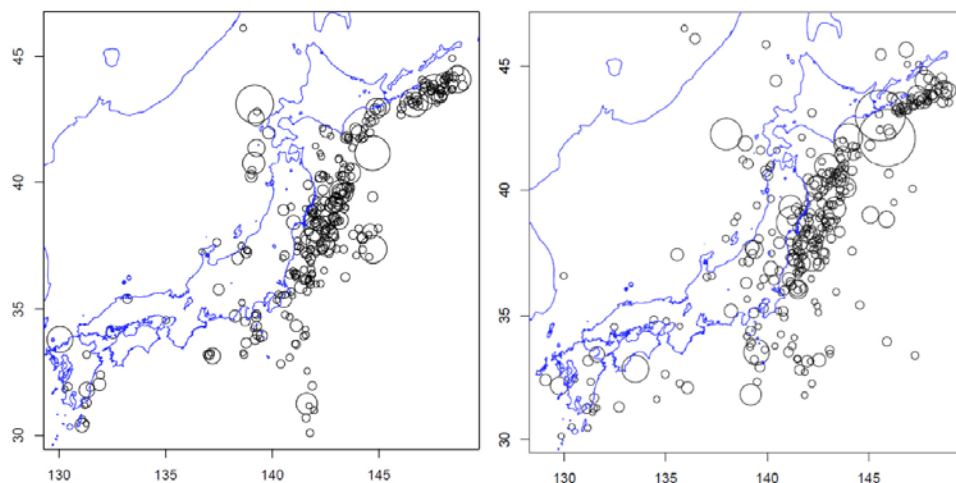
```
2441 Section16files/.
```

2442

2443 For the spatial plot, done in R:

```
2444 > source('delo2d-bvalues.R') ; which shows the following two plots (Fig. 15):
```

2445



2446

2447 Fig. 15. Simulated earthquake magnitudes on the epicenter coordinates of the JMA data (left  
2448 panel) and on the locations (right panel) simulated by the nonhomogeneous Poisson intensity.  
2449 Sizes of circle radius is proportional to exponential of simulated magnitudes ( $M > 5.95$ ) by the  
2450 interpolated  $b$ -values in §7.3.

2451

2452 After simulation we can make re-estimation of  $b$ -values, starting from  
2453 constructing the new Delaunay tessellation of the simulated data.

2454  
2455  
2456

## 16. HIST-ETAS simulation

2457       The programs in this section produce simulated data files for given sets of  
2458 parameters in the point process model used in HIST-ETAS models (See Ogata, 1981,  
2459 1998) for theoretical basis. It is noted that the intensity defined by a combination of  
2460 parameter values should be well-defined; due to some combinations of parameter  
2461 values, the simulated data can be explosive (Zhuang and Ogata, 2006).

2462       There are two options; either using magnitudes in `delone2.out` or simulating  
2463 magnitude by (modified) Gutenberg-Richter's Law. The first option simulates the  
2464 same number of events that are not less than threshold magnitude in the data, this is  
2465 the present option, and therefore the parameter  $b$ -value is not used in this particular  
2466 example. For the second option, you have to provide  $b$ -value of G-R law and number  
2467 of events to be simulated; you can simply modify the FORTRAN program  
2468 `histetasim.f` below by changing the commented line to execute for simulating  
2469 magnitude sequence.

2470       Furthermore, simulation can start based on an occurrence history of precursory  
2471 period; the users may also extend these program.

2472       Finally, the program `histetasim.f` here support only the case of isotropic  
2473 clustering that ignores the last three columns of `delone2.out`, but, if necessary, this can  
2474 be extended by modifying `histetasim.f` in reference of subroutine `func17` of the  
2475 optimization programs `hist-etas-mk.f` or `hist-etas5pa.f` in sections 9 and 10  
2476 or forecasting programs in Section 13, with the same the format of the current  
2477 `delone2.out`.

2478

2479       The FORTRAN program `histetasim.f` needs configuration `histetasim.conf`  
2480 as explained below. The example of input file is the same as `hist-etas-mk.upda` or  
2481 `hist-etas5pa.upda` which was the output in sections 9 and 10, respectively. All used  
2482 files in this section are selected in the program directory of `Section16files/` in the  
2483 program package .  
2484

2485

2486

### 16.1 File names

2487       For the simulation, done in FORTRAN:

```
2488 Program: histetasim.f
2489 Object: histetasim
2490 Configuration: histetasim.conf
2491 Reads: delone2.out,
2492         hist-etas-mk.upda, or
2493         hist-etas5pa.upda
2494 Writes: histetasim.prt, fort.7, fort.2
```

2495

2496       For the spatial plot, done in R:

2497 Program: histetasim.R  
2498 Reads: fort.2, fort.7,  
2499 drawmap.r, ../MapsData/jp.br.dat & jp.pp.dat  
2500 Writes: Rplots.pdf (= 7pa1993,1119,1046.pdf or 5pa1993,1119,1046.pdf)

2501  
2502

## 2503 16.2 Configuration File Format

2504 Explanation of the configuration file `histetasim.conf` consists of:

2505 5 !Choose either of simulation model 7 or 5 for `hist-etas-mk` or  
2506 `hist-etas5pa`, respectively

2507 1.1 6.0 128.0 21.0 30.0 17.0 14012.0 !bmg,cm0,tx0,tx,ty0,ty,tend  
2508 1993 1119 1046 !Seeds of uniform random number series; triplet four digits.

2509 The variable `bmg` and `cm0` stand for *b*-value, lower cutoff magnitude, respectively; `tx0`  
2510 and `ty0` stand for the longitude and latitude origin of the focal region, respectively;  
2511 `tx` and `ty` stand for the length of the rectangular region, respectively; and `tend` stands  
2512 for the time length.

2513 Different random number seeds are assumed working independent simulation  
2514 experiments.

2515  
2516

## 2517 16.3 Executing the Program

2518 The following command executes the compiled FORTRAN code.

2519 `./histetasim |tee histetasim.prt (= histetasimuk.prt or`  
2520 `histetasim5pa.prt),`

2521 where all output files listed below are selected in the program directory of  
2522 `Section17files`.

2523

## 2524 16.4 Output Produced by Program with configuration file of different first line

### 2525 16.4.1 `hist-etas-mk` case:

2526 If the number in the first line of `histetasim.conf` is 7, representing  
2527 `hist-etas-mk` model simulation, then the output files are:

2528 `histetasim.prt (= histetasimuk.prt), fort.2(= fort.2.muk),`  
2529 `fort.7 (= fort.7.muk)` which are all selected in the program directory of  
2530 `Section17files/`, and they have the same format as those by the simulation of  
2531 `hist-etas-mk` model. Calculated record of the program `histetasim` is stored  
2532 by the name `histetasim.prt (= histetasimuk.prt)` which shows some  
2533 key parameters to compare with the key parameters for checking consistency together

2534 with hypocenter data that are same as fort . 7 .

2535

2536 fort . 2 includes:

2537	308	21.00000	17.00000	6.00000	1701.00000
2538	1	146.37236	43.22112	7.70000	33.96782
2539	2	147.45493	43.47246	6.00000	34.02402
2540	3	145.96078	43.80458	7.10000	34.12867
2541	4	140.58100	36.19143	6.60000	37.06475
2542	5	143.57109	41.56049	6.00000	39.57438
2543				.....	
2544	304	142.19733	35.97812	6.10000	1680.84593
2545	305	141.96287	40.80838	6.20000	1683.40119
2546	306	140.64088	33.22854	6.00000	1684.12163
2547	307	143.43240	39.97664	6.10000	1692.37786
2548	308	148.13354	44.18092	6.10000	1700.54208
2549					

2550 where the first line shows the number of events, rectangular side lengths in degrees,  
2551 cutoff magnitude and the entire time span. The rest lines indicate the serial number of  
2552 events, epicenter coordinates, magnitude that are same as those in delone2.out in  
2553 §13.1.

2554

2555 fort . 7 (= fort . 7 . muk) includes:

2556	308							
2557	1	146.372	43.221	7.70	33.96782	0	0.00	1
2558	2	147.455	43.472	6.00	34.02402	1	7.70	1
2559	3	145.961	43.805	7.10	34.12867	1	7.70	1
2560	4	140.581	36.191	6.60	37.06475	0	0.00	2
2561	5	143.571	41.560	6.00	39.57438	0	0.00	3
2562	6	147.592	43.674	6.50	40.59455	0	0.00	4
2563	7	146.909	44.236	6.10	40.61836	6	6.50	4
2564	8	143.568	41.716	6.00	41.64508	5	6.00	4
2565	9	140.782	35.176	6.70	47.89052	0	0.00	5
2566	10	140.718	35.286	6.10	48.30271	9	6.70	5
2567				.....				
2568	299	142.177	36.975	6.00	1613.69128	298	6.10	183
2569	300	142.531	38.418	7.10	1651.89759	128	7.30	183
2570	301	145.575	43.010	6.60	1656.22287	0	0.00	184
2571	302	141.519	34.460	6.20	1671.84874	0	0.00	185
2572	303	146.391	43.451	6.00	1680.62511	0	0.00	186
2573	304	142.197	35.978	6.10	1680.84593	241	9.00	186
2574	305	141.963	40.808	6.20	1683.40119	0	0.00	187
2575	306	140.641	33.229	6.00	1684.12163	0	0.00	188
2576	307	143.432	39.977	6.10	1692.37786	0	0.00	189
2577	308	148.134	44.181	6.10	1700.54208	0	0.00	190

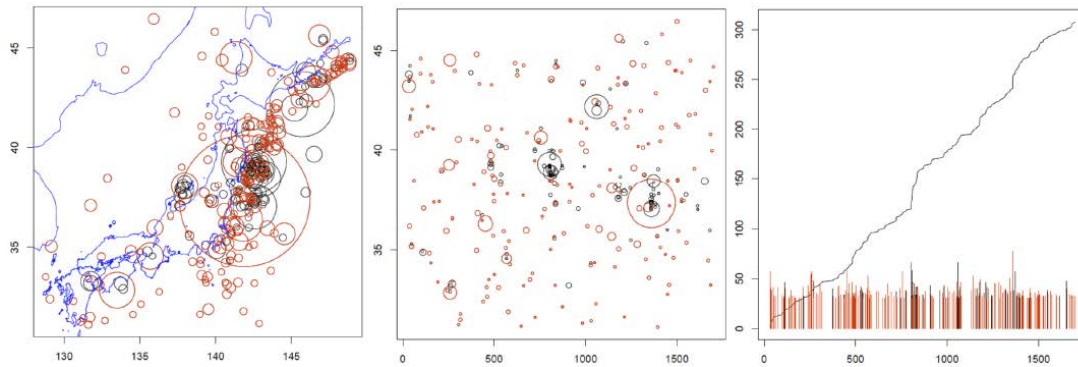
2578

2579 where the first to five columns are same as those of fort.2, sixth and seventh columns  
2580 represent shows the identification of parent and its magnitude, where 0 represents the  
2581 0-generation event that is simulated by the contribution of background intensity  
2582  $\mu(x,y)$ ; and the last columns show cluster number of the same family trees.

2583

2584 For the plot, done in R, then R.plots.pdf(7pa1993,1119,1046.pdf) shows  
2585 below plots (Fig. 16):

2586



2587

2588

2589 Fig. 16: Simulated data by the HIST-ETAS-mK model. Left panel shows epicenters with sizes of  
2590 circle radii are proportional to exponential of the same magnitude series ( $M > 5.95$ ) of the original  
2591 JMA data. Middle panel shows latitude versus time plots. Right panel shows the cumulative  
2592 number curve and magnitude versus time plots. In all panels, red ones indicate 0-th generation  
2593 earthquake events generated by the background intensity.

2594

2595 After simulation we can make reestimation starting from constructing 2D Delaunay  
2596 tessellation for the simulated data sets.

2597

2598 16.4.2 hist-etlas-5pa case:

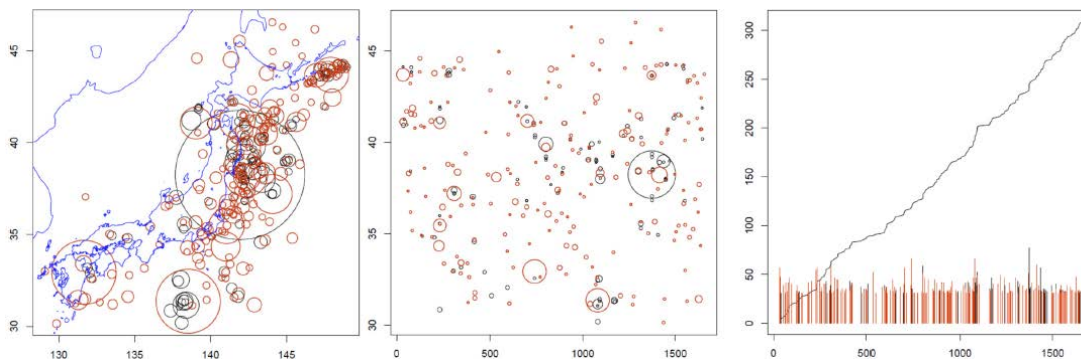
2599 If the number in the first line of `histetasim.conf` is 5 representing  
2600 `hist-etlas-5pa` model simulation, then the output files are:

2601 `histetasim.prt` (= `histetasim5pa.prt`), `fort.2` (= `fort.2.5pa`), and `fort.7` (= `fort.7.5pa`) which are selected in the program directory of `Section16files/`,  
2602 and have the same format as those by the simulation of `hist-etlas-mk` model.

2603

2604  
2605 For the plot, done in R, then `R.plots.pdf` (5pa1993,1119,1046.pdf) show below  
2606 plots (Fig. 17):

2607



2608

2609

2610 Fig. 17: Simulated data by the HIST-ETAS-5pa model. Left panel shows epicenters with sizes of  
2611 circle radii are proportional to exponential of the same magnitude series ( $M > 5.95$ ) of the  
2612 original JMA data. Middle panel shows latitude versus time plots. Right panel shows the

2613 cumulative number curve and magnitude versus time plots. In all panels, red ones indicate 0-th  
2614 generation earthquake events generated by the background intensity.

2615

2616 After simulation we can make re-estimation, but we need to start from  
2617 constructing new 2D Delaunay tessellation for the simulated data sets.

2618

2619

## 2620 APPENDICES

### 2621 A. Mathematical Outline of Models

2622 The ETAS model (Ogata, 1985, 1988, 1989) was extended for space-time data, and  
2623 among the possible modelings for the space component, the best form described in  
2624 §A.3 (Ogata, 1998) is selected by the goodness-of-fit comparison using the Akaike  
2625 information criterion (*AIC*: Akaike, 1974). Incidentally, see Zhuang *et al.* (2005) and  
2626 Ogata and Zhuang (2006) for further improvement of the space-time ETAS model,  
2627 but we do not consider this for the hierarchical extensions of the parameters.

2628 We give a brief outline here of the space-time ETAS models that are fitted by this  
2629 software. We initially define the space-time ETAS model in a general way that  
2630 encompasses all of the specific models fitted by this software. We then describe what  
2631 constraints are imposed by specific models. Further details are available in Ogata  
2632 (2010) for an example.

#### 2633 A.1 Determination of Anisotropic Clusters

2634 Before fitting the space-time ETAS models with anisotropic spatial clustering  
2635 effect, we aim at compiling similar solution as the centroid Moment tensor solution  
2636 (Dziewonski *et al.* 1981) using early aftershocks activity, which was first investigated  
2637 by Utsu and Seki (1955) and Utsu (1969). Also, see Ogata *et al.* (1995) and Ogata  
2638 (1998).

2639 The large earthquakes of  $M \geq M_m$  in the catalogue are selected, and their immediate  
2640 aftershocks are determined. The threshold magnitude  $M_m$  of the main shocks is  
2641 determined appropriately, taking account of the cutoff magnitude  $M_c$  of the  
2642 earthquakes in the catalog, such as  $M_m = M_c + 1.0$ . For example, the space window is  
2643 a square centered at the epicenter of the main shock, with sides of length  $3.33 \times 10^{0.5M-2}$   
2644  $+\varepsilon$  centered at the epicenter location, where  $M$  is the magnitude of the main shock.  
2645 The last term  $\varepsilon$  is to quantify the error of epicenter estimates, usually takes 0 but we  
2646 take  $\varepsilon = 66.6$  km (0.3 degree in latitude) in early days in offshore Japanese events. For  
2647 the time span for estimation purpose, we can set one day (24 hours) or the shorter.  
2648 The time window can be longer than 1 day in a low detection region or during an  
2649 earlier period. On the other hand, from a forecasting perspective nowadays, one might  
2650 set “0.05”, i.e. about one hour, to quickly determine the centroid location and  
2651 orientation characteristics of the impending aftershock sequence after a main shock  
2652 event using all detected earthquakes.

2653 For each main shock and its aftershock sequence, a bivariate normal distribution is  
2654 fitted to the spatial values. In particular, for each, the covariance matrix

2655

$$S = \begin{pmatrix} \sigma_1^2 & \rho\sigma_1\sigma_2 \\ \rho\sigma_1\sigma_2 & \sigma_2^2 \end{pmatrix}$$

2656 and the centroid of the main shock and its aftershock sequence are estimated.

2657 The null model assumes that  $S$  is the identity matrix, and the cluster center is at  
 2658 the location of the main shock. There are three possible alternative models:

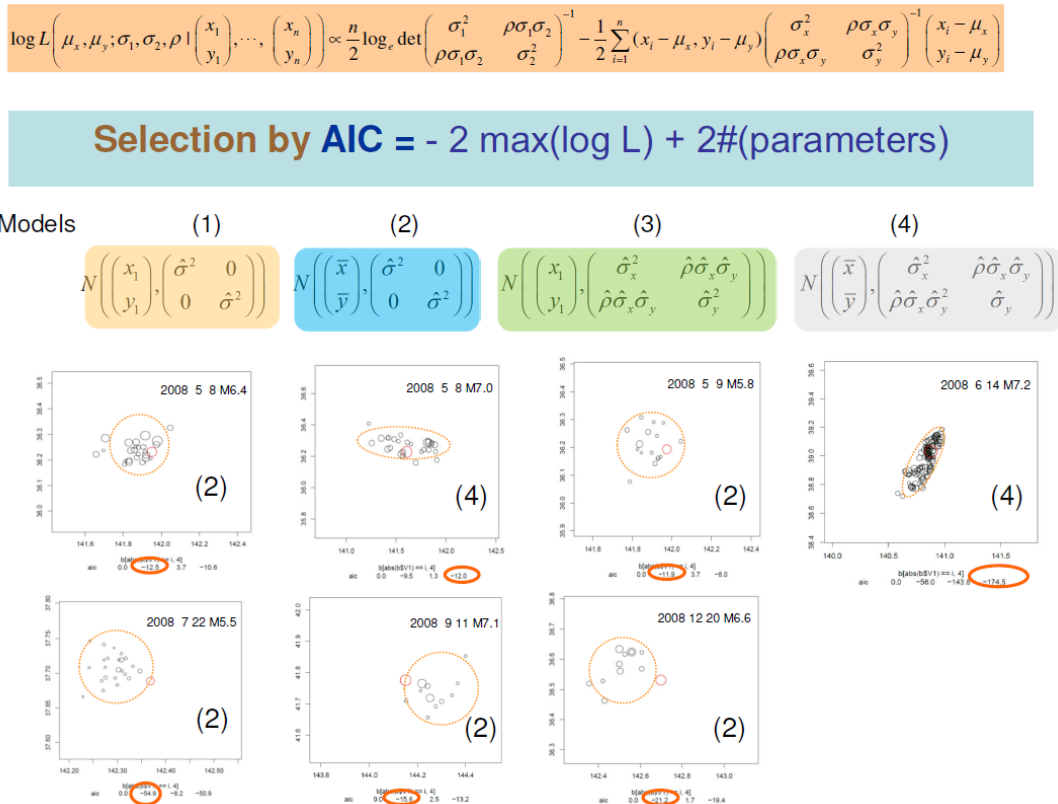
- 2659 1.  $S$  is different to the identity matrix but the cluster center is not different to that  
 2660 of the main shock;  
 2661 2.  $S$  is not different to the identity matrix but the cluster centre is located at the  
 2662 centroid;  
 2663 3.  $S$  is different to the identity matrix and the cluster center is located at the  
 2664 centroid.

2665 Cases 2 and 3 are achieved by relocating the main shock to the centroid location. For  
 2666 each of the four models of a given cluster, the AIC is calculated. That model with the  
 2667 smallest AIC is selected for each cluster.

2668 See Ogata (1998, 2010), Ogata (2004, Appendix B) and Ogata and Zhuang (2006,  
 2669 Appendix A) for more details. This procedure is executed by the program  
 2670 `aniSo2etas`.

2671

2672 The procedure is illustrated below (Fig. 18):  
 2673



2674

2675 Fig. 18: These panels show aftershocks occurring during the first hour after the main shock that is  
 2676 indicated by a small red circle  $(x_l, y_l)$ . The occurrence date and magnitude of the main shock are  
 2677 printed. The AIC values of Models (1) ~ (4) relative to the largest one are listed in each panel,  
 2678 where the model of the smallest value is adopted for the forecast of the aftershock cluster

2679 anisotropy. Namely, we compare the goodness-of-fit of the following four 2-dimensional Normal  
 2680 distributions by the AIC. The model (1) stands for isotropic cluster with the centroid as the original  
 2681 epicenter. The model (2) stands for isotropic cluster, but the centroid coordinates are different from the  
 2682 original epicenter. The model (3) stands for anisotropic cluster with the centroid as the original  
 2683 epicenter. And the model (4) stands for anisotropic cluster but the centroid coordinates are different  
 2684 from original epicenter. The model with the smallest AIC value is adopted, and each panel illustrates a  
 2685 contour of the selected model.

2686  
 2687 The isotropic Space-Time Epidemic-Type Aftershock Sequence (ST-ETAS) model

$$2688 \quad \lambda(t, x, y | H_t) = \mu(x, y) + \sum_{\{i: t_i < t\}} \frac{K_0}{(t - t_i + c)^p} \left[ \frac{(x - x_i)^2 + (y - y_i)^2}{e^{\alpha(M_i - M_0)}} + d \right]^{-q}$$

2689 can be extended to non-isotropic clusters for the earthquakes indicated by the output  
 2690 aniso2etas.out3, aiming at a better fit of the models to an earthquake catalog. For this,  
 2691 each response function is extended in such a way that the isotropic term in the  
 2692 response functions is replaced by

$$2693 \quad \frac{1}{\sqrt{1 - \rho^2}} \left( \frac{\sigma_2}{\sigma_1} x^2 - 2\rho xy + \frac{\sigma_1}{\sigma_2} y^2 \right),$$

2694 so that the corresponding iso-circle and iso-ellipse as a cross-section of the function at  
 2695 the same height have the same area as each other. Namely, the corresponding circle  
 2696 and ellipse as a cross-section of  $z = z_c$  have the same area to each other. Then the  
 2697 integral of the above conditional intensity function remains the same (cf., Ogata,  
 2698 1998).  
 2699

## 2700 A.2 Delaunay Tessellation

2701 The Delaunay tessellation is a rather elegant method that can be used to estimate  
 2702 background seismicity or, in fact, to get estimates of anything that may vary in space  
 2703 where we have values of the entity of interest at any given points. It involves drawing  
 2704 triangles where the vertices are points, and no point falls within any of the  
 2705 circumcircles of the drawn triangles. Algorithms for the implementation of the  
 2706 techniques can be found in the Wikipedia, for example.

2707 In the case of a two-dimensional surface, each triangle provides a flat surface where  
 2708 the height of the surface is known at the three vertices. At any other point on the  
 2709 surface within a triangle, the height of the surface can be estimated using linear  
 2710 interpolation. The program `interpolated.f` performs such an interpolation. In  
 2711 regions where point density is large, the triangles will be very small and hence the  
 2712 interpolation error will be small, and conversely, where the point density is small the  
 2713 interpolation error will be relatively larger. Further, the rate at which points occur in a  
 2714 given region will be inversely proportional to the area of the triangles within that  
 2715 region.

2716 Consider the Delaunay triangulation (e.g., Green and Sibson, 1978); that is to say,  
 2717 the whole rectangular region  $A$  is tessellated by triangles with the vertex locations of  
 2718 earthquakes and some additional points  $\{(x_i, y_i), i=1, \dots, N+n\}$ , as given in Fig. 19,  
 2719 where  $N$  is the number of earthquakes and  $n$  is the number of the additional points on  
 2720 the rectangular boundary including the corners. Here, for successfully fulfilling a  
 2721 Delaunay tessellation, we sometimes need very small perturbation of epicenters to  
 2722 avoid lattice structure or duplicated locations in a local domain. The panel below

2723 shows such a tessellation based on the epicenters of a JMA dataset and the additional  
 2724 points on the boundaries. Then, define the piecewise linear function  $\phi(x, y)$  on the  
 2725 tessellated region such that its value at any location  $(x, y)$  in each triangle is linearly  
 2726 interpolated by the three values at the vertices. Specifically, consider a Delaunay  
 2727 triangle and the coordinates of its vertices  $(x_i, y_i), i = 1, 2, 3$ . Then, for the values  
 2728  $\phi_i = \phi(x_i, y_i), i = 1, 2, 3$ , the function value at any location inside the triangle is given  
 2729 as follows: Consider the linear equations

$$\begin{aligned} 2730 \quad & a_1x_1 + a_2x_2 + a_3x_3 = x \\ 2731 \quad & a_1y_1 + a_2y_2 + a_3y_3 = y \\ 2732 \quad & a_1 + a_2 + a_3 = 1 \end{aligned}$$

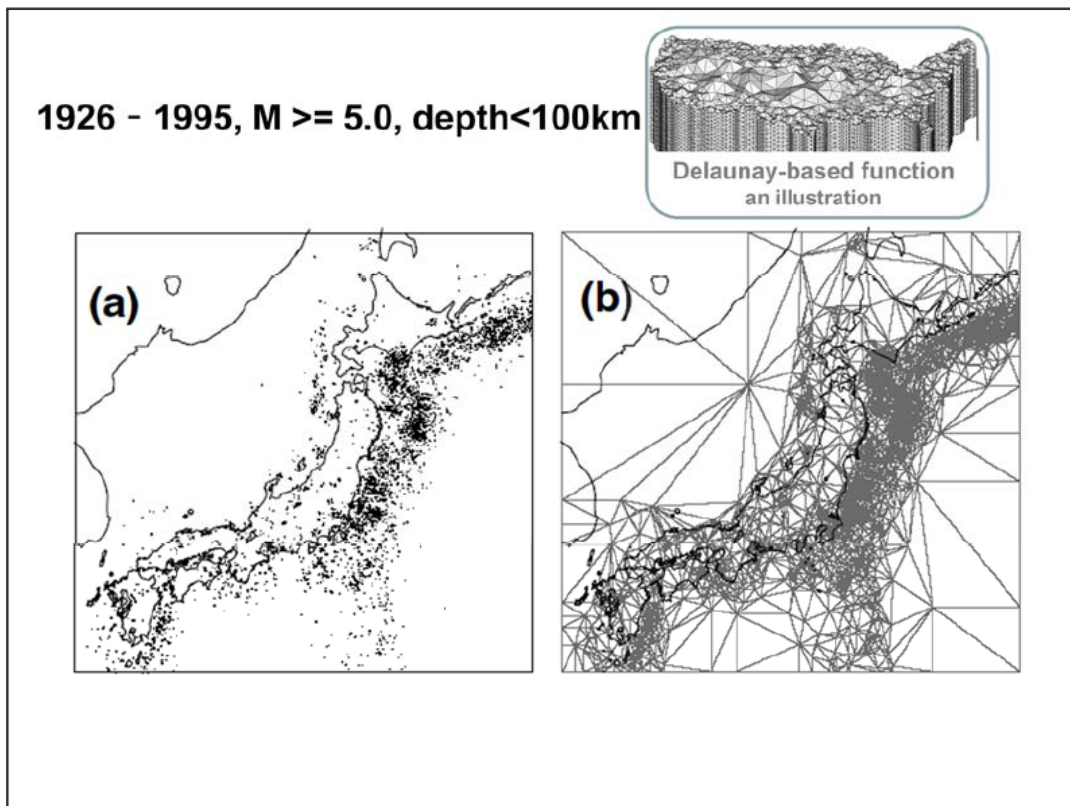
2733 to obtain the non-negative solution  $\hat{a}_1, \hat{a}_2$  and  $\hat{a}_3$  so that we have

$$2734 \quad \phi(x, y) = \hat{a}_1\phi_1 + \hat{a}_2\phi_2 + \hat{a}_3\phi_3.$$

2735 Such a function suitably represents the variation of the samples on a highly  
 2736 non-homogeneous or clustered point pattern. That is to say, we can estimate detailed  
 2737 changes of rate in a region where the observations are densely populated.

2738 For further details on Delaunay tessellations, see the [wikipedia](#), Tanemura *et al.*  
 2739 (1983), Ogata (2004), Ogata *et al.* (2003), and Green and Sibson (1978).

2740  
 2741



2742 Fig. 19: (a) Epicenter locations (dots) of earthquakes of  $M \geq 5.0$  in and around Japan for the  
 2743 target period 1926-1995 together with those of  $M \geq 6.0$  from the period 1885-1925 that are  
 2744 used as the history of the ETAS model, and (b) Delaunay tessellation connecting the  
 2745

2746 epicenters and some points on the boundary.

2747

2748

### 2749 A.3 Spatial Non-homogeneous Poisson Model

2750 An objective method is developed for the estimation of the spatial intensity of the  
 2751 point locations. Consider superimposed epicenters throughout a period. Let us  
 2752 estimate the spatial seismicity from the earthquake locations. Now, we can consider  
 2753 two possible parameterizations for an intensity function  $\lambda_\theta(x, y)$  of the  
 2754 nonhomogeneous Poisson processes. The first one is a bi-linear cubic spline function  
 2755 (Ogata and Katsura, 1988). However, this does not work efficiently relative to the  
 2756 number of necessary coefficients unless the locations are rather uniformly distributed  
 2757 throughout the region. The alternative is the Delaunay triangulation of this region  
 2758 tessellated by the earthquake locations, namely, a 2-dimensional piecewise linear  
 2759 function defined on the tessellation where the function value at any location is  
 2760 determined by the values at the vertices of Delaunay triangles. The modelling using  
 2761 Delaunay tessellation is suited for observations of clustered points. Namely, we can  
 2762 see detailed changes in the region where the observations are densely populated while  
 2763 smoother changes are expected in the sparsely populated regions. For the random  
 2764 location data  $\{(x_i, y_i); i = 1, 2, \dots, n\}$  in a region  $A$ , we can write the log-likelihood  
 2765 function as

$$2766 \ln L(\theta) = \sum_{i=1}^n \ln \lambda_\theta(x_i, y_i) - \iint_A \lambda_\theta(x, y) dx dy$$

2767 where we have about the same number of parameters, or even more, as the number of  
 2768 earthquakes. Hence, we consider the penalized log likelihood

$$2769 R(\theta | w) = \ln L(\theta) - Q(\theta | w),$$

2770 where, in the case of a Delaunay piecewise function,

$$2771 Q(\theta | w) = w \iint_A \left\{ \left( \frac{\partial \lambda_\theta(x, y)}{\partial x} \right)^2 + \left( \frac{\partial \lambda_\theta(x, y)}{\partial y} \right)^2 \right\} dx dy$$

$$2772 = \sum_{j: \text{Delaunay triangles}} w \Delta_j \left( \left| \begin{array}{ccc} \phi_1^j & y_1^j & 1 \\ \phi_2^j & y_2^j & 1 \\ \phi_3^j & y_3^j & 1 \end{array} \right|^2 + \left| \begin{array}{ccc} x_1^j & \phi_1^j & 1 \\ x_2^j & \phi_2^j & 1 \\ x_3^j & \phi_3^j & 1 \end{array} \right|^2 \right) / \left| \begin{array}{ccc} x_1^j & y_1^j & 1 \\ x_2^j & y_2^j & 1 \\ x_3^j & y_3^j & 1 \end{array} \right|^2.$$

2773 The objective tuning of the weight  $w$  is carried out by the Bayesian method  
 2774 described in §A6 below, hence we obtain unique solutions of both the optimal weight  
 2775 and then the maximum a posterior estimate (in short, the MAP estimate) of the  
 2776 intensity function.  
 2777

### 2778 A.4 $b$ -value estimate and forecasting seismicity

2779 Initially assume that the  $b$ -value of the Gutenberg-Richter's magnitude frequency law  
 2780 (Gutenberg and Richter, 1944) is location independent. Historically, based on the  
 2781 moment method, Utsu (1965) proposed the estimator  $\hat{b} = N \log e / \sum_{i=1}^N (M_i - M_c)$   
 2782 for the observation of magnitude sequence  $\{M_i, i = 1, \dots, N\}$  where  $M_c$  is usually the

2783 lowest bound of the magnitudes above which almost all the earthquakes are detected.  
 2784 This is modified by Utsu (1970) to replace  $M_c$  by  $M_c - 0.05$  for the unbiased estimate  
 2785 of the  $b$ -values in case when the given magnitudes are rounded into values with 0.1  
 2786 unit, and hereafter we follow this modification for the JMA catalog. Aki (1965)  
 2787 showed that the Utsu's  $b$ -estimator is nothing but the maximum likelihood estimate  
 2788 (MLE) that maximizes the likelihood function

$$2789 \quad L(b) = \prod_{i=1}^N \beta e^{-\beta(M_i - M_c)}, \quad M_i > M_c \text{ and } \beta = b \ln 10.$$

2790 Here, we want to assume that the  $b$ -value, or coefficient of the exponential  
 2791 distribution of magnitude, is dependent on the location in such a way that  $\beta_{\theta}(x, y) =$   
 2792  $b_{\theta}(x, y) \ln 10$  where  $\theta$  is a parameter vector characterizing the function (Ogata *et al.*,  
 2793 1991). We will solve these problems by a Bayesian procedure. Having observed the  
 2794 magnitude data  $M_i$  for each hypocenter's coordinates  $(x_i, y_i)$  with  $i = 1, 2, \dots, N$ , the  
 2795 current likelihood function of  $\theta$  can be written by

$$2796 \quad L(\theta) = \prod_{i=1}^N \beta_{\theta}(x_i, y_i) e^{-\beta_{\theta}(x_i, y_i)(M_i - M_c)}$$

2797 for  $M_i > M_c$ . Since  $\beta$ , or  $b$ , is positive valued, we make the re-parameterization of the  
 2798 function  $\beta_{\theta}(x, y) = e^{\phi(x, y)} / \log_{10} e$ , so that the estimate of the  $b$ -values in space is  
 2799 given by  $b_{\theta}(x, y) = e^{\phi(x, y)}$ , where the  $\phi$ -function is piecewise linear on the Delaunay  
 2800 tessellation, as given above. For a set of clusters of earthquakes, the Delaunay-based  
 2801 function fits better than the bi-cubic B-spline function that was used in Ogata &  
 2802 Katsura (1988) and Ogata *et al.* (1991). The estimation of the coefficients is  
 2803 undertaken by the penalized log-likelihood,

$$2804 \quad R(\theta | w) = \ln L(\theta) - w \iint_A \left\{ \left( \frac{\partial \beta_{\theta}(x, y)}{\partial x} \right)^2 + \left( \frac{\partial \beta_{\theta}(x, y)}{\partial y} \right)^2 \right\} dx dy$$

2805 where the penalty weight  $w$  is tuned by a similar Bayesian procedure based on the  
 2806 ABIC (see Appendix B).  
 2807

## 2808 A.5 Space-Time ETAS Models: General Model Formulation

2809 Denote the history of the process up to but not including time  $t$  as  $H_t$  where

$$2810 \quad H_t = \{(t_i, x_i, y_i, M_i) : t_i < t\}$$

2811 and where  $(t_i, x_i, y_i, M_i)$  represents the time-space-magnitude outcome of the  $i$ -th event.

2812 The model parameters are  $\mu$ ,  $K_0$ ,  $c$ ,  $\alpha$ ,  $p$ ,  $d$ , and  $q$ . In the fitted models, some or all of  
 2813 these parameters will vary in space, and will be denoted as  $\mu(x, y)$ ,  $K(x, y)$ ,  $c$ ,  $\alpha(x, y)$ ,  
 2814  $p(x, y)$ ,  $d$ , and  $q(x, y)$ .

2815 Let

$$2816 \quad f_j(t, x, y) = [t - t_j + c]^{-p(x, y)}$$

2817 and

$$2818 \quad g_j(x, y) = \left[ \frac{(x - x_j, y - y_j) S_j (x - x_j, y - y_j)^t}{e^{\alpha(x, y)(M_j - M_0)}} + d \right]^{q(x, y)} \quad (a1)$$

2819 where  $M_0$  is a reference magnitude (`xmg0`) that can be usually a threshold magnitude  
 2820 of completely detected (`cutm` in §4.2),  $(x_j, y_j)$  is the centroid location of the main  
 2821 shock-aftershock sequence associated with the  $j$ th event, and  $S_j$  describes the major  
 2822 and minor axes of the spatial intensity associated with the  $j$ th event. Note that in many  
 2823 cases,  $S_j$  will just be the identity matrix and  $(x_j, y_j)$  will be the location of the  
 2824 epicenter in the original catalog. Alternative spatial response functions to (a1) are  
 2825 examined in Ogata (1998) to show the predominance of (a1) in and around Japan.  
 2826 The conditional intensity function can now be written as

$$2827 \quad \lambda(t, x, y | H_t) = \mu(x, y) + K_0(x, y) \sum_{\{j: t_j < t\}} g_j(x, y) f_j(t, x, y)$$

2828 Using the Delaunay tessellations, the spatial versions of the model parameters can  
 2829 be expressed as

$$2830 \quad \mu(x, y) = \bar{\mu} e^{\phi_1(x, y)} \quad (\text{a2})$$

$$2831 \quad K_0(x, y) = \bar{K}_0 e^{\phi_2(x, y)} \quad (\text{a3})$$

$$2832 \quad \alpha(x, y) = \bar{\alpha} e^{\phi_3(x, y)} \quad (\text{a4})$$

$$2833 \quad p(x, y) = \bar{p} e^{\phi_5(x, y)} \quad (\text{a5})$$

$$2834 \quad q(x, y) = \bar{q} e^{\phi_7(x, y)} \quad (\text{a6})$$

2835 In the programs, we assume that the temporal scaling parameter  $c$  and the scaling  
 2836 parameter  $d$  are location independent. See Ogata *et al.* (2003) and Ogata (2004).

2837

### 2838 **A.5.1 Anisotropic space-time ETAS model (etas2aniso)**

2839 The simplest model (`st-etas`) is where no model parameters vary in space, i.e.

2840

$$2841 \quad \phi_1(x, y) = \phi_2(x, y) = \phi_3(x, y) = \phi_5(x, y) = \phi_7(x, y) = 0,$$

2842 for all  $x$  and  $y$  for functions in (a2) – (a6).

2843 This model includes an approximate version to shorten the long computation time  
 2844 by considering a range within a certain prescribed distance for each earthquake that is  
 2845 useful for the application to seismicity in wide regions. For this version, we need to  
 2846 indicate a spatial distance bound of the triggering range. The input parameter is how  
 2847 many times of the Utsu Spatial Distance  $USD = 3.33 \times 10^{0.5M-2}$  km (cf., §A.1). As the  
 2848 default value, it is set to be 2 times of  $USD$  in the configuration file. Hence, for the  
 2849 exact calculation, we put the parameter `bi2` such that `bi2`  $\times$   $USD$  exceeds the largest  
 2850 distance between earthquakes in the region.

2851

### 2852 **A.5.2 HIST-ETAS model of location dependent $\mu$ and $K_0$ -parameters**

2853 In this model (`hist-etas-mk`), we assume that only  $\mu$  and  $K_0$  vary over space,  
 2854 i.e.

$$2855 \quad \phi_3(x, y) = \phi_5(x, y) = \phi_7(x, y) = 0$$

2856 and  $\phi_1(x, y)$  and  $\phi_2(x, y)$  are not zero for all  $x$  and  $y$  for functions in (a2) – (a6). The  
 2857 model is fitted by using the values of the other parameters as estimated by the model

2858 in §A.5.1, as the initial values to start, and fitting the two spatial functions given by  
 2859 Eqs. 1 and 2. Here, all seven baseline parameters  $\bar{\mu}, \bar{K}_0, c, \bar{\alpha}, \bar{p}, d,$  and  $\bar{q}$  are  
 2860 re-estimated along with  $\phi_1(x,y)$  and  $\phi_2(x,y)$ ; i.e., Eqs. (a2) ~ (a6).

### 2861 **A.5.3. HIST-ETAS model (hist-etasspa)**

2862 In this model, we assume that five of the parameters vary in space:  $\mu, K_0, \alpha, p$  and  $q,$   
 2863 i.e. Equations 1~ 5, respectively. The values of the two constant parameters ( $c$  and  $d$ )  
 2864 are those as estimated by the model in §A.5.1. In addition to the parameters  $c$  and  $d,$   
 2865 the baseline parameters of  $\alpha, p$  and  $q$  as estimated by the model in §A.5.1 are fixed  
 2866 throughout the computation. Namely, those are same as obtained in hist-etassmk.  
 2867 Effectively we are fixing the parameter values to those estimated in A.5.2 and only  
 2868 estimating the  $\phi_i$ 's,  $i = 1, 2, 3, 5, 7.$

2869

### 2870 **A.5.4. Forecasting by HIST-ETAS models**

2871 In a short-term span after a large earthquake  $j,$  we can make space-time forecast of  
 2872 aftershock activity. First, we only make a real time forecast using the isotropic matrix  
 2873  $S_j$  (see §A1) within one hour after the occurrence of the earthquake  $j;$  but during the  
 2874 same period, a cluster analysis for the  $S_j$  is carried out. Specifically, the centroid  
 2875 hypocenter and variance-covariance matrix of a spatial cluster of aftershocks are  
 2876 formed using all detected and located earthquakes during the first hour, say, after the  
 2877 large earthquake. Then, based on this, the general non-isotropic space-time  
 2878 forecasting is performed after that.

2879 Then, in principle, the short-term probability forecast in space-time-magnitude bin  
 2880 is calculated, by the simple joint distribution of the separable combination between  
 2881 seismicity and magnitude, given by:

$$2882 \lambda(t, x, y; M | H_i) dt dx dy = \lambda(t, x, y | H_i) \cdot \hat{\beta}(x, y) e^{-\hat{\beta}(x, y)(M - M_c)} dt dx dy,$$

2883 where the estimation procedure of the location-dependent parameter

2884  $\hat{\beta}(x, y) = \hat{b}(x, y) \ln 10$  for magnitude frequency could be applied.

2885 However, the  $\hat{b}(x, y)$ -values represent the frequency feature near the small  
 2886 earthquake near the threshold magnitude, but the magnitude distribution in many local  
 2887 regions do not follow the GR law for larger magnitudes such as taking shapes of  
 2888 tapering or characteristic earthquake type. For example, maximum likelihood  
 2889 estimates are obtained for many modified Gutenberg-Richter magnitude frequency  
 2890 distributions (see Utsu, 1999). Another issue is that  $b$ -values for the mainshocks and  
 2891 aftershocks can be significantly different (Utsu, 1971). Also, Ogata et al. (2018) did  
 2892 not confirm that the magnitude forecasts by location dependent  $b$ -value throughout  
 2893 Japan region outperform the baseline G-R law with the  $b$  value of 0.9. Hence, at this  
 2894 moment, we may rather assume generic magnitude frequency  $\hat{\beta} = \hat{b} \ln 10$  with  
 2895  $\hat{b} = 0.9$  throughout the entire target region, instead of location-dependent estimate  
 2896  $\hat{\beta}(x, y),$  for a stable forecasting.

2897

2898 **A.6 Likelihoods and Penalized Likelihoods**

2899 **A.6.1 log-likelihood function and its maximization**

2900 Now we start with the simplest space-time ETAS model in which all the parameters  
 2901  $\theta = (\mu, K, c, \alpha, p, d, q)$  of the ASTETAS model in §A3.1 are constant throughout the  
 2902 whole region, equivalently, all the functions  $\phi_k(x, y)$ ,  $k = 1, 2, 3, 5, 7$  defined are equal  
 2903 to zero. The maximum likelihood estimates (MLE) are obtained by the maximizing  
 2904 the log-likelihood function

2905 
$$\ln L(\theta) = \sum_{\{i; S < t_i < T\}} \ln \lambda_\theta(t_i, x_i, y_i | H_{t_i}) - \int_S^T \iint_A \lambda_\theta(t, x, y | H_t) dx dy dt, \quad (a7)$$

2906 for the earthquakes in the target period  $[S, T]$ , where  $H_t$  is the history of earthquake  
 2907 occurrences before time  $t$  including those from the precursory period  $[0, S]$ . For the  
 2908 detailed numerical description of the log-likelihood function, especially of the second  
 2909 integral term in (a7), the reader is referred to Ogata (1998). Then we use a  
 2910 quasi-Newton method (Fletcher and Powell, 1963; Kowalik and Osborne, 1968, etc.)  
 2911 for the numerical maximization.

2912 When the number of earthquakes (say,  $n$ ) in the data is large, the computing take a  
 2913 substantial time due to the double sum of  $n^2/2$  terms in the first part of the log  
 2914 likelihood (a7). Unlike the computation using the Markovian recursive relation in the  
 2915 conditional intensity of the ETAS model (Ogata *et al.*, 1993), such a recursive  
 2916 calculation of the conditional intensity of the space-time ETAS is not available.  
 2917 Instead, one may be interested in a quicker spatially approximate computation by only  
 2918 taking the double sum of the earthquake pairs closer than a certain distance, such as 2  
 2919 times the Utsu Spatial Distance  $3.33 \times 10^{0.5M-2}$  km (cf., §A.1). The HIST-ETAS  
 2920 models in A5 and A6 use this restriction.

2921

2922 **A.6.2 Penalised log-likelihood function and its optimization**

2923 Here we consider the hierarchical models with location dependent parameters in §A.3  
 2924 to describe spatial heterogeneity. These models require a large number of further  
 2925 parameters for the coefficients of functions  $\phi_k(x, y)$ ,  $k = 1, 2, \dots, 5$ . Let such  
 2926 coefficients be described by the parameter set  $\{\theta = (\theta_i) \in \Theta\}$ , and let the likelihood  
 2927 function be given by  $L(\theta | \text{data})$ . To estimate the parameters, we frequently use the  
 2928 penalised log likelihood (Good and Gaskins, 1971)

2929 
$$R(\theta, \tau | \text{data}) = \ln L(\theta | \text{data}) - Q(\theta | \tau), \quad (a8)$$

2930 where the function  $Q$  represents a positive valued penalty function, and  $\tau = (w_1, w_2)$   
 2931 or  $\tau = (w_1, \dots, w_5)$  is a vector of the hyper-parameters that control the strength of  
 2932 some constraints between the parameters bundled by  $\theta$ . Greater constraints will  
 2933 impose more smoothness in  $\phi_k(x, y)$ , less constraints allows greater roughness. For  
 2934 the penalties, besides the simplest penalty in §A3 and §A4, we can consider

2935 
$$Q(\theta | \tau) = w \iint_A \left\{ \left( \frac{\partial \phi}{\partial x} \right)^2 + \left( \frac{\partial \phi}{\partial y} \right)^2 \right\} dx dy$$

2936 for  $b$ -values of the location-dependent G-R law and non-homogeneous Poisson  
 2937 processes, we use

$$2938 \quad Q(\theta | \tau) = \sum_{k=1}^2 w_k \iint_A \left\{ \left( \frac{\partial \phi_k}{\partial x} \right)^2 + \left( \frac{\partial \phi_k}{\partial y} \right)^2 \right\} dx dy \quad (a9)$$

2939 for the HIST-ETAS with location dependent  $\mu$  and  $K$  parameters, and

$$2940 \quad Q(\theta | \tau) = \sum_{k=1}^5 w_k \iint_A \left\{ \left( \frac{\partial \phi_k}{\partial x} \right)^2 + \left( \frac{\partial \phi_k}{\partial y} \right)^2 \right\} dx dy \quad (a10)$$

2941 for the HIST-ETAS with location dependent  $\mu$ ,  $K$ ,  $\alpha$ ,  $p$  and  $q$  parameters. Furthermore,  
 2942 in addition to each penalty, we sometimes need damping constraints for  $\phi_1$  and  $\phi_2$

2943 corresponding to  $\mu$  and  $K_0$ ,  $\sum_{k=1}^2 w_0 \iint_{\partial A} \phi_k(x, y)^2 dx dy$ , only on the boundary of the

2944 region  $\partial A$ , where  $w_0$  is fixed throughout the optimization procedure of other

2945 hyperparameters (weights).

2946 The penalized log-likelihood in (a8) defines a trade-off between the goodness of fit to  
 2947 the data and the uniformity of each function, namely, the facets of the piecewise linear  
 2948 function being as flat as possible. A smaller weight leads to a higher regional  
 2949 variability of the  $\phi$ -functions. The crucial point here is the tuning of the vector  $\tau$ .  
 2950 From the Bayesian viewpoint, the penalty function is related to the prior probability  
 2951 density

$$2952 \quad \pi(\theta | \tau) = e^{-Q(\theta | \tau)} / \int_{\Theta} e^{-Q(\theta | \tau)} d\theta,$$

2953 and the exponential to the penalized log likelihood function  $R$  is proportional to the  
 2954 posterior function. For determining suitable values of the hyper-parameters  $\tau$ ,  
 2955 consider the posterior probability density function

$$2956 \quad p(\theta | \text{data}; \tau) = L(\theta | \text{data}) \pi(\theta | \tau) / \Lambda(\tau | \text{data})$$

2957 with normalizing factor

$$2958 \quad \Lambda(\tau | \text{data}) = \int_{\Theta} L(\theta | \text{data}) \pi(\theta | \tau) d\theta. \quad (a11)$$

2959 The maximization of this normalizing factor or its logarithm with respect to the  
 2960 hyper- parameters  $\tau$  is called the method of the Type II maximum likelihood due to  
 2961 Good (1965). Given a set of data, one seeks to compare the goodness-of-fit of  
 2962 Bayesian models that have distinct likelihoods or distinct priors and to search for the  
 2963 optimal hyper-parameter values. For instance, Ogata *et al.* (1991) compared the use of  
 2964 different priors for isotropic and anisotropic smoothness constraints, which need two  
 2965 and five hyper-parameters, respectively. For such a purpose, Akaike (1980) justified  
 2966 and developed Good's method based on the entropy maximization principle (Akaike,  
 2967 1978) and defined

2968 
$$\text{ABIC} = -2\max_{\boldsymbol{\tau}} \ln \Lambda(\boldsymbol{\tau} | \text{data}) + 2\text{dim}(\boldsymbol{\tau}) \quad (\text{a12})$$

2969 for consistent use with the Akaike Information Criterion (AIC; Akaike, 1974). Here,  
 2970  $\text{dim}(\boldsymbol{\tau})$  is the number of the hyper-parameters. Both ABIC and AIC are to be  
 2971 minimized for the comparison of Bayesian and ordinary likelihood-based models,  
 2972 respectively, for better fit to the data. The normalizing factor  $\Lambda(\boldsymbol{\tau} | \text{data})$  in (a11) is  
 2973 called the likelihood of the Bayesian model with respect to the hyper-parameters  $\boldsymbol{\tau}$ .

2974 For practical computation of the normalizing factor  $\Lambda(\boldsymbol{\tau} | \text{data})$  in (a11), see the  
 2975 §B.2 below.

## 2976 **B Background to Computation Algorithms**

2977 This Appendix gives a description of the computing algorithms that are used to fit the  
 2978 models.

### 2979 **B.1 Nonlinear optimization for the maximum likelihood estimates (MLE)**

2980 For the maximum likelihood procedure of a space-time ETAS model  
 2981 (etasSelectAniso) in §A3.1, we use a quasi-Newton optimization for non-linear  
 2982 functions called Davidon-Fletcher- Powell algorithm (Fletcher and Powell, 1963).  
 2983 Also see Kowalik and Osborne (1968) or *Wikipedia* for an introduction.

2984 To get the optimal parameters, we repeat the following steps (A) - (D):

2985 (A) For a given fixed  $\boldsymbol{\tau}$ , calculate the negative log-likelihood and its gradient vector  
 2986  $\boldsymbol{u}$  at an initially given parameter vector  $\boldsymbol{\theta}_0$ .

2987 (B) Search the smallest negative log likelihood function (a7) with respect to  $\boldsymbol{\theta}$  on the  
 2988 one-dimensional straight line determined by the initial parameter vector  $\boldsymbol{\theta}_0$  and the  
 2989 gradient vector  $\boldsymbol{u}$  (Linear Search; e.g., Kowalik and Osborne, 1968).

2990 (C) Replace the minimizing parameter  $\hat{\boldsymbol{\theta}}$  in step (B) by  $\boldsymbol{\theta}_0$ . Then, compute the gradient  
 2991 vector  $\boldsymbol{u}_0$  at  $\boldsymbol{\theta}_0$ . Solve the equation  $H_{\boldsymbol{\tau}} \boldsymbol{u} = \boldsymbol{u}_0$  by an estimated Hessian to get a  
 2992 vector  $\boldsymbol{u}$  for the direction of the next linear search in step (B).

2993 (D) Repeat A-C until the negative log-likelihood function  $T$  attains the minimum  
 2994 overall  $\boldsymbol{\theta}$ , which is the maximum likelihood estimate (MLE).

2995  
 2996 In quasi-Newton methods the Hessian matrix (second derivatives of the function)  
 2997 need not be computed. An estimated inverse Hessian matrix is calculated by using the  
 2998 gradients during the steps of searching for the minimum of the negative log-likelihood  
 2999 function.

3000

### 3001 **B.2 Computations of Bayesian models through Gaussian approximations**

3002 In general, it is hard to get the high dimensional integration (a11) analytically  
 3003 unless the posterior distribution is Gaussian. This is because the likelihood function of  
 3004 the point-process model is not Gaussian distributed. Nevertheless, by virtue of the  
 3005 Gaussian prior distribution, Gaussian approximation of the posterior function is useful.  
 3006 Namely, we take the Gaussian approximation of the posterior distribution, utilising

3007 the quadratic form around the log-posterior maximum solution. That is to say, the  
 3008 penalized log-likelihood is well approximated by the quadratic form

$$3009 \quad T(\boldsymbol{\theta} | \boldsymbol{\tau}) \equiv \ln L(\boldsymbol{\theta} | \mathbf{Y}) + \ln \pi(\boldsymbol{\theta} | \boldsymbol{\tau}) \approx T(\hat{\boldsymbol{\theta}} | \boldsymbol{\tau}) - \frac{1}{2}(\boldsymbol{\theta} - \hat{\boldsymbol{\theta}})H_T(\hat{\boldsymbol{\theta}} | \boldsymbol{\tau})(\boldsymbol{\theta} - \hat{\boldsymbol{\theta}})^t \quad (\text{b1})$$

3010 around  $\hat{\boldsymbol{\theta}} = \arg\{\max_{\boldsymbol{\theta}} T(\boldsymbol{\theta} | \boldsymbol{\tau})\}$ , and  $H_T(\boldsymbol{\theta} | \boldsymbol{\tau})$  is the Hessian of  $T(\boldsymbol{\theta} | \boldsymbol{\tau})$  consisting of  
 3011 its negative second-order partial derivatives with respect to  $\boldsymbol{\theta}$ .

3012 We further assume that the Hessian matrix in (b1) is well approximated by a block  
 3013 diagonal matrix of five sub-matrices,  $H_T = \text{diag}\{H_T^1, H_T^2, H_T^3, H_T^4, H_T^5\}$ , relying on  
 3014 the Hessian of the prior where each block relates the model parameters  $\mu, K_0, \alpha, p,$   
 3015 and  $q$ , respectively. Namely, we assume independency between the coefficients of the  
 3016 different  $\phi_k$ -functions in the penalized log-likelihood (a8). Thus, the logarithm of the  
 3017 likelihood (11) of the Bayesian model is given by

$$\begin{aligned} 3018 \quad \ln \Lambda(\mathbf{Y}) &= \log \int_{\boldsymbol{\theta}} L(\boldsymbol{\theta} | \mathbf{Y}) \pi(\boldsymbol{\theta} | \boldsymbol{\tau}) \, d\boldsymbol{\theta} \\ &\approx T(\hat{\boldsymbol{\theta}} | \boldsymbol{\tau}) - \frac{1}{2} \ln \det\{H_T(\hat{\boldsymbol{\theta}} | \boldsymbol{\tau})\} + \frac{1}{2} \dim\{\boldsymbol{\theta}\} \log 2\pi \\ &= R(\hat{\boldsymbol{\theta}} | \boldsymbol{\tau}) - \frac{1}{2} \ln \det\{H_R(\hat{\boldsymbol{\theta}} | \boldsymbol{\tau})\} + \frac{1}{2} \ln \det\{H_Q(\hat{\boldsymbol{\theta}} | \boldsymbol{\tau})\}, \end{aligned}$$

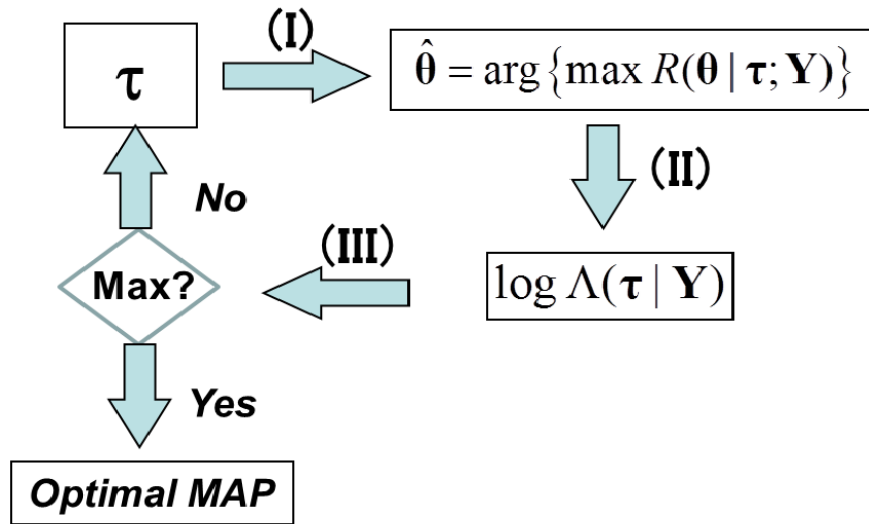
3019 where  $H_R$  and  $H_Q$  is the block diagonal Hessian matrix of the function  $R$  and  $Q$  in  
 3020 (a8), respectively, and ‘ $\det\{\cdot\}$ ’ indicates the determinant of the matrices.

3021 Then, we implement the maximization of the penalized log-likelihood (a8) with  
 3022 respect to the coefficients of the  $\phi$ -functions.

3023 In the maximization with respect to the  $2(N+n)$  dimensional coefficient vectors, we  
 3024 alternately adopt a linear search procedure and the incomplete Cholesky conjugate  
 3025 gradient (ICCG) method by inverting a block diagonal Hessian matrix  $H_R(\hat{\boldsymbol{\theta}} | \boldsymbol{\tau})$  (see  
 3026 §B.2), where  $N$  is the number of earthquakes and  $n$  is the number of the additional  
 3027 points on the rectangular boundary including the corners (see §6.4 and the figure in  
 3028 §6.5). This procedure makes the convergence very rapid regardless of the high  
 3029 dimensionality of  $\boldsymbol{\theta}$  if the Gaussian approximation at Equation (b1) is adequate for  
 3030 the posterior function.

3031 Having attained such convergence for a given hyper-parameter  $\boldsymbol{\tau}$ , we further need  
 3032 to perform the maximization of  $\Lambda(\boldsymbol{\tau})$  defined in (a11) with respect to  $\boldsymbol{\tau}$  by a direct  
 3033 search such as the simplex method (e.g., Kowalik and Osborn, 1968) in either 2 or 7  
 3034 dimensional space depending on the programs. Thus, we perform the double  
 3035 optimizations with respect the parameters (coefficients)  $\boldsymbol{\theta}$  and the hyper-parameters  
 3036 (weights)  $\boldsymbol{\tau}$ . These are alternately repeated until the latter maximization converges  
 3037 (see the diagram in Fig. 20 below). The whole optimization procedure usually  
 3038 converges when initial vector values for  $\boldsymbol{\tau}$  are set in such a way that the penalty is  
 3039 reasonably close to the correct value; otherwise, it may take very many steps to reach  
 3040 the solution, or it may even diverge. Eventually, we obtain the optimal maximum  
 3041 posterior (OMAP) solution  $\hat{\boldsymbol{\theta}}$  for the maximum likelihood estimate  $\hat{\boldsymbol{\tau}}$ .

3042



3043 Fig. 20. Diagram of Double Optimizations. (I) performs the maximization of the function  $R$   
 3044 with respect to  $\theta$ . (II) calculates the log likelihood of the Bayesian model using the quadratic  
 3045 approximation expanded at  $\hat{\theta}$ . (III) maximizes the log likelihood with respect to  $\tau$ .  
 3046  
 3047

3048 To get the optimal hyper-parameters, we repeat the following steps (A) - (D):

3049 (A) For a given  $\tau$  being fixed, set the gradient of the penalized log-likelihood,  $\mathbf{u} =$   
 3050  $\partial T / \partial \theta$  at an initial parameter  $\theta_0$ .

3051 (B) Maximize  $T$  in (b1) with respect to  $\theta$ , that is, on the one-dimensional straight line  
 3052 determined by the initial parameter vector  $\theta_0$  and the gradient vector  $\mathbf{u}$  (Linear Search;  
 3053 e.g., Kowalik and Osborne, 1968).

3054 (C) Replace the maximizing parameter  $\hat{\theta}$  in step (B) by  $\theta_0$ . Then, compute the gradient  
 3055 vector  $\mathbf{u}_0 = \partial T / \partial \theta$  at  $\theta_0$ . Solve the equation  $H_T \mathbf{u} = \mathbf{u}_0$  by the Incomplete Cholesky  
 3056 Conjugate Gradient (ICCG) method (e.g., Mori, 1986) to get the vector  $\mathbf{u}$  for the  
 3057 direction of the next linear search in step (B) until the function  $T$  attains the overall  
 3058 maximum  $\theta$ , which is the maximum posterior (MAP) solution for the given  $\tau$ .

3059 (D) Calculate  $\log \Lambda(\tau)$  using the quadratic approximation around the MAP  $\hat{\theta}$ , and  
 3060 go to step (A) with the other  $\tau$  to maximize  $\log \Lambda(\tau)$  by the direct-search  
 3061 maximizing method, such as the simplex method (e.g., Kowalik and Osborne, 1968;  
 3062 and Murata, 1992). The steps (A) ~ (D) are repeated in turn until  $\log \Lambda(\tau)$   
 3063 converges.

3064 According to our experience, the convergence rate in step (C) is very fast in spite  
 3065 of the very high dimensionality of  $\theta$ . This is expected when the quadratic  
 3066 approximations of  $T$  are adequate in a region around the MAP solution, otherwise it is  
 3067 likely to take endless iterations or even diverge. After all, by assuming a uni-modal  
 3068 posterior function, we can get the optimal MAP solution  $\hat{\theta}$  for the maximum  
 3069 likelihood estimate  $\hat{\tau}$  of the hyper-parameters. The reader is referred to Ogata and  
 3070 Katsura (1988, 1993), Ogata *et al.* (1991, 2000, 2001), and related references therein  
 3071 which further describe computational details.  
 3072

3073 **B.3 Notes on location-dependent  $\mu$  and  $K_0$  ETAS fitting (hist-et-as-mk)**

3074 The penalized log-likelihood in (a8) defines a trade-off between the goodness of fit  
 3075 to the data and the uniformity of each parameter function. We obtain the optimal  
 3076 weights  $\hat{\tau} = (\hat{w}_1, \hat{w}_2)$  together with the maximizing baseline parameters  $(\bar{\mu}, \bar{K})$  for  
 3077 the first two programs or  $(\bar{\mu}, \bar{K}, c, \alpha, p, d, q)$  for the last two, by the principle of  
 3078 maximizing the integrated posterior function (a11). Here note that the baseline  
 3079 parameters  $\bar{\mu}$  and  $\bar{K}$  are automatically determined by the zero-sum constraint of the  
 3080 corresponding  $\phi$ -function. This overall maximization can be eventually attained by  
 3081 repeating alternate procedures of the separated maximizations with respect to the  
 3082 parameters (coefficients) and hyper-parameters (weights) described as follows.

3083 First of all, for the initial inputs, we use the MLEs  $\hat{\theta} = (\hat{\mu}, \hat{K}, \hat{c}, \hat{\alpha}, \hat{p}, \hat{d}, \hat{q})$  obtained  
 3084 by the primary space-time ETAS model (st-et-as), for the baseline parameter, and  
 3085 also set all the coefficients of  $\phi$ -functions to be zero such that  $\phi_1(x, y) = \phi_2(x, y) = 0$ .

3086 Since the penalty functions already have the quadratic form with respect to the  
 3087 parameters  $\theta$ , the prior density is of a multivariate Gaussian distribution, in which the  
 3088 Hessian matrix  $H_Q$  consists of the elements of the negative second order partial  
 3089 derivatives of the penalty function  $Q$ . Actually, the present penalty function implies  
 3090 that the Hessian is a block diagonal matrix of five sub-matrices corresponding to each  
 3091  $\phi_k$ -function in (a2)~(a6) such that  $H_Q = \text{diag}\{H_\mu^1, H_\kappa^2\}$ . This is because we do not  
 3092 consider any restrictions a priori between the different  $\phi_1$  and  $\phi_2$ -functions. Here, all  
 3093 sub-matrices of  $H_Q^k$  are sparse, and have the same configuration of non-zero elements.  
 3094 Specifically, the  $(i, j)$ -element is non-zero if and only if the pair of points  $i$  and  $j$  are  
 3095 vertices of the same Delaunay triangle; cf., §6.3.

3096 **B.4 Notes on location-dependent  $\mu, K, \alpha, p$  and  $q$  ETAS fitting (hist-et-as5pa)**

3097 Having obtained the optimal weights  $\hat{\tau} = (\hat{w}_1, \hat{w}_2)$  and the MAP coefficients of  
 3098  $\hat{\phi}_1(x, y)$  and  $\hat{\phi}_2(x, y)$  with the baseline parameters  $\hat{\mu}, \hat{K}, \hat{c}, \hat{\alpha}, \hat{p}, \hat{d}, \hat{q}$  in the  
 3099  $\mu K$ -HIST-ETAS model, we use all of these for initial inputs to stably estimate the  
 3100 HIST-ETAS model in §A.3 with five spatially varying parameters in (a2) - (a6). Also,  
 3101 set other coefficients of  $\alpha, p$  and  $q$  parameter functions being zero such that  $\phi_3(x, y) =$   
 3102  $\phi_4(x, y) = \phi_5(x, y) = 0$  with the estimated baseline values  $\hat{\mu}, \hat{K}, \hat{c}, \hat{\alpha}, \hat{p}, \hat{d}$  and  $\hat{q}$  of  
 3103 the  $\mu K$ -HIST-ETAS model (hist-et-as-mk).

3104 Here, we consider the penalized log-likelihood function (a8) with the penalty  
 3105 function

$$3106 \quad Q(\theta | \tau) = \sum_{k=1}^5 w_k \iint_A \left\{ \left( \frac{\partial \phi_k}{\partial x} \right)^2 + \left( \frac{\partial \phi_k}{\partial y} \right)^2 \right\} dx dy \quad (b2)$$

3107 of  $\tau = (w_1, \dots, w_5)$ . In addition, we need damping constraints for  $\phi_1$  and  $\phi_2$

3108 corresponding to  $\mu$  and  $K_0$ ;  $\sum_{k=1}^2 w_k \iint_{\partial A} \{ \partial \phi_k(x, y) / \partial x \}^2 + \{ \partial \phi_k(x, y) / \partial y \}^2 dx dy$  only

3109 on the boundary of the region  $\partial A$ . For technical reasons, the baseline values

3110  $\hat{\mu}$ ,  $\hat{K}$ ,  $\hat{c}$ ,  $\hat{\alpha}$ ,  $\hat{p}$ ,  $\hat{d}$ ,  $\hat{q}$  and  $w_0$  in the programs are fixed throughout the whole  
 3111 computations. Thus the optimal weights  $\hat{\tau} = (\hat{w}_1, \hat{w}_2, \hat{w}_3, \hat{w}_4, \hat{w}_5)$  are obtained by the  
 3112 similar procedure of maximizing the integrated posterior function (see A.5.2) to that  
 3113 of the  $\mu K$ -HIST-ETAS model in §B.3.

3114 Since the penalty function in (b1) already has the quadratic form with respect to the  
 3115 parameters  $\theta$ , the prior density is of a multivariate Gaussian distribution, in which the  
 3116 Hessian matrix  $H_Q$  consists of the elements of the negative second order partial  
 3117 derivatives of the penalty function  $Q$ . Actually, the present penalty function implies  
 3118 that the Hessian is a block diagonal matrix of five sub-matrices corresponding to each  
 3119  $\phi_k$ -function in (a2)~(a6) such that  $H_Q = \text{diag}\{H_Q^1, H_Q^2, H_Q^3, H_Q^4, H_Q^5\}$ . This is because  
 3120 we do not consider any restrictions a priori between the different  $\phi_k$ -functions. Here,  
 3121 all sub-matrices of  $H_Q^k$  are sparse, and have the same configuration of non-zero  
 3122 elements. Specifically, the  $(i, j)$ -element is non-zero if and only if the pair of points  $i$   
 3123 and  $j$  are vertices of the same Delaunay triangle; cf., §6.3.

3124 Specifically, this maximization is performed sequentially and alternately as  
 3125 follows. First, we implement the maximization of the penalized log-likelihood (a8)  
 3126 with respect to the coefficients of the  $\phi$ -functions; see Eqs. (a2) - (a6). For the  
 3127 calculation, we adopt a linear search using the incomplete Cholesky conjugate  
 3128 gradient (ICCG) method for  $5(N+n)$  dimensional coefficient vectors, where  $N+n$  is the  
 3129 same number as given in §6.3. Alternately, we implement the simplex algorithm in the  
 3130 5-dimensional space of  $(\hat{w}_1, \hat{w}_2, \hat{w}_3, \hat{w}_4, \hat{w}_5)$  to maximize  $\mathcal{A}(\tau)$  until this converges. Here,  
 3131 before doing the 5-dimensional simplex search, we recommend to firstly make a  
 3132 lattice search of  $(w_3, w_4, w_5)$  in the logarithmic orders, such as  $(10^i, 10^j, 10^k)$ , for  
 3133 possible sets of integers  $i, j$  and  $k$  to compare the respective ABIC values  $h$ , while  
 3134  $(w_1, w_2)$  remain fixed to those  $(\hat{w}_1, \hat{w}_2)$  obtained in §9.3. It is a limitation of this  
 3135 procedure that this maximization may not converge for small sets of integers because  
 3136 the convergence relies on the quadratic approximation penalized log likelihood (see  
 3137 Appendix and the ICCG method). From our experience, selection from 2 or 3 or 4 for  
 3138 the above  $i, j$  and  $k$ , can be a good choice of the starting values. Then, using the set of  
 3139 weights with the smallest ABIC value, we can implement the 3-dimensional simplex  
 3140 search of  $(w_3, w_4, w_5)$  or even the 5-dimensional simplex search of  $(w_1, w_2, w_3, w_4, w_5)$   
 3141 for a global minimum. Here it is important to make use of the previously converged  
 3142 solutions of parameters (coefficients) for the next initial parameters of such large  
 3143 dimensions.

3144 It is also useful to examine whether or not the characteristic parameters, particularly  
 3145  $\alpha(x, y) = \hat{\alpha} \exp\{\phi_3(x, y)\}$ ,  $p(x, y) = \hat{p} \exp\{\phi_4(x, y)\}$  and  $q(x, y) = \hat{q} \exp\{\phi_5(x, y)\}$  are  
 3146 significantly uniform (i.e., spatially invariant). For this we can calculate the Akaike  
 3147 Bayesian Information Criterion (ABIC; see Appendix) as a byproduct of the above  
 3148 simplex optimization. A model with a smaller ABIC value indicates a better fit. For  
 3149 example, we can compare the ABIC values of the HIST-ETAS model for the optimal  
 3150 weights  $(\hat{w}_1, \hat{w}_2, \hat{w}_3, \hat{w}_4, \hat{w}_5)$  with the one for  $(\hat{w}_1, \hat{w}_2, \hat{w}_3, \hat{w}_4, 10^8)$  to examine whether  
 3151  $q$ -value is location dependent or not.

3152  
3153

### 3154 **Acknowledgement**

3155 We are grateful for the comments by Yicun Guo (former Ph. D. student of Peking  
3156 University), Taku Ueda (Ph. D. student of Earthquake Research Institute, University  
3157 of Tokyo) based on the use of previous version of HIST-PPM program package;  
3158 which were very useful for the revised version. The careful reading of this manual and  
3159 many comments by anonymous reviewer for publishing in the ISM Computer Science  
3160 Monographs the manual are greatly appreciated. Authors are supported by the JSPS  
3161 KAKENHI grant 17H00727.

### 3162 **References**

- 3163 Akaike, H. (1974). A new look at the statistical model identification, *IEEE Trans.*  
3164 *Autom. Control*, **AC-19**, 716– 723.
- 3165 Akaike, H. (1978). A new look at the Bayes procedure, *Biometrika*, **65**, 53–59.
- 3166 Akaike, H. (1980). Likelihood and Bayes procedure, in *Bayesian Statistics*, eds. J. M.  
3167 Bernard, *et al.*, 1 –13, Univ. Press, Valencia, Spain.
- 3168 Aki, K. (1965). Maximum likelihood estimate of  $b$  in the formula  $\log N=a-bM$  and its  
3169 confidence limits, *Bull. Earthq. Res. Inst.*, **43**, 237-239.
- 3170 Dziewonski, A.M., T.A. Chou, and J.H.Woodhouse (1981). Determination of  
3171 earthquake source parameters from waveform data for studies of global and  
3172 regional seismicity, *J. Geophys. Res.*, **86**, 2825-2852.
- 3173 Fletcher, R. and M.J.D., Powell (1963). A rapidly convergent descent method for  
3174 minimization, *Comput. J.*, **6**, 163-168.
- 3175 Good, I.J. (1965), *The Estimation of Probabilities*, M.I.T. Press, Cambridge,  
3176 Massachusetts.
- 3177 Good, I.J. and R.A. Gaskins (1971), Nonparametric roughness penalties for  
3178 probability densities, *Biometrika* **58**, 255-277.
- 3179 Green, P.J.and Sibson, R. (1978). Computing Dirichlet tessellations in the plane.  
3180 *Computer Journal* **21(2)**, 168–173. DOI:10.1093/comjnl/21.2.168
- 3181 Gutenberg, R. and C.F. Richter (1944). Frequency of earthquakes in California, *Bull.*  
3182 *Seismol. Soc. Amer.*, **34**, 185-188.
- 3183 Kowalik, J. and M.R. Osborne (1968). *Methods for Unconstrained Optimization*  
3184 *Problems*, American Elsevier, New York.
- 3185 Mori, M. (1986). *FORTRAN 77 Numerical Analysis Programming*, 342pp., Iwanami  
3186 Publisher, Tokyo, (in Japanese).
- 3187 Murata, Y. (1992). Estimation of optimum surface density distribution only from  
3188 gravitational data: an objective Bayesian approach, *J. Geophys. Res.*, **98**,  
3189 12097-12109.
- 3190 Ogata, Y. (1981), On Lewis' simulation method for point processes, *IEEE Information*  
3191 *Theory*, IT-27, 23-31.
- 3192 Ogata, Y. (1985). Statistical models for earthquake occurrences and residual analysis  
3193 for point processes, Research Memorandum, No. 288, The Institute of Statistical  
3194 Mathematics, Tokyo, <http://www.ism.ac.jp/editsec/resmemo-e.html>.

- 3195 Ogata, Y. (1988). Statistical models for earthquake occurrences and residual analysis  
3196 for point processes, *J. Amer. Statist. Assoc.*, 83, 9-27.
- 3197 Ogata, Y. (1989), Statistical model for standard seismicity and detection of anomalies  
3198 by residual analysis, *Tectonophysics*, **169**, 159-174.
- 3199 Ogata, Y. and Katsura, K. (1993). Analysis of temporal and spatial heterogeneity of  
3200 magnitude frequency distribution inferred from earthquake catalogues, *Geophys. J.*  
3201 *Int.*, **113**, 727-738.
- 3202 Ogata, Y., Matsu'ura, R. S. and Katsura, K. (1993). Fast likelihood computation of  
3203 epidemic type aftershock sequence model, *Geophys. Res. Lett.*, **20**(19),  
3204 2143-2146.
- 3205 Ogata, Y. (1998). Space-time point-process models for earthquake occurrences. *Ann.*  
3206 *Inst. Statist. Math.* **50**, 379–402. DOI:10.1023/A:1003403601725
- 3207 Ogata, Y. (2004). Space-time model for regional seismicity and detection of crustal  
3208 stress changes. *J. Geophys. Res.* **109**(B3), B03308. DOI:10.1029/2003JB002621.  
3209 See corrections in *J. Geophys. Res.* **109**(B6), B06308.  
3210 DOI:10.1029/2004JB003123.
- 3211 Ogata, Y. (2006). *Statistical Analysis of Seismicity, Updated Version*  
3212 *(SASeis2006)*, Computer Science Monograph, No 33, Institute of Statistical  
3213 Mathematics, Tokyo.
- 3214 Ogata, Y. (2008), Occurrence of the large earthquakes during 1978~2007 compared  
3215 with the selected seismicity zones by the Coordinating Committee of Earthquake  
3216 Prediction (in Japanese), *Report of the Coordinating Committee for Earthquake*  
3217 *Prediction*, 79, 623-625.
- 3218 Ogata, Y. (2010). Significant improvements of the space-time ETAS model for  
3219 forecasting of accurate baseline seismicity. *Earth, Planets and Space* **63**, 217-229,  
3220 doi:10.5047/eps.2010.09.001.
- 3221 Ogata, Y., M. Imoto and K. Katsura, (1991). 3-D spatial variation of b-values of  
3222 magnitude-frequency distribution beneath the Kanto District, Japan, *Geophys. J. Int.*  
3223 **104**, 135-146.
- 3224 Ogata, Y. and K. Katsura (1988). Likelihood analysis of spatial inhomogeneity for  
3225 marked point patterns, *Ann. Inst. Statist. Math.*, **40**, 29-39.
- 3226 Ogata, Y. and K. Katsura (1993). Analysis of temporal and spatial heterogeneity of  
3227 magnitude frequency distribution inferred from earthquake catalogues, *Geophys. J.*  
3228 *Int.*, **113**, 727-738.
- 3229 Ogata, Y., Utsu, T. and Katsura, K. (1995). Statistical features of foreshocks in  
3230 comparison with other earthquake clusters, *Geophys. J. Int.*, **121**, 233-254.
- 3231 Ogata, Y., Katsura, K., Tanemura, M. (2003). Modelling heterogeneous space-time  
3232 occurrences of earthquakes and its residual analysis. *Applied Statistics* **52**(4), 499–  
3233 509. DOI:10.1111/1467-9876.00420
- 3234 Ogata, Y., Katsura, K., Zhuang, J.C. (2006). *TIMSAC84: Statistical Analysis of Series*  
3235 *of Events (TIMSAC84-SASE), Version 2*. Computer Science Monograph, No 32.  
3236 Institute of Statistical Mathematics, Tokyo.
- 3237 Ogata, Y., Matsu'ura, R.S., Katsura, K. (1993). Fast likelihood computation of  
3238 epidemic type aftershock sequence model. *Geophys. Res. Lett.* **20**(19), 2143–2146.  
3239 DOI:10.1029/93GL02142

3240 Ogata, Y., Zhuang, J.C. (2006). Space-time ETAS models and an improved extension.  
3241 *Tectonophysics* **413(1-2)**, 13–23. DOI:10.1016/j.tecto.2005.10.016

3242 Ogata, Y. and Katsura, K. (2012). Prospective foreshock forecast experiment during  
3243 the last 17 years, *Geophys. J. Int.*, **191**, Issue3, 1237–1244,  
3244 doi:10.1111/j.1365-246X.2012.05645.x

3245 Rproject R Development Core Team. (2009). *R: A Language and Environment for*  
3246 *Statistical Computing*. R Foundation for Statistical Computing, Vienna. ISBN:  
3247 3-900051-07-0, URL: <http://www.R-project.org>

3248 Tanemura, M., Ogawa, T., Ogita, N. (1983). A new algorithm for three-dimensional  
3249 Voronoi tessellation. *Journal of Computational Physics* **51(2)**, 191–207.  
3250 DOI:10.1016/0021-9991(83)90087-6

3251 Tsuruoka, H. (1996). Development of seismicity analysis software on workstation.  
3252 *Tech. Res. Rep. 2*, 34–42, Earthquake Res. Inst., Univ. Tokyo (in Japanese).

3253 Utsu, T. (1965). A method for determining the value of b in a formula  $\log n = a - bM$   
3254 showing the magnitude frequency relation for earthquakes (in Japanese), *Geophys.*  
3255 *Bull. Hokkaido Univ.*, **13**, 99-103.

3256 Utsu, T. and A. Seki (1955). Relation between the area of aftershock region and the  
3257 energy of the main shock, *Zisin (J. Seismol. Soc. Japan)*, 2nd Ser., ii, **7**, 233-240 (in  
3258 Japanese with English summary).

3259 Utsu, T. (1969). Aftershocks and earthquake statistics (I): some parameters which  
3260 characterize an aftershock sequence and their interaction, *J. Faculty Sci., Hokkaido*  
3261 *Univ.*, Ser. VII (geophysics) **3**, 129-195.

3262 Utsu, T. (1970). Aftershocks and earthquake statistics (II): Further investigation of  
3263 aftershocks and other earthquake sequences based on a new classification of  
3264 earthquake sequences, *J. Faculty Sci., Hokkaido Univ.*, Ser. VII (geophysics), **3**,  
3265 198-266.

3266 Utsu, T. (1982), Catalog of Large Earthquakes in the Region of Japan From 1885  
3267 Through 1980, *Bull. Earthq. Res. Inst., Univ. Tokyo*, **57**, 401-463.

3268 Utsu, T. (1985). Catalog of large earthquakes in the region of Japan from 1885  
3269 through 1980: Correction and supplement. *Bull. Earthq. Res. Inst., Univ. Tokyo*, **60**,  
3270 639-642.

3271 Zhuang, J., C. Chang, Y. Ogata, and Y. Chen (2005). A study on the background and  
3272 clustering seismicity in the Taiwan region by using point process models, *J.*  
3273 *Geophys. Res.*, **110**, B5, B05S18, doi:10.1029/2004JB003157, 2005.

3274 Zhuang J. and Ogata Y. (2006). Properties of the probability distribution associated  
3275 with the largest event in an earthquake cluster and their implications to foreshocks.  
3276 *Physical Review, E*, **73**, 046134. doi: 10.1103/PhysRevE.73.046134

3277